Flood defenses Washington D.C.

multidiscipinary project

by

Lisa van der Linde[1], Vincent Leclercq[2], and Ligaya Wopereis[1]

[1] *MSc student Hydraulic Engineering, Delft University of Technology*
[2] *MSc student Geotechnical Engineering, Delft University of Technology*

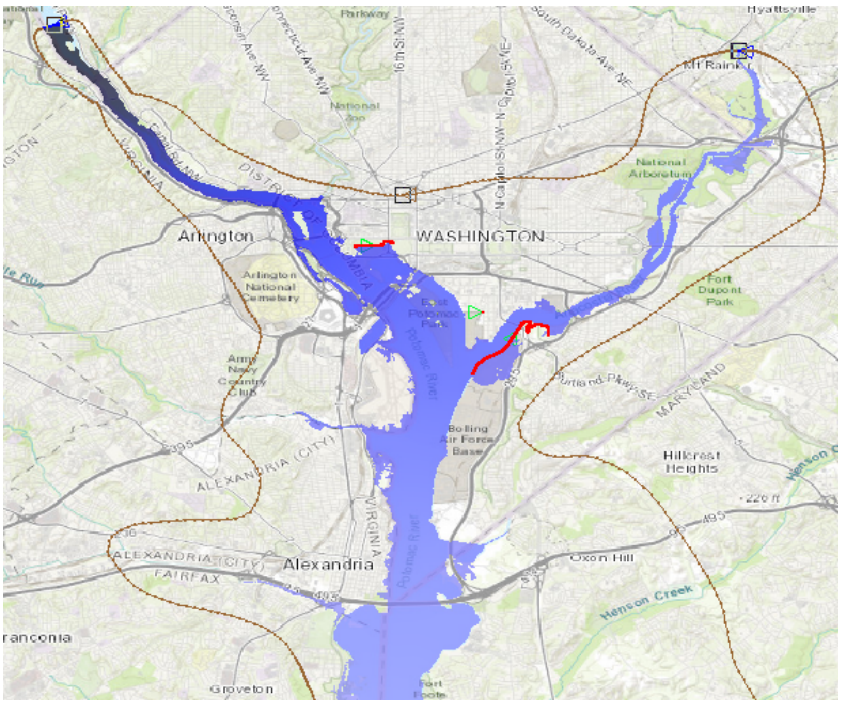

Student numbers respectively:	4342852, 4283732, 4393600	
Project duration:	September 5, 2018 – Oktober 27, 2018	
Project supervisors:	Dr. ir. J. Bricker,	TU Delft
	Dr. ir. M. Zijlema,	TU Delft
	Prof. Dr. ir. C. Jommi,	TU Delft
	Dr. ir. C. Ferreira,	George Mason University

Preface

This report was written for the course Multidisciplinary Project - CIE4061-09 at Delft University of Technology. The research was conducted at the George Mason University, Flood Hazards Lab. The project aims at creating a better understanding of the flood risk in Washington DC by means of modelling the floods and in-situ inspections, because the area is flooded frequently. Based on the modelling and area inspection, improved flood protections were to be designed. However, during the course of the project, instabilities in the model occurred, which could not be solved in time. Therefore, the flood protection design was based on historic data instead, and the modelling part of the project shifted towards understanding these instabilities.

Lisa van der Linde[1], Vincent Leclercq[2], and Ligaya Wopereis[1]

[1] *MSc student Hydraulic Engineering, Delft University of Technology*
[2] *MSc student Geotechnical Engineering, Delft University of Technology*
Washington DC, 09/11/2018

Contents

List of Figures

List of Parameters

Parameter	Unit	Description
ACC	$	Annualized Construction Costs
ACT	-	Activity of a clay
A_{levee}	m^2	Area of the levee
Bc	m	Crest width
Bc_0	m	Crest width existing levee
$B_{x,y}$	m^2/s	Bottom friction
C_α	-	Secundary coefficient of compression
C_c	-	Primary coefficient of compression
C_D	-	Quadratic friction coefficient
C_r	-	Courant number
C_u	kPa	Undrained shear strength
C_v	-	Coefficient of consolidation
c	-	Unit construction cost per volume
$D_{x,y}$	m^2/s	Bottom friction
DS	-	Discriminant Factor
e0	-	Initial void ratio
e_ref	-	Void ratio at reference time
E_h	m^2/s	Lateral eddy viscosity
E_u	kPa	Undrained modulus of elasticity
f	m^2/s	Coriolis
f_0	m	Diameter of inner circle of the smallest mesh element
g	m/s^2	Gravitational acceleration
H	m	Total water depth
H_L	m	Levee height
H_0	m	Levee height existing levee
H0	-	Initial thickness of compressible layer
h	m	Average water depth
h_c	m	Capillary rise in porous medium
I	-	Influence factor
I(z)	-	Coefficient of Influence
K_{slip}	m/s	Linear friction coefficient
k_h	m/s	Horizontal hydraulic conductivity
k_v	m/s	Vertical hydraulic conductivity
L	m	Levee length
LI	-	Liquidity Index
LL	-	Liquid Limit
$M_{x,y}$	m^2/s	Bottom friction
N	-	SPT Number of blow
N60	-	Normalized SPT number of blows
n	$years$	Lifetime of levee
OCR	-	Over Consolidation Ratio
PI	-	Plasticity Index
PL	-	Plastic Limit
p_a'	kPa	Athmospheric pressure
$Q_{x,y}$	m^3/s	Discharge
r	m	Radius of the pores
S	-	Degree of Saturation
s	-	Cost multiplier

t	s	Time
$tan(\alpha)$	-	Inner slope angle of levee
$tan(\beta)$	-	Outer slope angle of levee
U, V	m/s	Velocities in x,y direction
UC	$\$/m^3$	Unit land cost
V_{levee}	m^3	Volume of the levee
w	-	Water content
w_c	m	Settlements due to consolidation
w_i	m	Instantaneous undrained settlements
w_s	m	Settlements due to creep
w_t	m	Total Settlements
α	m^2/s	Bottom friction
$\alpha_{1,2,3}$	-	Time weighing factors for k+1, k, k-1
γ	[N/m]	Surface tension of water
ζ	m	Surface elevation
η	m/s	Tidal potential
θ_r	Degrees	Receding contact angle
μ	-	Mean
ξ	-	Shape parameter
ρ	kg/m^3	Density of water
σ	-	Scale parameter
σ	kPa	Total stress
σ'	kPa	Effective stress
σ_p'	kPa	Preconsolidation pressure
$\sigma_{penetrometer}$	kPa	Penetrometer stress level measurement
σ_{vo}'	-	Initial vertical effective stress
τ_b	m^2/s	Bottom friction
τ_s	m^2/s	Surface tension
τ_0	-	Weighing factor in GWCE
ϕ	m^2/s	Weighing factor
ϕ'	degrees	Effective friction angle

Abstract

The United States of America have a safety standard for flood protection of 1/100 year. However the flood protections in the Washington D.C. do not comply with this requirement. During this study the levees in Washington D.C. area were analysed and it was found, that in order to comply with the 1/100 safety standard the levees in the National Mall needs to be heighten by 0.5 m and those near the Anacostia river by 1.5m. The safety standard of 1/100 imposed in the United States of America is not based on exact calculation, therefore another design method was applied, which uses an optimal safety level based on the damage cost of floods and investment cost of flood protections.

The calculation of the optimal return period was based on the 'Standaardmethode 2017' and it was found that the optimal return period at the National Mall levee is 1/263 years. At the southern bank of the Anacostia river this optimal return period is 1/373 year. With these return periods new levees were designed in order to ensure the safety of the area of Washington D.C. There were two new levees needed around the National mall. The first was situated north of the Lincoln memory along the Potomac river and the second replaces the temporary flood defence by the 2nd street SW and had an L-shape facing the Potomac river. The Anacostia levee was stretched on the East side in order to comply with the new 1/373 year safety standard. The old and new National mall levees needed a height of 3.5 m and those by the Anacostia needed a height of 8.5 m. It is important to take caution with these new levees as some houses needed to be removed. An attempt was made at modelling the above mentioned floods in ADCIRC to improve the accuracy of the design water levels and to verify the final design. However, the model showed instabilities, preventing the results from being used. Explanations for these instabilities are the incoming water not being properly ramped up, the large vertical gradients in shallow areas and the upstream and downstream boundaries being too close to each other.

1 Introduction

The Washington metropolitan area, including Washington DC, is a low-lying urbanized area on reclaimed wetlands. Due to the low lying bathymetry the area is subjected to frequent floods. The damage caused by these floods is extensive especially because the area is the political centre of the country, has great historical monuments and the entire metropolitan area has a population of more than 6.1 Million inhabitants. The cause of these reoccurring floods are the following: Extreme discharges from the Potomac and Anacostia rivers, extensive rainfall and storm surge from Chesapeake Bay, which is connected to the Atlantic Ocean. Historically, there have been 13 major floods recorded of which 4 were caused by rainfall, the remaining floods were caused by either extreme river discharge, or storm surge by hurricanes. The largest flood recorded occurred in 1933 by an unnamed hurricane which coincided with high astronomical tide. The most recent non-rainfall flood was cause by hurricane Isabel, requiring temporary flood barriers to be placed (NCPC, 2008). This report focuses on understanding the full extent of the risk and providing possible solutions. The main research question is:

What is the extend of floods in Washington DC and what measures can be taken to prevent these floods?

Which will be answered by means of the following sub-questions.

- What is the current state of flood protections in Washington DC?
- What are relevant floods against which Washington DC should be protected?
- What is the extend of the floods?
- How can these floods be modelled?
- What additional protection is required to comply with the local safety standards?
- What are the optimal design standards?
- What additional and new protection is required to comply with the optimal safety standard?

All sub questions will be answered for the following study area and levee condition.

Description of the study area

Figure 1.1 below shows the computational domain of the project. In the north two boundary conditions are found, the Potomac river on the West and the Anacostia river on the East. The downstream boundary can be seen in figure 3.3. In the district of Columbia there are two levees serving as flood protection. The national mall levee is approximately 3.9 m high and is interrupted by the 17th street, one of the largest streets in Washington DC, at this location, there is the possibility to place temporary flood defenses in case of high water. The other levee consists of a brick wall, which can be closed of in case of a flood. Another region of interest is the Anacostia riverbank, just south of the District of Columbia, this levee is maintained by the army, since it is connected to a military base and has a height of approximately 5.0m.

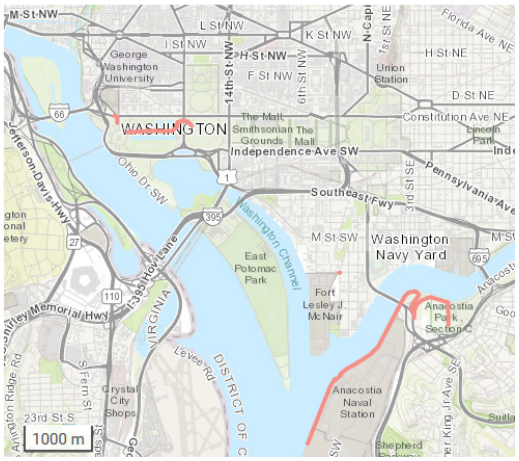

Figure 1.1: Sight investigation National Mall

Current levee condition

The state of the National Mall and Anacostia bank levee's were assessed in order to get an overview of the situation at hand. The same conclusions as the Army Corps were drawn as to the state of the levees. Both the Anacostia bank and National Mall levee presented unwanted amount of vegetation, as can be seen in Figure J.2 and J.1 in Appendix J. The National Mall levee also presented signs of unwanted fauna, while the Anacostia bank Levee had non-water retaining structures on the levee that were in poor condition. These factors made the levee system unsuitable as reliable flood defense. On top of this, settlements have lead the height of the levee to be too small for the 1/100 year return period. The lowest point on the National Mall levee had a height of + 5m NAVD 88 and the Anacostia bank levee + 3.96 m NAVD 88.

This report bases its research on the situation described above. The first chapter explains how the floods are modelled, which parameters were used and which assumptions were made. Chapter 3, goes into the details about the preparation and parameters of the model used. In chapter 4 the data collection for the soil parameters is shown, as well as the methods applied to design the levee. The results are shown in chapter 5 followed by a discussion of the results and its implications. In the final chapter the limitations of the research are mentioned, recommendations are given and conclusions are drawn.

2

Flood return period

To determine the probability of occurrence for different floods, historical data was analyzed near Washington DC. For this multiple measuring stations were used. In figure 2.1 the different measuring stations can be observed. Station A is United States Geological Survey (USGS) station 1646500, where the discharge of the Potomac river was recorded. The discharge of the Anacostia river was derived as the sum stations C and D which were USGS stations 1651000 and 1649500. Station B recorded the waterlevel near Washington DC this was a station by NOAA Tides and Currents with as identifaction 8594900. Further downstream near the Chesapeake Bay there was another station of NOAA Tides and Currents, used for the downstream boundary conditions, station 8635750 (Lewisetta, VA).

Figure 2.1: Measuring stations

Any trends in the data were removed, after which a probability density function could be fitted through the data. The function could be transformed into a cumulative density function that was used to determine the design water level for a specific return period. The trends were added again on top of the return period water level to obtain the design water level. For the boundary conditions of the model a multivariate cumulative density function was created.

2.1. Sea level rise trend removal

In the historical data of the tidal level a rising trend could be observed. This trend was removed in the probabilistic analysis, to be added after the return period water level was obtained. A linear trend was assumed, fitted through the mean sea level at the location of the gauge. The results of the original water level at NOAA gauge 8594900, the mean sea level trend and the trendless water level can be found in figure 2.2 for Washington DC and in figure 2.3 for the downstream boundary. The trend that was removed from the water level was found to be of 3.14 mm/year.

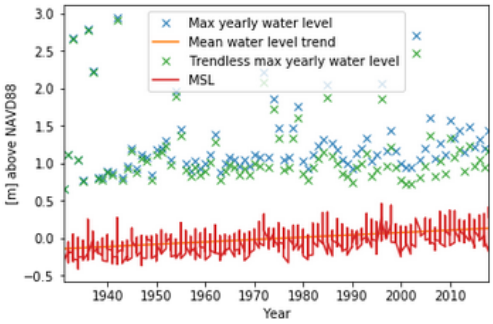

Figure 2.2: Historical water levels near Washington DC

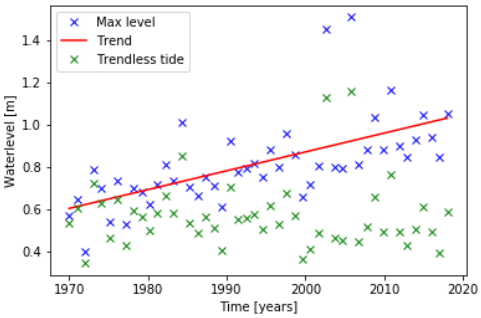

Figure 2.3: Historical water levels at the downstream boundary

2.2. Curve fitting

Extreme value distributions were made from the historical data, by taking the block maximua of historical data. The sampling interval was chosen to be 1 year. The probability density functions that could fit the data properly were the Weibull, Gumbel or Frechet distribution. These are all specific cases of the Generalized Extreme Value distribution, or GEV which uses distribution described in Eq. 2.1.

$$GEV = \exp(-(1+\xi * \frac{x-\mu}{\sigma})^{-\frac{1}{\xi}}) \tag{2.1}$$

The GEV relies on 3 parameters, a location μ, a scale σ and a shape parameter ξ. These were found using the in2extRemes tool of R-studio. This tool provided the best fit by iterating the maximum likelihood. It returned the return period curve, presented in 2.4.

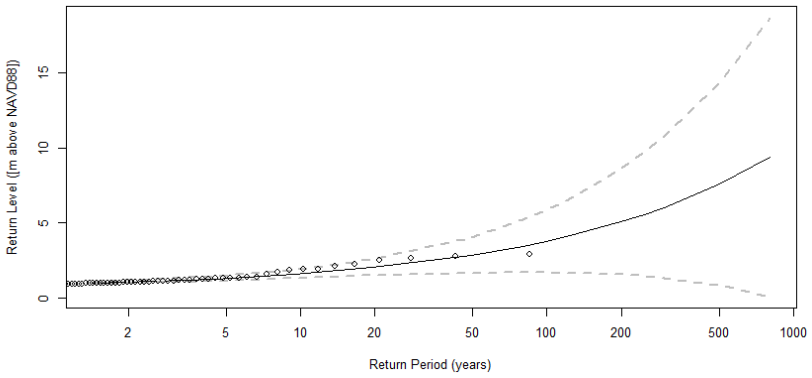

Figure 2.4: Return level curve of water level in DC

With the Generalized Extreme Value parameters obtained from the R-studio curve fit, the Probability Density Function (PDF) and Cumulative Density Function (CDF) were plotted in Python. These plots are presented in figure 2.5.

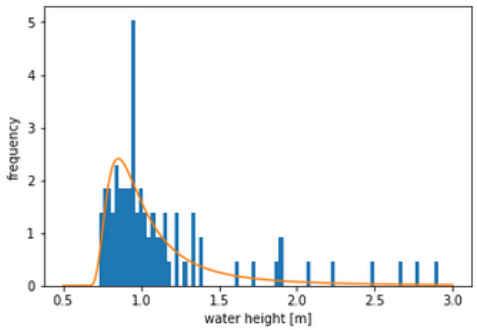

Figure 2.5: Curve fit of GEV PDF through water level histogram

Through the histograms of these annual maxima, different probability density functions were fitted, these were evaluated by calculating the Root Mean Square Error (RMSE) to determine the best fit.

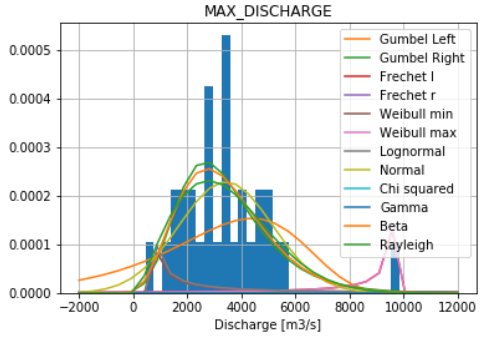

Figure 2.6: PDF fitting of the yearly maximum discharges

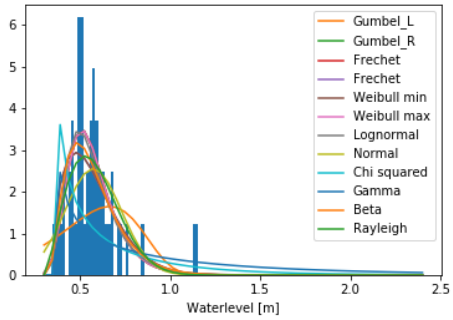

Figure 2.7: CDF fitting of the pick discharges

With an RMSE of $3.69E^{-7}$ the Rayleigh distribution is the best fit for the Potomac historical data, while for the Chesapeake Bay the optimal distribution is a Weibull distribution with an RMSE of 114.69. In figures 2.8 and 2.9 the fitted distribution functions can be found.

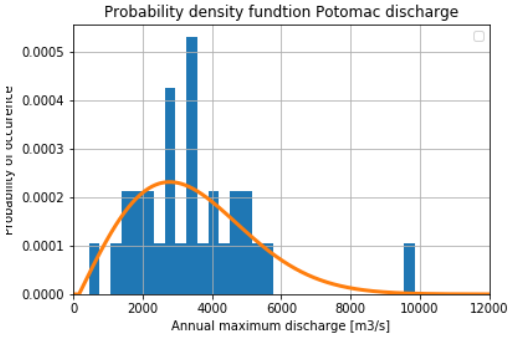

Figure 2.8: Most accurate PDF, Rayleight distribution

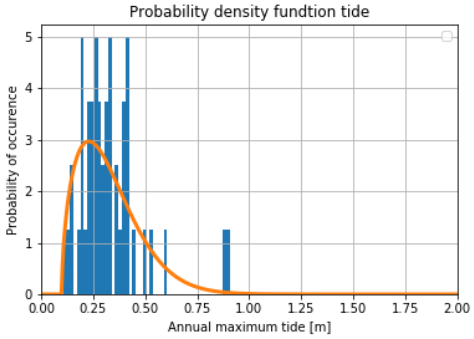

Figure 2.9: Most accurate CDF, Weibull distribution

2.3. Return period determination

Flood level optimization is used to minimize all flood related cost on the long term. For the purpose of this study, solely levee construction cost and flood damage are taken into account.

To determine the optimal safety level, the bathtub overflow related to certain water heights were looked at with ArcGIS. Failure due to over topping is assumed to happen after water levels exceed levee heights. The flood levels were then related to the previously determined return periods, see paragraph **??**. The flood maps for the respective flood heights can be found in A.

Damage cost

To estimate the flood damage per return period, the flood maps were given a raster with a resolution of 100m by 100 m. The raster points were then divided into groups, depending on the usage of the land. The financial worth of the classes of real estate or land usage were calculated using the average of real estate prices per class in the study area. Additional land usage worth and vehicle worth has been adopted from Standaardmethode 2017, as well as losses from business disruption (Slager and Wagenaar, 2017). A high land value in downtown Washington DC however, might culminate to cost estimations on the low end. The amount of vehicles was assumed to be 0.86 times the number of households.

Depending on the water depth and category, every raster point was given a damage factor. In order to do this, the damage curves from Standaardmethode 2017 where used (Slager and Wagenaar, 2017). The damage that one raster point accounts for is its maximum damage cost previously computed, multiplied by the damage factor. This makes the total cost of one flood scenario the sum of the cost of every individual raster point as shown in Eq. 2.2.

$$S = \sum_{i=1}^{n} \alpha_i * n_i * S_i \tag{2.2}$$

Where:
S [$]: total damage cost
α_i [-]:damage factor of one raster block
n_i [-]:raster block
S_i [$]:Maximum damage of one raster block

An overview of the damage costs per flood scenario are given in Appendix A for both Washington DC and the Anacostia river bank. The yearly damage cost per scenario was determined by multiplying the actual cost with the probability of the scenario. This is plotted in the figure below for both flood planes with a linearly fitted line to extrapolate the estimated cost.

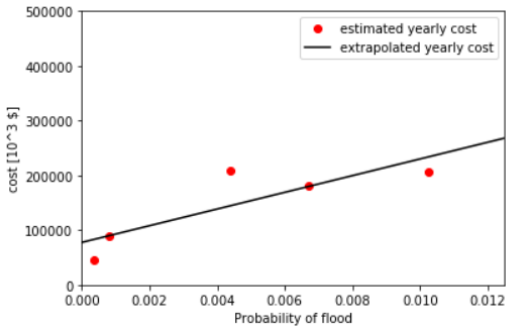

Figure 2.10: Damage costs downtown Washington DC

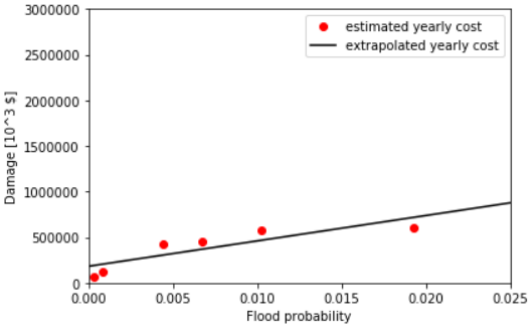

Figure 2.11: Damage cost Anacostia riverbank

Investment cost

The investment cost for a single levee is based on its geometric properties and was calculated using the following formula: (Hui et al., 2016).

$$ACC = \left[\frac{r*(1+r)^n}{(1+r)^n-1}\right] * (s*c*V_{levee} + UC*A_{levee}) \tag{2.3}$$

$$V_{levee} = L\left[Bc*H_L + \frac{1}{2}\left(\frac{1}{tan(\alpha)} + \frac{1}{tan(\beta)}\right)*H_L^2\right] - L_0\left[Bc_0*H_0 + \frac{1}{2}\left(\frac{1}{tan(\alpha)} + \frac{1}{tan(\beta)}\right)*H_0^2\right] \tag{2.4}$$

$$A_{levee} = L\left[Bc + \left(\frac{1}{tan(\alpha)} + \frac{1}{tan(\beta)}\right)*H_L\right] - L_0\left[Bc_0 + \left(\frac{1}{tan(\alpha)} + \frac{1}{tan(\beta)}\right)*H_0\right] \tag{2.5}$$

Where:

ACC [$]: annualized construction cost
n [years]:levee lifespan
s [$/ m^3]:soil cost per unit of volume
c [$/ m^3]:unit construction cost per volume
V_{levee} [m^2]: volume of the levee
UC [$/ m^2]:local land value
A_{levee} [m^2]: area occupied by levee
L [m]:levee length
L_0 [m]: previous levee length
α [rad]: levee slope
β [rad]: levee slope
H_L [m]: levee height
H_0 [m]: previous levee height
Bc [m]: crown width
Bc_0 [m]: previous crown width

The landvalue Unit Cost (UC) depends on the distance of the land from downtown Washington DC. Land values depend on the distance from the city center in a quartic polynomial distribution (Albouy and Ehrlich, 2012). This distribution can be found in Appendix A. The needed land area is related to the length of the levee. The levee length differs per design return period, as is shown in the figures below.

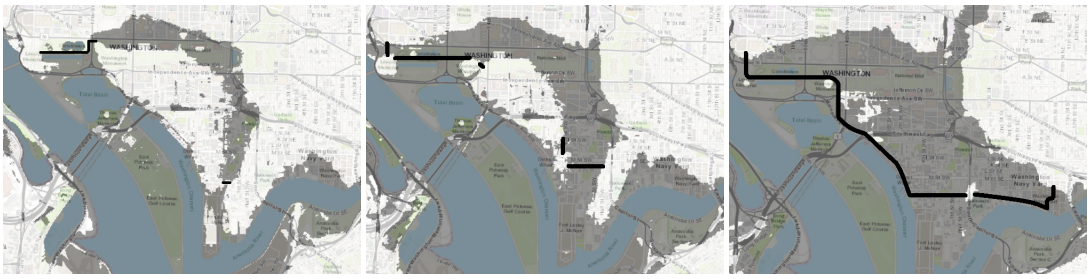

Figure 2.12: Levees in downtown Washington DC for flood levels of respectively 4m, 6m and 10 m

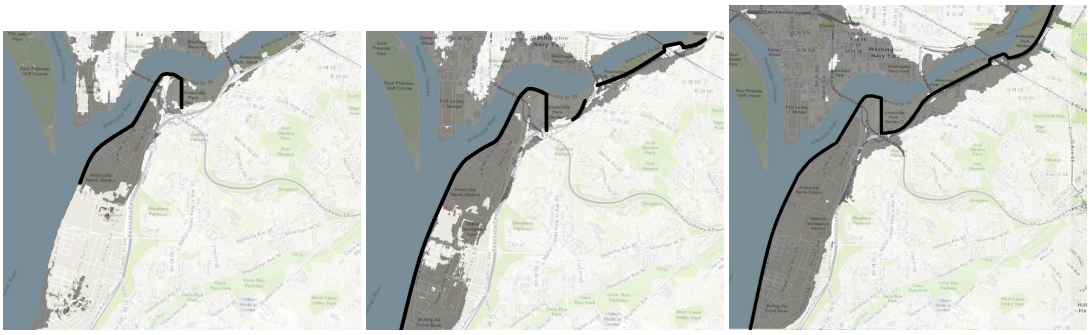

Figure 2.13: Levees on the Anacostia river bank for flood levels of respectively 4m, 6m and 10 m

Since the cost benefit analysis considers long term solutions, a lifespan of 50 years is taken into consideration for the levees. Furthermore, it is assumed that the levees have to be rebuild after these 50 years, which makes this a conservative estimation. The annual investment costs would then be the total levee cost divided by the 50 year lifespan. This is plotted in figures 2.14 and 2.15 below, including the extrapolated exponentially fitted curve.

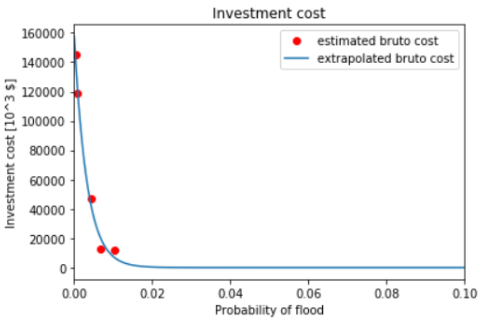

Figure 2.14: Investment costs downtown Washington DC

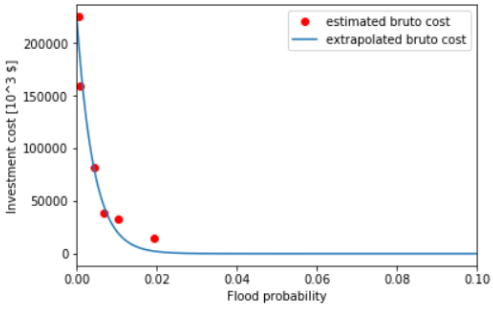

Figure 2.15: Investment cost Anacostia riverbank

Total

The total cost associated with a certain probability would be the linked damage cost and investment cost added up. Doing so with the damage curves and the investment curves, this gives curves with the optimal return period at their minima. As seen in figures 2.16 and 2.17, this gives optimal return periods for downtown DC and the Anacostia river bank of respectively 263 and 373 years.

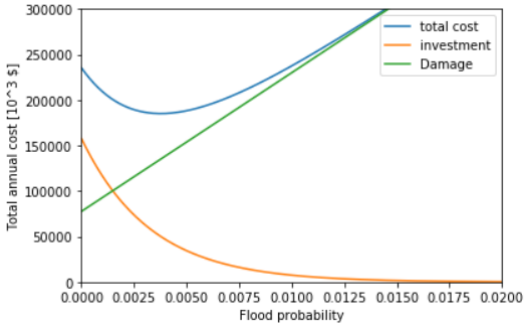

Figure 2.16: Annual costs downtown Washington DC

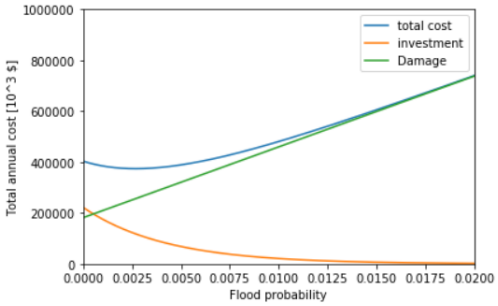

Figure 2.17: Annual cost Anacostia riverbank

2.4. Boundary conditions

The boundary conditions of the model were defined at three different locations, the Potomac and Anacostia rivers served as upstream boundaries and the Potomac river right before Chesapeake Bay was used as downstream boundary. The input data for both upstream boundaries are discharges and the input data for the downstream boundary was the water level condition.

The Potomac river and the downstream water level are combined in a multivariate probability density function to determine the once in X years storm event. Where X will be a 100 years, 263 years and 376 years, respectively, as shown in the section above. Because of the small discharge of the Anacostia in comparison to the Potomac river, the average discharge of the Anacostia river will be used in the simulations.

There are multiple methods available for determining the once in X years flood of a combination of factors. Since we are only working with two variables, the most reliable method is determining the joint probability distribution. The probability density functions are combined to a multivariate distribution function by multiplying the distributions with each other as shown in Eq. 2.6.

$$f(x,y)dxdy = f_x(x) * f_y(y)dxdy \tag{2.6}$$

The multivariate probability density function is shown in figure 2.18.

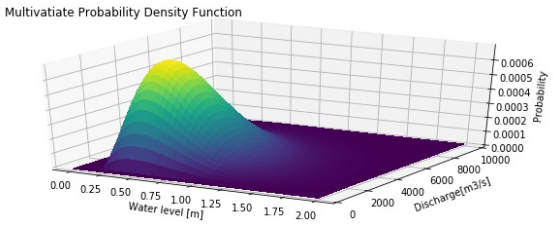

Figure 2.18: Multivariat probability density function

To obtain boundary conditions for certain return periods the multivariate cumulative distribution function is computed by calculating the cumulative area underneath the probability density function. By doing this, all combinations for a certain return period can be computed and used in the model (Jonkman et al., 2011).

$$F(x,y) = \int_{-\infty}^{\infty} f_x(x) * f_y(y) dx dy \tag{2.7}$$

The multivariate cumulative distribution function, calculated using Eq. 2.7 is shown in figure 2.19.

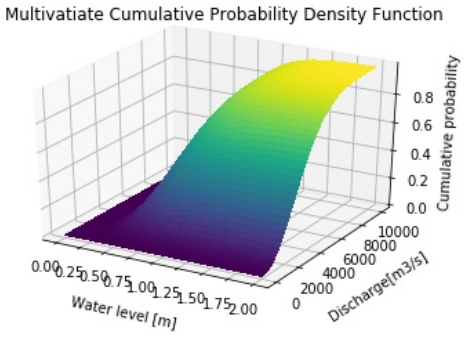

Figure 2.19: Cumulative distribution function

To determine the potential extreme events for a certain return period T the intersection of the cumulative distribution function and the plain at $1-\frac{1}{T}$ must be determined. Figure 2.20 shows the potential storm events for a once in a 100 year, a 263 year and a 373 year return period.

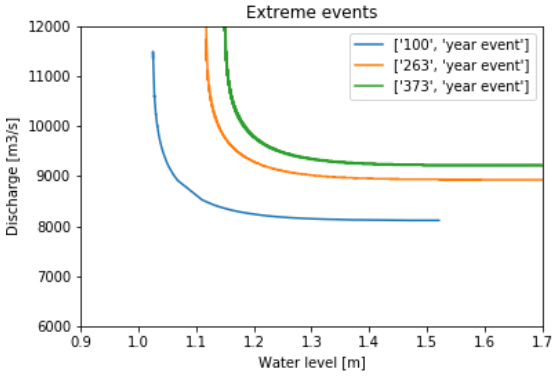

Figure 2.20: Extreme events for different return periods

The time series for the downstream boundary was created by assuming the once in a X year elevation to be half of the tidal amplitude. The upstream boundary was created by assuming the discharge to develop

with the shape of a Gaussian distribution, starting of at mean flow conditions, followed by an increase until the statistically calculated water level. The time series can be found in Appendix H.

These boundaries were used to model the study area, how this was done can be found below.

3

Flood modelling

In order to have a better understanding of the frequent floods occurring in the National Capital of the United States of America, the ADvanced CIRCulation (ADCIRC) model was used to simulate different extreme flood scenarios. ADCIRD is a finite-element hydrodynamic model computed in FORTRAN 90 language and based on the generalized wave continuity equation (GWCE) to accurately model a moving fluid on a rotating earth. In this research, ADCIRC was used to model storms and heavy discharges in floodplains. ADCIRC is widely used in the United States, especially by the Army Corps, companies and universities such as George Mason university. To stay consistent with the research done here at the Flood Hazard department of GMU, ADCRIC was chosen to simulate flooding scenarios around Washington DC.

The area of study as mentioned previously, was the District of Columbia and comprised the Potomac and Anacostia rivers, see figure 3.1 below. The boundary conditions were; water levels from tide and storm surges for the downstream boundary, and discharges for the two upstream boundaries; the Potomac river on the West and the Anacostia river on the East.

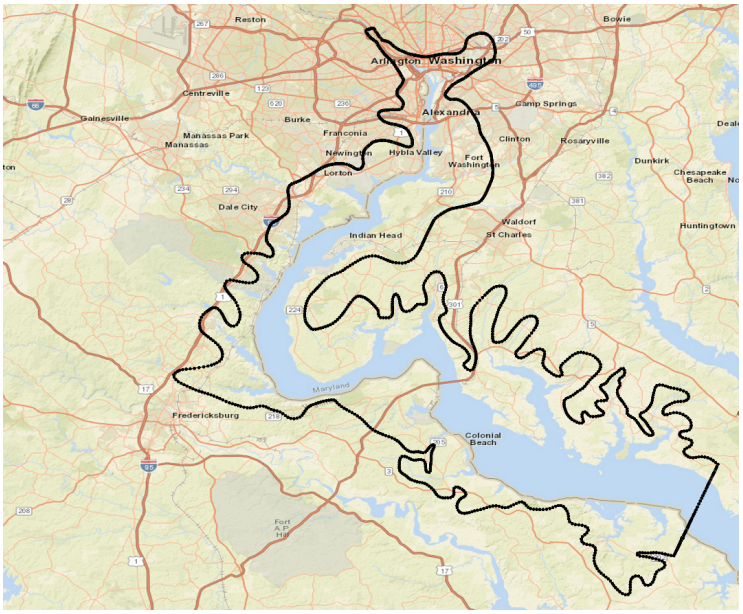

Figure 3.1: Region of study

In order to model the flow of this area with ADCIRC, a mesh describing the domain was required. SMS, which provides a graphical interface for ADCIRC, was used for this purpose.

3.1. ADCIRC

ADCIRC computes the water levels at nodes by means of the Generalized Wave Continïty equation, which is integrated in space and discretized in time. Eq. 3.1 shows the GWCE. For the discretization and derivation view Appendix B.

$$\frac{\partial^2 \zeta}{\partial t^2} + \frac{\partial \tilde{J}_x}{\partial x}(VH) + \frac{\partial \tilde{J}_y}{\partial y}(VH) - UH\frac{\partial \tau_0}{\partial x} - VH\frac{\partial \tau_0}{\partial y} = 0 \tag{3.1}$$

where

$$\begin{aligned} \tilde{J}_x &\equiv \frac{\partial}{\partial t}(UH) + \tau_0 UH = H\frac{\partial U}{\partial t} + U\frac{\partial \zeta}{\partial t}\tau_0 UH \\ \tilde{J}_y &\equiv \frac{\partial}{\partial t}(VH) + \tau_0 VH = H\frac{\partial V}{\partial t} + V\frac{\partial \zeta}{\partial t}\tau_0 VH \end{aligned} \tag{3.2}$$

The velocities are determined by solving the momentum equations as are shown in Eq. 3.3.

$$\begin{aligned} \frac{\partial U}{\partial t} + U\frac{\partial U}{\partial x} + V\frac{\partial U}{\partial y} - fV &= -g\frac{\partial[\zeta + P_s/g\rho_0 - \alpha\eta]}{\partial x} + \frac{\tau_{sx}}{H\rho_0} - \frac{\tau_{bx}}{H\rho_0} + \frac{M_x}{H} - \frac{D_x}{H} - \frac{B_x}{H} \\ \frac{\partial V}{\partial t} + U\frac{\partial V}{\partial x} + V\frac{\partial V}{\partial y} - fU &= -g\frac{\partial[\zeta + P_s/g\rho_0 - \alpha\eta]}{\partial y} + \frac{\tau_{sy}}{H\rho_0} - \frac{\tau_{by}}{H\rho_0} + \frac{M_y}{H} - \frac{D_y}{H} - \frac{B_y}{H} \end{aligned} \tag{3.3}$$

In these equations the baroclinic, surface tension and dispersion Coriolis components were neglected. Because only the 2 dimensional depth integrated model was used, not enough information was supplied for the baroclinic and dispersion Coriolis components to be calculated. Also no wind forcing was used cancelling out the surface tension.

3.2. The Mesh

The mesh created for this project as state above, was made in SMS and was based on an already existing mesh of a wider part of the region, see figure 3.2. The existing mesh was cut to fit into the area of interest and its different boundary conditions, see figure 3.3. The boundary conditions were chosen conforming to the location of the measuring stations available on NOOA Tides and Current. Therefore the bottom part of the existing mesh was cut to level with the chosen measuring station: 8635750 Lewisetta, VA.

The element size of the existing mesh were considered applicable to the research needed, therefore a size function called 'Gridspacing' was used in order to keep the same element size for the model. This led to elements of the new mesh having a size between 20 to 700m. The creation of the new mesh was done in UTM projection, zone 18 (78W - 72W - Northern Hemisphere), datum NAD83, planar units meter. All meshing was done in an irregular triangulation.

Figure 3.2: Existing mesh with wider region

Figure 3.3: Adjusted mesh with region of interest

The elevation of the new mesh was defined using the same technique as the one used to find the elements sizes: using a size function containing the elevations of the existing mesh (see figure 3.4). This led to a mesh with as minimum elevation 30.29m and as maximum elevation -101.43m, elevations in ADCIRC are positive downwards and negative upwards.

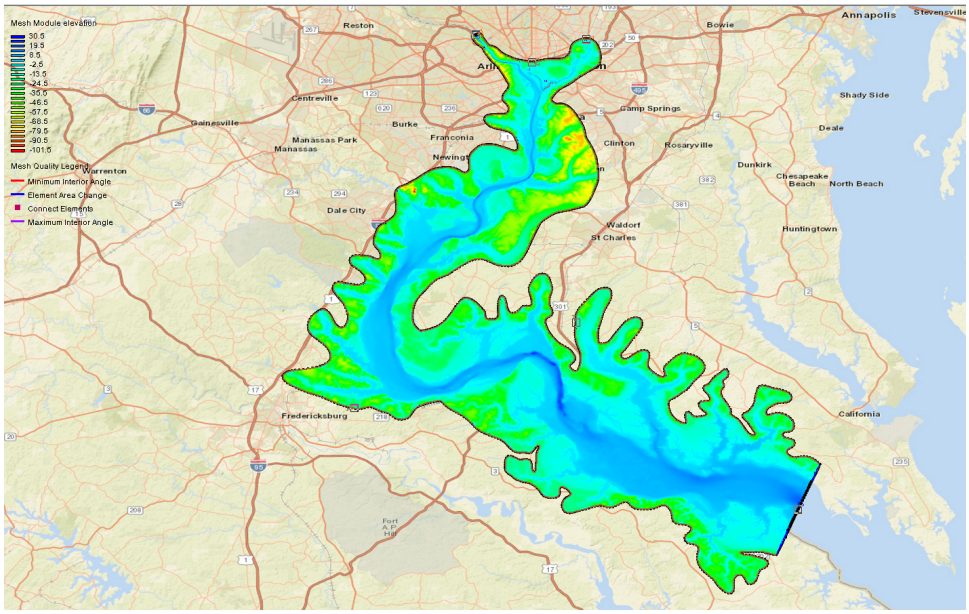

Figure 3.4: Elevation of the model

The existing mesh didn't contain any levees, in order to add them the newly created mesh needed some refining. The first step was to cut out the nodes and elements of the mesh around the levees. The nodes around the hole created were then converted to nodestrings and the mesh was converted to a map. In the map arcs were placed to represent the existing levees in the Washington Mall and near the Anacostia river. A total of 2 levees were placed and 2 temporary flood defences, see figure 3.5. Finally, polygons were created in regions containing the levees which was needed to convert the map back to a mesh. The elevation of these polygons were set to the same elevation as the previous mesh using a size function and the element size was set to 'Paving'. The map was then converted back into a mesh which contained only the levees.

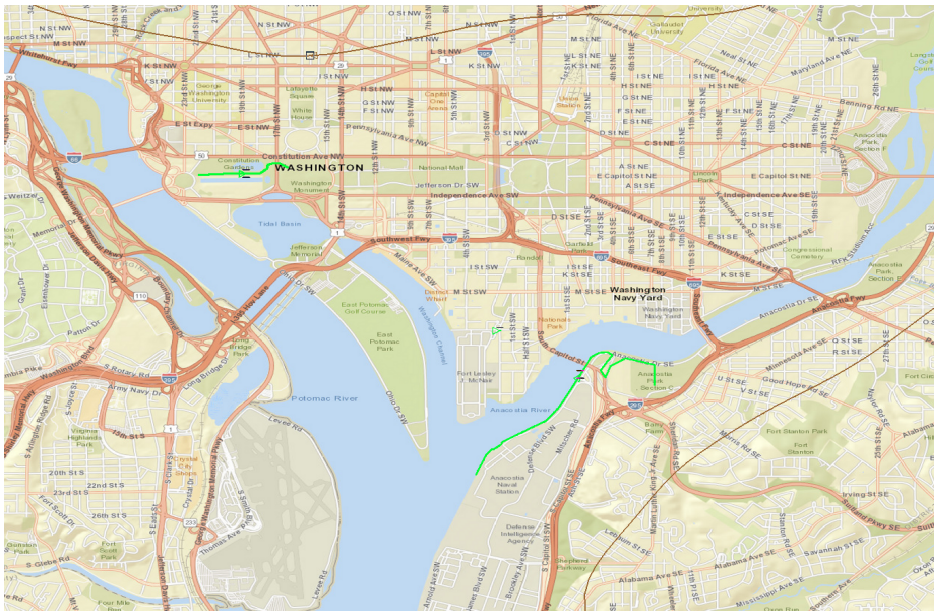

Figure 3.5: Bathymetry of the region

Due to the steep slope required to accurately model the levees, a grid spacing of approximately 5m was chosen. This fine grid spacing was chosen in order to model the dikes accurately: Due to their small width, approximately 8m, an equal or smaller grid spacing was needed to model the flow around the levees. This

was required due to the high gradients which could not be computed on a coarse grid.

The mesh containing the holes and the newly created mesh, containing exclusively the levees, were then merged in order to obtain the final mesh. The heights of the levee were then inserted according to data from the National levee database, see appendix C.

The final mesh contained the following:

- Number of elements: 981037;
- Number of nodes: 492399;
- Element type: linear;
- Number of triangular elements: 981037.

All the information created in this mesh was stored by ADCIRC in a file called fort.14. This file contained all the grid spacing and elevation information of the mesh. In order to finalize the mesh more information had to be establish, which will be explained in the following sub sections.

3.2.1. Boundary Type

The boundary conditions are essential to run a simulation, many boundary types exist in ADCIRC, for this research only 4 were needed:

- Mainland;
- Normal flow;
- Ocean;
- Island barrier.

Boundaries were represented by nodestrings in the mesh. The 'Mainland' boundaries were set all around the computational domain where land was present. This boundary type allowed the model to know that no water could flow pass this point and information about this boundary was stored in the fort.14 files.

The normal flow boundaries represented the Potomac and Anacostia rivers, their flow were set as 'Non-Periodic'. The discharge data for these boundaries were added by creating a hydrograph to represent heavy discharges characterizing a 1/100 flood, see section 2.4. Information about these boundaries were stored in a fort.20 file.

The Ocean boundary downstream was set to 'Ocean' and the option 'Specify single curve' was used to insert data characterizing the 1/100 flood. Information about this boundary was stored in a fort.19 file.

Finally, the nodestrings representing the dikes were set with a boundary condition of 'Island Barrier', this according to the SMS user manual (SMS, 2018) represents levees that are situated inside the computational domain. A non-zero flow is then assumed if the barrier is not over-topped and a normal flow is computed using either sub-critical or super-critical (free surface weir formula based on the water level on both sides of the barrier) if the barrier is over-topped. The height of the levees had to be inserted as positive numbers in ADCIRC.

3.2.2. Quality check

Once the mesh was created and its boundaries defined, the quality of the model needed to be inspected in order to avoid instabilities and for the model to run accurately. In general, for a mesh to function it is important that the following requirements are met (SMS, 2018):

- There cannot be overlapping elements;
- No disjointed vertices are allowed;
- The boundary of the mesh must be continuous;
- The vertices are numbered in counterclockwise manner.

These requirements are necessary for ADCIRC models to run, however errors can occur if no attention is paid to the size change of two neighbouring triangles. A decent measure was to assume a maximum area change of 0.5 times the area of the first triangle. Additionally the angles of the internal corners of the triangles cannot be too large or too small. A common practice is to use triangles with angles ranging from 10° to 150°, that way no too large errors are produced.

For this specific model the following conditions were met:

- Minimum interior angle: 10.0° ;
- Maximum interior angle: 130.0° ;
- Element area change: 0.5;
- Connecting elements: 8.

The connecting element conditions refers to the number of elements connected to one node, for this model each node did not connect more than 7 elements.

The mesh created now contained the dikes and approximately half a million nodes. This high number of nodes was especially due to the high definition that was needed around the dikes to have an accurate representation of the flow around the area of interest. However in other to run this mesh, some more parameters were needed.

3.3. ADCIRC model control

For ADCIRC to run a simulation it needs to create a control file (fort.15) that contains all the needed parameters to simulate the flow around Wahsinton DC. Another file containing parameters used by ADCIRC is the fort.13 which contains approximately the same parameters but with spatially varying values, in contrast to the fort.15 file which strictly contains constant values. The fort.13 file was not created for this simulation due to time restriction.

The fort.15 file is mandatory to run a model but the fort.13 file is not however it does make the simulation more stable and more realistic. Therefore, it is advise to create this file for future runs with this model.

3.3.1. Hydraulic conditions

In order to solve the equations a number of information about the area is required; such as the bathymetry, bottom friction coefficient and horizontal eddy viscosity. The bathymetry was given in the previously existing mesh. The other parameters were found using equations and literature studies.

Bottom friction

The bottom friction in the momentum equations is approximated using equation 3.4:

$$\frac{\tau_{bx}}{\rho_0} = K_{slip} U \frac{\tau_{by}}{\rho_0} = K_{slip} V \tag{3.4}$$

Where the drag coefficient K_{slip} can be a constant or approximated quadratically using equation 3.5:

$$K_{slip} = C_D \sqrt{U^2 + V^2} \tag{3.5}$$

For this research the quadratic approximation was used with a quadratic drag coefficient C_D of magnitude 0.0025. Another possibility was to overwrite this function to provide a Manning coefficient for every node in order to determine the bottom friction. This would have given more realistic results, due to the high variability in ground cover.

Closure assumption

Because the turbulent fluctuation in the flow cannot be computed directly for the model a closure assumption must be made to approximate the lateral stresses. The expression used by ADCIRC is given in Eq. 3.6.

$$H\tau_{i,j} = E_h \left[\frac{\partial Q_j}{\partial i} + \frac{\partial Q_i}{\partial j} \right]; i = x, y; j = x, y \tag{3.6}$$

Where the horizontal eddy viscosity E_h has a value of 10 m^2/s in meandering coastal estuaries according to (Colbo, 2005).

Weighting factor GWCE
In the generalized wave continuïty equation (GWCE) the τ_0 value determines the amount in which continuïty is taken into account. When τ_0 is 0, no contnuïty is used in the calculation, when τ_0 is 1, the full continuïty is included in the calculations. For the derivation of the GWCE see appendix B the derivations are based on Luettich and Westerink. Typical values of τ_0 are between 0.005 and 0.1, the first 0.005 being the standard value in ADCIRC (Cheryl Ann Blain, Robert S. Linzell, Philip Chu, 2010). A rule of thumb to use for this parameter is τ_0 is 1 to 10 time the quadratic drag coefficient C_D. Like the bottom friction τ_0 can be spatially varying.

With the parameters proper to the region established, other parameters are needed to ensure the stability of the simulation.

3.3.2. Stability

The stability of a model is essential in order to get results. However it can often happen that simulation are unstable and many explanations can be found for this. Here are of few parameters that could lead to instabilities.

Time step

To ensure stability the time step of a simulation should comply with the CFL condition. Which implies that numerical information should not travel faster than real information. For the CFL condition to be upheld the Courant number should be smaller than 1, Cr<1. On a triangular grid the Courant number is defined in Eq. 3.7 (Roberts and Pringle, 2018).

$$Cr = \frac{(|u| + \sqrt{gh}) * \Delta t}{f_0} < 1 \tag{3.7}$$

Where f_0 defines the diameter of largest circle fitting inside the triangle. The smallest inner diameter in the mesh is approximately 5 meters. Based on the area of the smallest mesh element and assuming it to be equilateral. The largest expected celerity is 10 m/s, based on a maximum height of 10 meters. The flow velocity is assumed to be 2 m/s at most. The resulting time step is found in Eq. 3.7.

$$\Delta t < \frac{f_0}{(|u| + \sqrt{gh})} = \frac{5}{12} = 0.42s \tag{3.8}$$

Simulations made with ADCIRC can have even stricter regulations of Cr « 0.1, if the simulation includes barrier islands, constricted inlets, or wetting and drying of near-shore elements, (Cheryl Ann Blain, Robert S. Linzell, Philip Chu, 2010). Therefore:

$$\Delta t < \frac{0,1 * f_0}{(|u| + \sqrt{gh})} = \frac{0,5}{12} = 0.04s \tag{3.9}$$

For this research a time step of 0,04s or smaller was needed. Smaller time step would increase the accuracy of the simulation but would also increase the time needed to simulate. Therefore, due to the lack of time, decreasing the time step was not advised and increasing it was preferred keeping in mind that it could lead to instabilities.

Wetting and Drying

Another important phenomenon that can lead to instabilities in ADCIRC even with the CFL condition met, are instabilities due to the wetting and drying attribute of the model. These instabilities occur especially during highly non linear events (J.C. Dietrich and Luettich). The wetting and drying algorithm determines whether elements should be included in the calculations or not.

If all three nodes of an element are wet, the element is considered wet and the element is taken into account in the calculations. If two nodes are wet and one is dry, the elevation of the wet nodes determines whether the dry node is artificially made wet, and thus the element. For this to occur, the water level must be $1.2 * H_0$ in which H_0 is a parameter specified in the model and typically is smaller than 0.1 meters (Blain et al., 2010, Dietrich et al., 2004). Additionally the velocity should be sufficient to wet the element, however since this has no influence on the stability of the model (Dietrich et al., 2004), it will not be further explained.

For drying to occur the element must have an elevation smaller than or equal to $0.8 * H_0$. If a node is dried the water level of that node artificially remains $0.8 * H_0$ (Dietrich et al., 2006), this may lead to instabilities if the node is immediately wet again. To prevent these instabilities a minimum number of time steps is

included in the model where an element can not get wet again. However this is not always enough and the value of H_0 and U_0 sometimes need to be adapted.

Parameters of direct relevance to the wetting and drying condition are the minimum water level (H_0) and minimum velocity (U_0) at which wetting and drying start. For ADCIRC both have a standard value of 0.05m and 0.05 m^2/s respectively.

3.3.3. Projection

The projection used for this simulation was a Geographic (Latitude/Longitude) projection with horizontal datum NAD83 and a planar Units of Arc Degrees. The horizontal datum NAD83 is only applicable in the United States and is proper to the area around the District of Columbia. The vertical datum used for the bathymetry of the model was NAVD88 with meters as units. However, at the tidal boundary the vertical datum used was the tidal datum with mean sea level as reference. Having a wrong projection or inconsistent projection references could also lead to instabilities.

With the parameters characterizing the region and those insuring stability found, ADCIRC was ready to run the model. All runs were computed without taking into account wind or sediment transport. Only the river discharges and the tide found in 2.4 were set as input parameters.

3.4. Stampede2

Many platforms exist to run ADCIRC models, this can be done in SMS, in python notebook or on a super computer. Due to the very high number of nodes the model was too heavy to run in SMS or python, therefore a platform called 'Stampede2' which represented a supercomputer was used.

Stampede2 is the flagship supercomputer at the Texas Advanced Computing Center (TACC) which is accessible at George Mason University and used by many other universities and many companies. Therefore, for each job submitted, a waiting time restricted considerably the amount of simulations that could be made. The waiting time in stampede2 was related to the number of job submitted and the length of the simulation. New users and low time consuming jobs had priority over others. For this reason it was chosen to model not more than 2days of simulation due to the time restriction of this project. In the future it is encourage to run longer simulations.

The graphical interfaces used to access stampede2 were winSPC and Putty. The first was used to visualize the files and the work sent. The second was the interface used to submit jobs, see appendix D for more information about the supercomputer used.

4

Soil Conditions

4.1. Design method

4.1.1. Geometry

The new flood protections for Washington DC were designed based on the return periods previously discussed. The normative water height for a 1/100 year flood and a $1/p_{opt}$ was obtained like previously discussed. The levees were designed to last at least 50 years, which means that a sea level rise of 50 years should be added to the return period water level. This is equivalent to a height of 0.15m. To account for wave overtopping, 1.25 m will be added on top of the design water level. The levee geometry will be decided based on the US guidelines (CIRIA, 2013), dictating a slope of 1:3 and a crest width of at least 6m.

4.1.2. Settlements

The settlements will be normative for the final levee height. It is therefore necessary to try to estimate these.

The settlements of a layer are dependent on the increase in stress in a layer due to an increase in load. The increase in stress at a specific depth under half an embankment due to the construction of an embankment was proposed by (Osterberg, 1957).

$$\Delta\sigma(z) = 2 * I(z) * \Delta\sigma \tag{4.1}$$

Where: σ: the total increase in stress due to the embankment construction. I(z) [-]: the coefficient of influence. Figure 4.1 shows I is based on a[m] the width of slope base and b[m] width of half levee crest

The total settlements of a soft soil due to an increase in load can be separated in 3: the instantaneous elastic undrained deformation of a soil, the primary compression due to consolidation (dissipation of excess pore pressures) and the secondary settlements, or creep. Elastic settlements in drained layers will be disregarded, meaning that sandy layers will be considered incompressible.

$$w_t = w_i + w_p + w_c \tag{4.2}$$

Where:
w_t [m]: total settlements
w_i [m]:instantaneous elastic undrained settlements
w_c [m]:settlements due to consolidation (or primary settlements
w_s [m]:settlements due to creep (or secondary settlements)

The instantaneous undrained settlements occur immediately after loading and depend on the undrained elasticity of the soil. These settlements were induced by deformation without volume loss, meaning that the soil will settle under the levee but heave next to it. These settlements can be approximated with elasticity theory.

$$w_i = \frac{\Delta\sigma}{E_u} * I \tag{4.3}$$

Where:

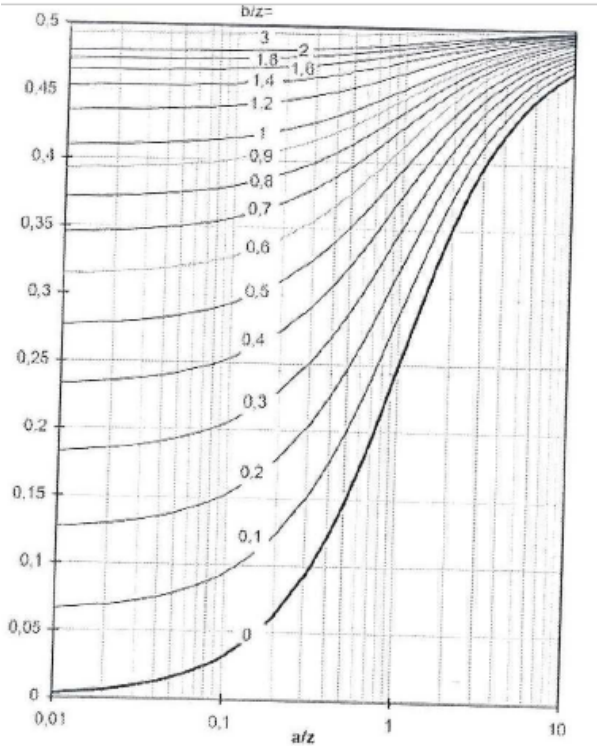

Figure 4.1: Determination of coefficient of influence for stress increase under an embankment at specific depth (Osterberg, 1957)

I[-] Influence factor
$\Delta\sigma$ [-]: vertical stress increment at the surface of the soil foundation
E_u[kPa]: elastic modulus of compressible soil for undrained condition

The influence factor for the initial undrained settlements can be estimated based on (Giroud, 1973) as can be seen in Figure 4.2.

Primary settlements are induced by the dissipation of the excess pore pressure. The method to compute primary settlements was developed by Terzaghi and is formulated in Eq. 4.4.

$$w_{c-inf} = \frac{H0}{1+e_0} * C_c * log\frac{\sigma'_{v0}+\Delta\sigma}{\sigma'_{v0}} \tag{4.4}$$

Where: H0[m]: Initial thickness of compressed layer e0[-]: Initial void ratio Cc[-]: Primary compression coefficient

Creep is a settlement of soft soils due to an increase in load that is infinite. For clayley and organic soils it can lead to big settlements over time. In contrary to primary compression creep is independent of the load increase, and is only dependent on the reference time at which it starts. Usually it is assumed that creep starts occurring after 90 percent of consolidation has happened. The creep settlements is expressed in Eq. 4.5.

$$w_{c-inf} = \frac{H0}{1+e_1} * C_\alpha * log\frac{t}{t_{ref}} \tag{4.5}$$

4.1.3. Stability

The stability of the levees will be assessed with the Slope-W software. The Morgenstine-Price slice method will be used to check the stability against rotational failure of the levee.

4.2. Lithography

In order to be design the levees and predict their stability and settlements knowledge of the subsurface is required. In absence of a national subsurface database the designs will be based on parameter correlation

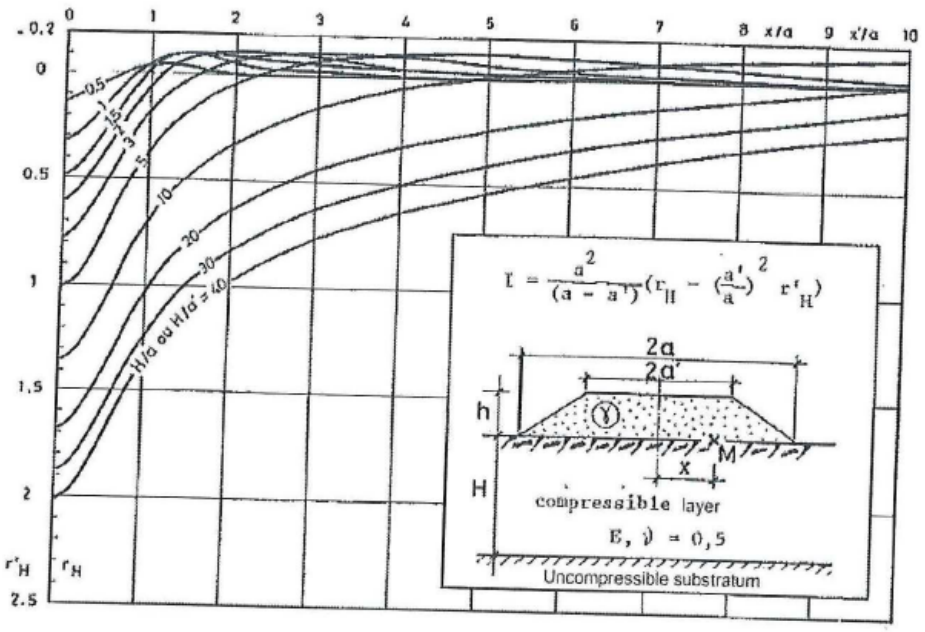

Figure 4.2: Determination of coefficient of influence for instantaneous settlements (Giroud, 1973)

from different sources like geological history, private soil investigations and data estimation based on Table 2b from Eurocode 7 presented in Appendix **??**.

4.2.1. Geological context

Little data of the subsurface is available to the public, as most of it is privately owned. This means that a assumptions will need to be made in order to estimate soil parameters. The geological context of the region will help to provide some insight. This information can be found from SSURGO database.

The area of interest for the design of levees is located at the Anacostia and Potomac river banks. From Appendix I it can be be noted that the top layer along the river banks is composed of alluvium and artificial fills, or in some cases river terrace deposits. This means that alternate layers of sand, silt and clay can be expected. This lithography is similar to that of the western part of the Netherlands, so Eurocode 7 can be used to approximate data values that are lacking. From Appendix I it is found that each layer can be up to 10 m thick above the bedrock, which is in the order of magnitude of the influence zone for the levee design.

4.2.2. Available private boreholes

Two geotechnical reports were found as source for the lithography at the site of the existing National Mall levee and Anacostia bank levee. The geotechnical report used as base for the National Mall levee was provided by Froehling & Robertson, Inc for the "NAMA Rehabilitate Potable Water Lines" project led by CH2M Hill (Froehling Robertson, 2014). The report that was chosen as base for the Anacostia bank levee was provided by ECS Mid-Atlantic LTD for the project "Kingman Island improvement" led by LEE + PAPA AND ASSOCIATES (ECS-Midatlantic-LTD, 2009). Both the geotechnical reports contain borehole information and the Atterberg limits of the clays and silts present in the boreholes. No information on the void ratio or the compressibility is however provided, so educated guesses will be made based on the state of the soil and Eurocode 7.

14 Boreholes were available for the Kingman Island improvement project. The summary of the lithography found in each borehole is presented in Appendix K. For ease of design it was decided only to chose one borehole as reference soil conditions for the design of the embankment of the Anacostia bank. Since the boreholes are not at the exact location of the Anacostia bank levee the poorest soil conditions can be chosen in order to get the safest design possible. A better approach would have been to investigate the exact soil conditions on site, but this was not an option considering the time frame. It can be noted that in the boreholes

the top soil layers are composed of a fill. This is not a good representation of the location of the site of interest, therefore one parameter to chose the normative borehole will be the size of the fill. The soil conditions that are the poorest, in combination with the smallest fill seem to be at the location of borehole ECS9. This will therefore be the normative borehole to design the levees on the Anacostia Bank. The level that will be used as reference for the toe level is +0m NAVD 88 instead of the borehole groundtable level. This is because the levee is directly adjacent to the river.

From the "Nama Rehabilitate Potable Water Lines" project 10 boreholes close to the National Mall levee were provided. From these two were in alignment with the levee location, boreholes 3 and 7. They can be found in Appendix K. Borehole 3 shows a more sandy subsurface than borehole 7, however it can be noted that the top 3.5 feet are composed of a fill. This fill is probably the levee that is already in place. Even when discarding this top layer of silt, the subsurface at borehole 7 still seems softer than at borehole 3 which is has more gravel and sand. Borehole 7 is therefore chosen as normative design for the National Mall levee. Note should be taken that the National Levee database states that the toe of the levee has an elevation of +2m NAVD88. This level will be used as reference level for the levee design instead of the borehole ground table elevation.

4.2.3. Groundwater conditions

The groundwater conditions are important to determine the stress conditions in the soil. The groundwater table that was encountered at the different locations can be found from the boreholes. For the National Mall location a GWT of 5.9 m below the surface was found, while for the Anacostia bank location a GWT of 7.6 m below the surface was encountered.

The boreholes indicated that the layers of silt above the GWT were moist. This could be an indication of capillary rise. Capillary rise would lead to suction pore pressures, inducing an enhanced effective stress in the soil. It is therefore of importance to estimate whether the wetness of the soil is due to capillary rise. The capillary rise in a porous medium can be expressed with Jurin's Law, Eq. 4.6.

$$h_c = \frac{2\gamma cos\theta_r}{\rho g r} \tag{4.6}$$

Where:

γ the surface tension of water = $71.9 * 10^{-3}$ [N/m]

θ_r the receding contact angle = 32 deg for Silts (Bachmann et al., 2010)

ρ the density of water = 1000 [kg/m3]

g the acceleration of gravity = 9.81 [m/s2]

r the radius of the pores = d/6 with d the diameter of grains (Azouni et al., 1957)

The layers above the GWT are composed of silt. The diameter of silt grains vary between $2 * 10^{-6}$ and $6.3 * 10^{-5}$ m. With this range a capillary rise range of 37.3m to 1.18 m would be present. Seeing as all the layers are described as moist and no further information on the grain size diameter is present, it will be assumed that the silt layers are saturated due to capillary rise.

A summary of the assumed soil lithography and groundwater conditions at the location of the National Mall levee and the Anacostia bank levee can be found in Figure 4.4 and 4.5.

4.3. Soil parameter correlation

In order to design the levees soil parameters like density, compressiblity, hydraulic conductivity, friction angle and preconsolidation pressure are required. Some of these will provide an estimation for the DSS undrained shear strength which is needed for the stability calculation.

Whenever available the parameter correlation will mostly depend on the Atterberg limits. The different methods of correlations will be compared to get an overview of which method can be deemeed the most trustworthy. The Atterberg limits are often expressed in Plasticity Index PI and Liquidity Index LI. These are expressed respectively in Eq. 4.7 and 4.8.

$$PI = LL - PL \tag{4.7}$$

$$LI = \frac{w - PL}{PI} \tag{4.8}$$

If these are not available the SPT N number of blows will be used for the estimation of strength properties. As last resort the table 2b from Eurocode 7 will be used, based on the lithography description from the boreholes. A summary of the different soil parameters required, and how they will be correlated to each other is provided in table 4.1.

Table 4.1: Summary of the required soil data their correlation

Parameter searched	Correlated parameters	Source
Unit weight γ	-	Eurocode 7
Specific gravity GS	-	(ASTMD85492, 2013)
Preconsolidation pressure σ_p'	Atterberg Limits, GS, γ	(Kootahi and Mayne, 2016)
Primary compression coefficient Cc	LL	(US.Army.Corps, 2000) or EC7
Secondary compression coefficient Cα	Cc	(Mesri and Godlewski, 1977)
Horizontal hydraulic conductivity k_h	D10	(US.Army.Corps, 2000) or (str)
Initial void ratio e0	Borehole description	(association of Swiss Road and traffic Engineers)
Initial void ratio e0	w	State relations
Coefficient of consolidation Cv	Atterberg limits	(Carrier, 1985)
Undrained shear strength Cu	OCR(σ_p')	(Ladd et al., 1977)
Undrained shear strength Cu	LL	(Gavin)
Undrained shear strength Cu	N60	(Clayton, 1985)
Effective friction angle ϕ'	N60	(Brown and Hettiarachchi, 2008)

A summary of the lithography at the 2 sites with each correlated parameter for the specific layers will be provided in Figures 4.4 and 4.5.

4.3.1. Density and specific gravity

The density of the different soil layers is required to establish the stress level. These are unfortunately not measured from the boreholes, and will therefore need to be estimated based on the layer description of the boreholes and Eurocode 7. The specific gravity of the grains is required in case the Atterberg limits of a layer are known. With the specific gravity, and the Atterberg limits an estimation of the preconsolidation pressure can be provided in the absence of an Oedometer test. (ASTMD85492, 2013)

For the National Mall MH layers a specific gravity of 2.65 was chosen while for the Anacostia bank ML layer 2.7 and CL 2.75 were chosen.

Preconsolidation pressure

The preconsolidation is of great importance to provide an idea of the stress state of a soil when loaded. For the design of a levee specifically it implies that loading until the preconsolidation pressure will lead to a reloading stress path, with consequences for the coefficient of compression and therefore the estimation of the final settlements. The preconsolidation pressure can also be of importance for the estimation of the undrained shear strength of a layer, as will be showed in the paragraph on undrained shear strength estimation.

The preconsolidation can be estimated based on the Atterberg limits and the effective stress in the soil (Kootahi and Mayne, 2016). The relation between the preconsolidation pressure σ'_p and the Atterberg limits

are expressed as in Eq. 4.9 and 4.10.

If DS>1.123

$$\frac{\sigma'_p}{p_a} = 1.62 * (\frac{\sigma'_{vo}}{p_a})^{0.89} * (LL)^{0.12} * (w)^{-0.14} \tag{4.9}$$

If DS<1.123

$$\frac{\sigma'_p}{p_a} = 7.94 * (\frac{\sigma'_{vo}}{p_a})^{0.71} * (LL)^{0.53} * (w)^{-0.714} \tag{4.10}$$

With DS being the Descriminant Factor being expressed as a function of the Atterberg limits and the Specific Gravity presented in Eq. 4.11.

$$DS = 5.152 * log_{10}(\frac{\sigma'_{vo}}{p_a}) - 0.061 * (LL) - 0.093 * (PL) + 0.0622 * GS * w_n \tag{4.11}$$

4.3.2. Hydraulic conductivity

The horizontal hydraulic conductivity of a layer can be approximated based in the D10 grain size diameter (US.Army.Corps, 2000). The sieves present in the geotechnical studies unfortunately do not show a fine enough passing percentage to get the D10 value. This means that values for the horizontal hydraulic conductivity will be assumed based on (str).

The hydraulic conductivity is of importance for the testing of the piping condition. If the layer under the levee is highly permeable, a risk of uplift can be present, leading to piping. A general relationship between horizontal and vertical hydraulic conductivity will be used, where:

$$k_h = 10 * k_v \tag{4.12}$$

4.3.3. Initial void ratio

The initial void ratio of the subsurface is of great importance to the estimation of the final settlements. With the assumption of full saturation due to capillary rise and the estimation of specific weight of grains the void ratio can be written as:

$$e_0 = w * Gs \tag{4.13}$$

In the absence of soil data about the compaction type assumptions will need to be made. (**?**). The state of the soil is described in the boreholes. In combination with the range of void ratio for each type of soil this provides an estimation of the initial void ratio that could be used to predict the settlements.

A summary of the void ratio range for the soil types present in the boreholes is presented in table 4.2

Table 4.2: Range of void ratio for different soil types (str)

Soil type	emin	emax
SM	0.33	0.98
ML	0.26	1.28
MH	1.14	2.10
SP	0.30	0.75
SC	0.17	0.59
CL	0.41	0.69

4.3.4. Compression Coefficients

Three compression coefficients are of need to predict the settlements of the levee to be constructed. The primary compression coefficient Cc that deals with the consolidation of a low permeability soil under an applied load, the secondary compression coefficient that deals with creep, and the unloading/reloading coefficient that is of importance to predict the settlements during the reloading phase of an over consolidated soft soil.

Where possible, the compression coefficients will be correlated to the liquid limit instead of through the Eurocode 7, as the latter also depends on the estimation of the initial void ratio, leading to a double estimation.

The primary compression coefficient Cc was correlated to the Liquid Limit LL (US.Army.Corps, 2000). This correlation relies on normally consolidated clays, which may lead to overestimation of the settlements in case over over consolidated soils. Figure 4.3 shows the relation between the primary consolidation ratio and the Liquid Limit.

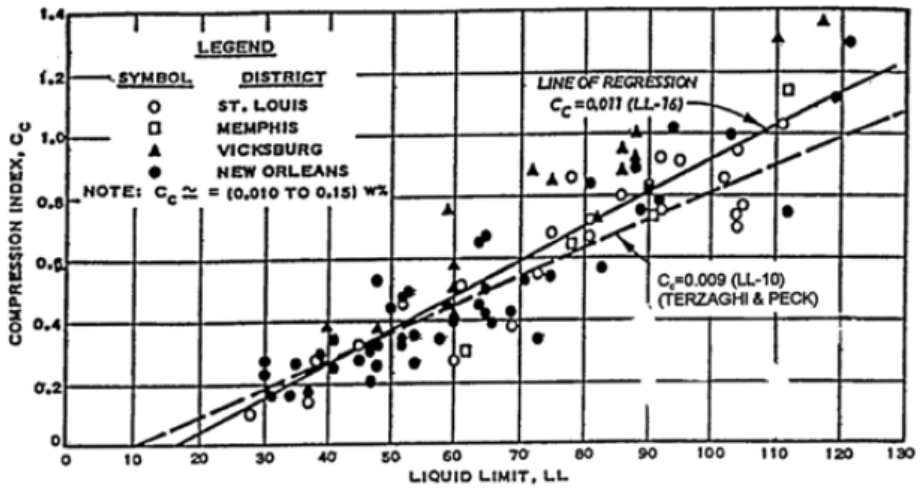

Figure 4.3: Correlation between Liquid Limit and the Primary compression coefficient of normally consolidated clays (US.Army.Corps, 2000)

The secondary compression coefficient that can be estimated as being a fraction of the primary compression coefficient. For clays and silts the ratio C_α/Cc is typically 0.05 (Mesri and Godlewski, 1977).

The unloading-reloading coefficient is more difficult to predict. It would usually be found based on the ratio between the change in pressure and change in void ratio in the loading until preconsolidation phase of an Oedometer test. Since this test is not available and no information is available on the void ratio the unloading-reloading coefficient needs to be assumed from Eurocode 7 (Figure L.1).

4.3.5. Coefficient of consolidation

The coefficient of consolidation is required to determine the rate of consolidation. This is necessary in case the constructor wants a certain percentage of settlements to have taken place after a handover, or to provide an estimation of creep settlements. In this report there is no restriction on the amount of settlement after handover, however it is necessary to remain on the safe side with the amount of settlement.

(Carrier, 1985) showed a relation between the coefficient of consolidation with the Atterberg limits and the activity of clays. The activity of a clay is defined as the ratio of the Plasticity Index and the percentage of clay particles (0.002 mm). The relation is expressed with Eq. 4.14.

$$Cv = \frac{9.09 * 10^{-7}(1.192 + ACT^{-1})^{6.993}(4.135LI + 1)^{4.29}}{PI(2.03LI + 1.192 + ACT^{-1})^{7.993}} \tag{4.14}$$

The sieve tests provided in the reports do not provide the percentage of clay particles, so it is impossible to calculate the activity of the clay. A high coefficient of consolidation leads to a lower consolidation time. Since it is assumed that creep starts after 90 percent of consolidation occurred, a high coefficient of consolidation will induce more creep settlements. Activity of clays usually varies between 0.75 and 1.25. a low value of activity leads to a higher coefficient of consolidation according to the relation above. The goal of this design is to provide a safe value of total settlements, therefore A=0.75 will be assumed for the estimation of Cv. Compressible layers that do not have Atterberg limits data (like the National Mall boreholes) will be assumed to have the same coefficient of consolidation as the layer that is provided with data.

4.3.6. Undrained shear strength

The critical loading type for a levee is often the construction phase, because the loads are applied fast compared to the hydrodynamic period of the fine grained soils, resulting in a reduced effective stress of the sub-

layers. In order to check the stability of levees a measure of the undrained shear strength of fine grained soils like clays and silts should therefore be provided. The undrainded shear strength is not a soil parameter. It is dependent in the method of testing, loading rate, stress history and sample extraction. The unconsolidated undrained shear strength in a triaxial apparatus can be approximated with different methods. Where possible these results will be compared in order to get a single value for each fine grained layer.

A direct measurement of the undrained shear strength was provided with the readings of the pocket penetrometer. With no confining pressure σ'_3 the stress read from the penetrometer is purely deviatoric„ with as reading σ'_1. This implies that the undrained shear strength, being the radius of the Mohr circle is equal to half of the value read from the pocket penetrometer. This value should be used with care since it is taken after the borehole was extracted. This means that the soil was no longer under confinement when the test was performed, which influences the undrained shear strength. Note should be taken that the values of pocket pen given in Figure K.7 are in TSF, with 1 TSF = 95.76 kPa.

$$Cu = \frac{\sigma_{penetrometer}}{2} \tag{4.15}$$

A correlation between the undrained shear strength and the normalized number of blows N_{60} (Clayton, 1985) will be used as reference when no other data is available. A summary of the correlation between the two parameters is presented in Figure 4.3

Table 4.3: Correlation between the undrained shear strength and the normalized SPT number of blows N60 (Clayton, 1985)

Undrained shear strength	**Cu [kPa]**	**SPT N60 value**
Extremely/very low	<10 to 20	0 to 4
Low	20 to 40	4 to 8
Medium	40 to 75	8 to 15
High	75 to 150	15 to 30
Very High	150 to 300	30 to 60
Extremely High	>300	>60

As previously discussed the over consolidation ratio can be estimated in the layers where the Atterberg limits were established. (Ladd et al., 1977) proposed a relation between the effective stress in a layer, the OCR and the undrained shear strength. The OCR being defined as the ratio between preconsolidation pressure and the effective stress.

$$c_u = \sigma'_v * 0.3 * OCR^0.8 \tag{4.16}$$

The last correlation that will be used as a reference will be between the Liquid index and the undrained shear strength which is shown in Eq. 4.17 (Gavin).

$$c_u = 2 * 100^{(1-LI)} \tag{4.17}$$

4.3.7. Effective friction angle

The drained shear strength for cohesionless soils can be estimated with the effective friction angle. (Brown and Hettiarachchi, 2008) proposed a conservative approach to estimate the effective friction angle from the SPT number of blows based on an energy balance method, as shown in Eq. 4.18. This method approached the SPT as a pile driving technique, and provided good results for the effective friction angle estimation.

$$\phi' = 0.3818 * tan^{-1}(0.25N_{60} * \frac{p_a}{\sigma'}) \tag{4.18}$$

Assumptions and results

An estimation of the different soil parameters and methods is provided in Figure 4.4 and 4.5. Where possible the different methods for the estimation of the undrained shear strength were compared to the values provided in the Eurocode 7. The final values chosen can be found highlighted in green. Correlation of effective friction angle with respect to N60 value was always preferred over EC7 friction angle, as this correlation was proven quite strong. Correlation with Liquid Limit for the primary compression coefficient was also preferred over EC7, because EC7 also relies on a estimation of initial void ratio, thereby increasing the estimation error.

In the MH an ML layers of the National Mall the N-value was extremely low, implying a layer that is extremely soft. In the deepest layer the layer did not provide enough resistance against the hammer blow, leading to a punchthrough.This means that the values for undrained shear strength were underestimated with that method. The OCR method gave values that were too big in comparison with the other methods, implying that that either the density was wrongly estimated, or the prediction of the Preconsolidation pressure may have been faulty. The Liquidity Index correlation also provide values that seemed extremely small for the type of soil on which the Atterberg limits were tested. For the National Mall location the pocket penetration test values were therefore chosen when available, for they were in a realistic range for the undrained shear strength of the layers.

For the Anacostia bank the ML layer presented undrained shear strength results in the same order of magnitude for the OCR and SPT method as the EC7. To remain consistent with the method for the National Mall it was therefor chosen to take the SPT method for the undrained shear strength. The bottom layer presented contradictory results. All the methods except the Liquid Limit correlation presented high values for undrained shear strength. It would appear that the SPT method overestimated the undrained shear strength due to the sand mixed in the layer. The Liquidity Index correlation providing results so different from the other 3, it was chosen not to rely on that one. As the EC7 gave a result that was halfway through the OCR and SPT correlation values, it was chosen to fall back on that value for the undrained shear strength of the bottom layer.

The subsurface around the region has a lot of silt. It will therefore be assumed that the levee itself will be made from the ML layer material at the location of the National Mall levee.

	Main Layer Comp.	Sec Layer Comp.	Layer Descripition	EC7 Description	γ (1) [kN/m3]	N [-]	N60 [-]	LL [%]	PL [%]	w [%]	σ'(p) [kPA]	OCR [-]	Cu(1) [kPa]	Cu(2) [kPa]	Cu(3) [kPa]	Cu(4) [kPa]	Cu(6) [kPa]	φ'(1) [°]	φ'(2) [°]	e0 [-] (7) (8)	Cc(1) (5)	Cα	kh [m/s]	cv [m2/s]
0 m																								
	SM		FILL: Brown, silty SAND with gravel, medium dense, moist	Strong silty Sand	19	12	17	NA	NA	n.d.	n.d.	n.d.	NA	NA	n.d.	n.d.	NA	30	34	0.5 (7)	0.0087 (1)	0.000435	5*10^(-7)	
1.2 m																								NA
	ML		Gray, sandy SILT, trace gravel, firm, moist	Strong sandy loam	19	6	9	n.d.	n.d.	n.d.	n.d.	n.d.	50	40	n.d.	n.d.	ND	NA	NA	0.5 (7)	0.0766 (1)	0.00383	1*10^(-8)	
1.8 m																								n.d.
	MH		Gray, ELASTIC SILT, contains wood fragments, very soft,	Soft loam	19	2	3	n.d.	n.d.	n.d.	n.d.	n.d.	50	10	n.d.	n.d.	ND	NA	NA	2 (7)	0.276 (1)	0.0138	1*10^(-9)	
2.4 m																								n.d.
	ML		Gray, SILT, contains wood fragments, very soft, moist	Soft loam	19	2	3	49	29	44	356	5.24	50	10	79	6.32	23.94	NA	NA	1.2 (7) 1.2 (8)	0.2024(1) 0.38(5)	0.019	1*10^(-9)	
3.0 m																								2E-08
	MH		Gray, ELASTIC SILT, contains wood fragments, very soft, moist	Soft loam	19	1	2	n.d.	n.d.	n.d.	n.d.	n.d.	50	5	n.d.	n.d.	35.91	NA	NA	2 (7)	0.276 (1)	0.0138	1*10^(-9)	
4.9 m																								n.d.
5.5 m	SM		Dark gray, silty SAND, very loose, moist	Strong silty Sand	18	2	3	NA	NA	n.d.	n.d.	n.d.	NA	NA	n.d.	n.d.	NA	25	14	0.9 (7)	0.021 (1)	0.00105	5*10^(-7)	
6.1 m																								NA
	MH		Dark gray, sandy ELASTIC SILT, very soft, wet	Soft loam	19	0	0	n.d.	n.d.	n.d.	n.d.	n.d.	50	0	n.d.	n.d.	11.97	NA	NA	1.8 (7)	0.2576 (1)	0.01288	1*10^(-8)	
7.6 m																								n.d.

(1) Based on EC7
(2) Based on SPT
(3) Based on OCR
(4) Based on LI
(5) Based on LL
(6) Based on Pocket Penetrometer
(7) Based on Swiss method
(8) Based on w

GT at + 2.93 m NAVD 88
GWT at 5.49 m below GT
Capillary rise at 1.22 m below GT

Figure 4.4: Estimated soil parameters of the National Mall

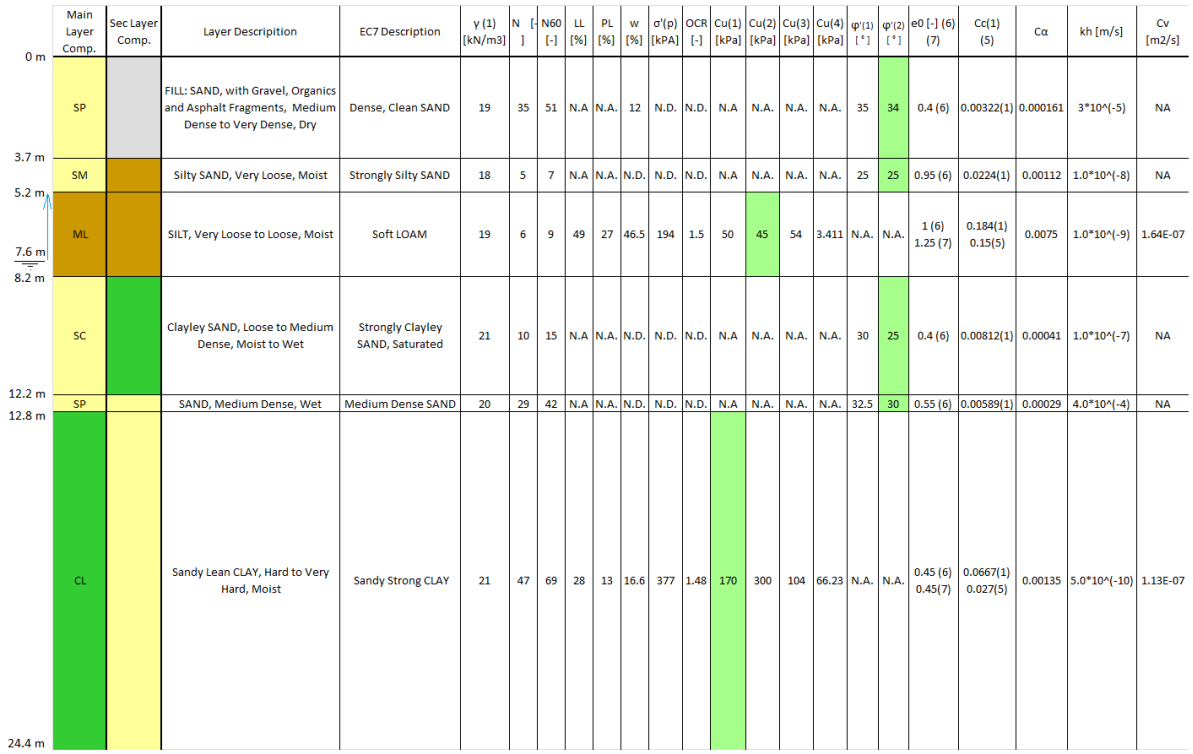

	Main Layer Comp.	Sec Layer Comp.	Layer Descripition	EC7 Description	γ (1) [kN/m3]	N [-]	N60 [-]	LL [%]	PL [%]	w [%]	σ'(p) [kPA]	OCR [-]	Cu(1) [kPa]	Cu(2) [kPa]	Cu(3) [kPa]	Cu(4) [kPa]	φ'(1) [°]	φ'(2) [°]	e0 [-] (6) (7)	Cc(1) (5)	Cα	kh [m/s]	Cv [m2/s]
0 m	SP		FILL: SAND, with Gravel, Organics and Asphalt Fragments, Medium Dense to Very Dense, Dry	Dense, Clean SAND	19	35	51	N.A	N.A.	12	N.D.	N.D.	N.A	N.A.	N.A.	N.A.	35	34	0.4 (6)	0.00322(1)	0.000161	3*10^(-5)	NA
3.7 m	SM		Silty SAND, Very Loose, Moist	Strongly Silty SAND	18	5	7	N.A	N.A.	N.D.	N.D.	N.D.	N.A	N.A.	N.A.	N.A.	25	25	0.95 (6)	0.0224(1)	0.00112	1.0*10^(-8)	NA
5.2 m	ML		SILT, Very Loose to Loose, Moist	Soft LOAM	19	6	9	49	27	46.5	194	1.5	50	45	54	3.411	N.A.	N.A.	1 (6) 1.25 (7)	0.184(1) 0.15(5)	0.0075	1.0*10^(-9)	1.64E-07
7.6 m	SC		Clayley SAND, Loose to Medium Dense, Moist to Wet	Strongly Clayley SAND, Saturated	21	10	15	N.A	N.A.	N.D.	N.D.	N.D.	N.A	N.A.	N.A.	N.A.	30	25	0.4 (6)	0.00812(1)	0.00041	1.0*10^(-7)	NA
8.2 m	SP		SAND, Medium Dense, Wet	Medium Dense SAND	20	29	42	N.A	N.A.	N.D.	N.D.	N.D.	N.A	N.A.	N.A.	N.A.	32.5	30	0.55 (6)	0.00589(1)	0.00029	4.0*10^(-4)	NA
12.2 m	CL		Sandy Lean CLAY, Hard to Very Hard, Moist	Sandy Strong CLAY	21	47	69	28	13	16.6	377	1.48	170	300	104	66.23	N.A.	N.A.	0.45 (6) 0.45(7)	0.0667(1) 0.027(5)	0.00135	5.0*10^(-10)	1.13E-07
12.8 m																							
24.4 m																							

(1) Based on EC7
(2) Based on SPT
(3) Based on OCR
(4) Based on LI
(5) Based on LL
(6) Based on Swiss method
(7) Based on w

GT at +2.13 m above NAVD 88
GWT at 7.6 m below GT
Capillary rise at 5.2 m below GT

Figure 4.5: Estimated soil parameters of the Anacostia bank

5
Results

5.1. ADCIRC model

Many simulations were made using Stampede2 to model the 1/100 year flood around Washington DC, however none of them were stable. Due to the time restriction, most of the simulations were made using the created model with dikes and with the right area of interested. The original plan was, to first make simulations with the existing mesh, then with the cut mesh and no dikes, and finally with the mesh cut and containing the dikes. This was too ambitious and it was therefore decided to focus on the model with dikes to get it running. Many adjustments were made to get the model stable, unfortunately none of them worked.

The results were analysed with winSCP that gave an result file called myMPI.o*runID*. This file was also used to check for instabilities and understand occurring errors. The main issue faced throughout the multiple simulations made were 'elevation errors' near the downstream boundary. In the following section more explanation is giving about the different techniques used to make the simulation stable.

5.1.1. Influence of parameters

The first explanation found for the instabilities in the model was incorrect input parameters. These input parameters were tested by changing one parameter at the time. The resulting simulation times were then compared to each other and the model with the largest simulation time was considered the most stable model and its parameter was then kept.

- The model type;
- Ramp function;
- Spatially variable GWCE parameter, τ_0;
- Eddy horizontal viscosity;
- The wetting and drying algorithm;
- The time step;
- The nonlinear bottom friction coefficient.

All these parameters have influence on the stability of the simulation and all are correlated to each other. Therefore understanding them was difficult and many simulations were made changing just one parameters at the time, see appendix E. However, the data obtained from these experiments was not enough and in order to get a better understanding of the influence of each parameters more data was needed. Below are the different changes made and their consequences on the simulation time of the model according to the data collected.

The model type

Two model types were tested here, the 2 dimensional depth integrated model and the 2D dimensional depth integrated explicit model. The first model seemed the most stable and was the most used. The second model was expected to run faster, however instabilities occurred sooner and was therefore not used after few failed simulations. Implicit methods such as the 2DDI usually allow more stability with larger time steps.

Ramp function

The ramp function used was a hyperbolic tangent function of a 2 days length and applied for forcing from surface elevation specified boundary conditions, nonzero flux boundary conditions, and tidal potential. The value of 2days was the most used in simulations as it should better results, however values of 0,5 and 1 day were also tested but showed poor quality results. Figure 5.1 shows that the best results occur with a ramp time of 2 days. a further increase in stability is possible by increasing the ramp time even further.

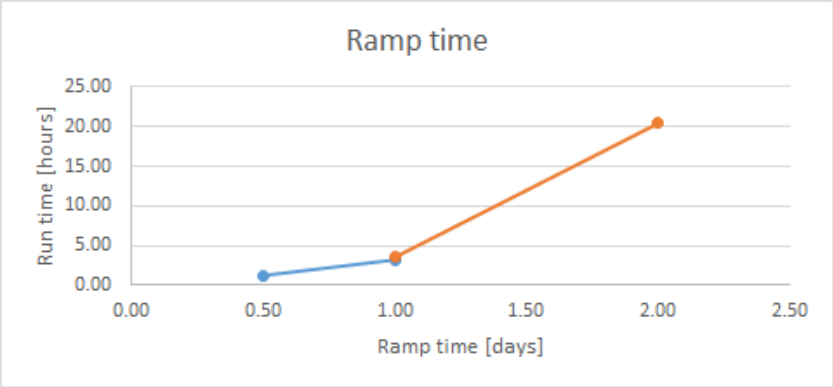

Figure 5.1: Testing the Ramp function of ADCIRC

Spatially variable GWCE parameter τ_0

According to (SMS, 2018) the values for tau0 usually vary in a range between 0.005 and 0.1. For these simulations different value of Tau0 were tested: 0.005; 0.05; 0.025; 0.5; 0.01; 0.03; -1 and -2. The last two options were a special feature of ADCIRC v45.11 where the tau0 is spatially varying.

For TAU0 is -1 the value of tau0 is calculated according to the depth, when the depth is higher or equal than 10m TAU0 is set to 0.005; and if the depth is smaller than 10m TAU0 is set to 0.020.

Similarly when TAU0 is equal to -2 the values are calculated according to the depth, when the depth is higher or equal than 200m TAU0 is set to 0.005; when it is smaller than 200m but higher than 1m it is set to 1/depth; and finally when the depth is smaller or equal than 1m TAU0 is set to 1.0.

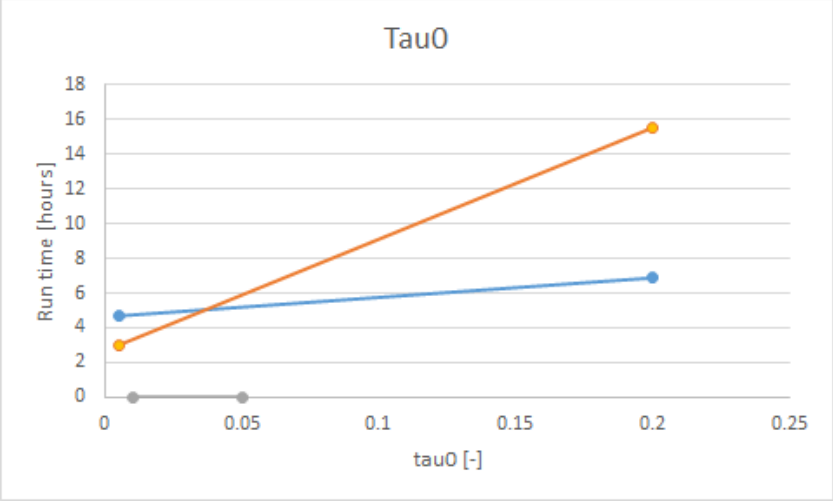

Figure 5.2: Testing the Tau0 parameter of ADCIRC

The Tau0, Figure 5.2, value shows a clear preference for a value of 0.2 which represents in this figure the TAU0 = -1 value.

From the multiple simulations run the value of TAU0 = -1 gave the best results and was therefore the most used.

Eddy viscosity

The standard value of the horizontal eddy viscosity is set to 2 m^2/s in ADCIRC. For this area of interest the horizontal eddy viscosity was mostly set to 10 m^2/s as it is the common value for coastal estuaries. Other higher values were used such as 20 m^2/s or 50 m^2/s but this led to instabilities sooner.

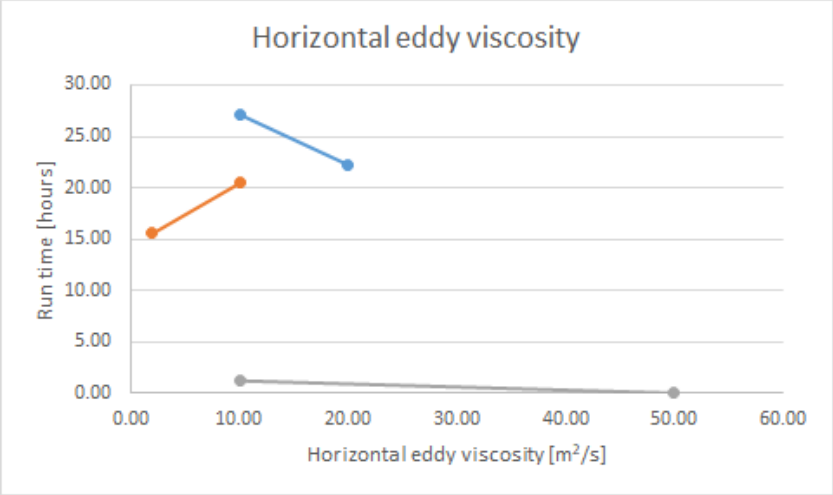

Figure 5.3: Testing the horizontal EDDY viscosity

The optimal value for the lateral eddy viscosity is 10 m^2/s as can be seen in The figure 5.3.

Wetting and drying algorithm

One possible explanation for the elevation errors by the downstream boundary was that the water level was oscillating to fast, which results in artificial additions of water. As explained before, the wetting and drying parameters were introduced to prevent this. The value of H_0 was set to 0.01 m and the values of U_0 to 0.01 m/s. This however didn't seem to improve the instabilities problem and therefore the values 0.01 m for H_0 and 0.5 m/s for U_0 were tested which also led to fast instabilities. In most simulations the values were thus kept as the standards of 0.05 m for H_0 and 0.05 m/s for U_0. The H_0 was also tested with 0.1 m but also led to unstable results.

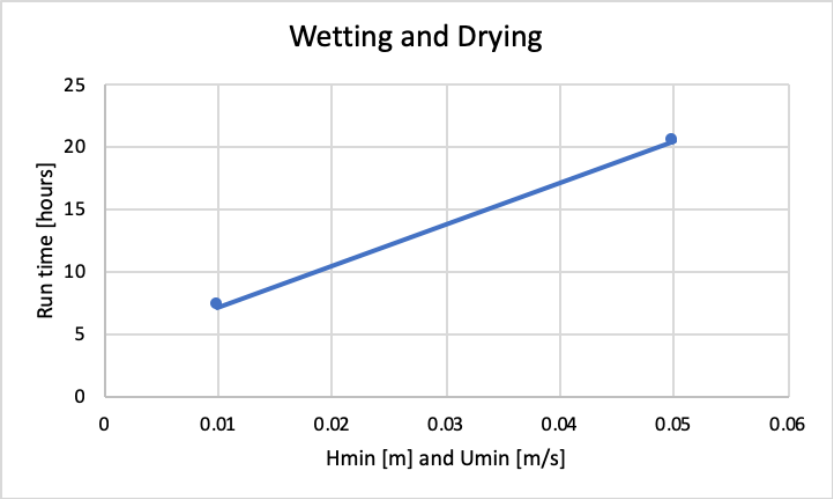

Figure 5.4: Testing the Wetting and Drying parameters of ADCIRC

Figure 5.4 shows a preference for the standard values of H_0 = 0.05 m and U_0 = 0.05m/s. More runs should be preformed to give an optimal value.

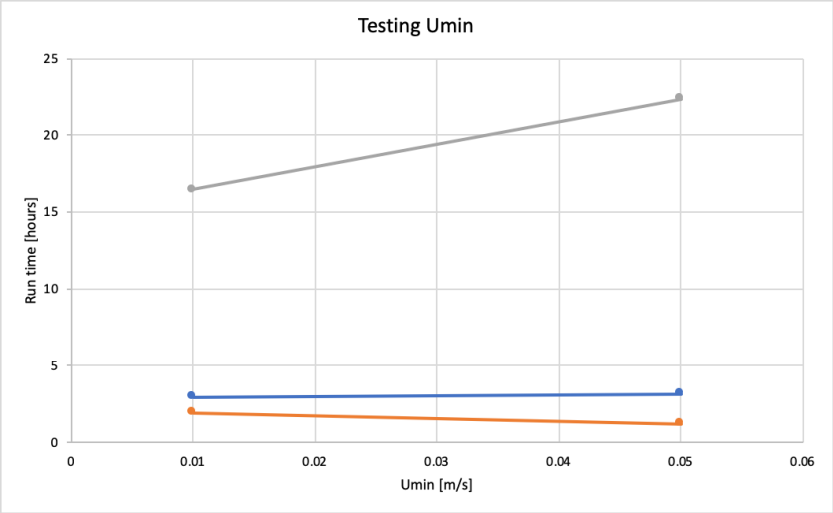

Figure 5.5: Testing the minimum velocity of ADCRIC

The minimum velocity of the wetting and drying parameter, Figure 5.5, shows contradictory results. In some cases U_0 is better with a value of 0.01 m/s and others with a value of 0.05 m/s. Therefore no conclusion can be drawn from this analysis, more runs should be performed.

The time step

The time step was based on the courant number which would usually result in time steps of 0.4 seconds, however it was found in literature that to prevent instabilities the courant number should be 10 times smaller resulting in a time step of 0,04 seconds. The time steps tested ranged from 0.1 to 0.01 seconds. Since none of these time steps solved the problem of the instabilities most runs were performed using a time step of 0.1 seconds to decrease the computational time.

The non linear bottom friction coefficient

The quadratic drag coefficient C_D is usually 0.0025 for natural flow. Other higher values were tested for simulation on a range from 0.0025 to 0.5 as seen in figure 5.6. It can be seen that the stability increases with an increasing bottom friction. However, the bottom friction was not increased further to prevent unrealistic results.

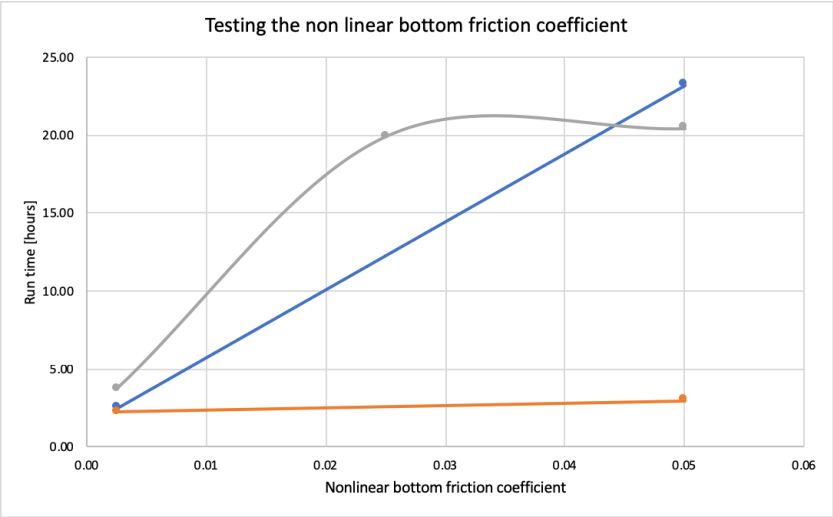

Figure 5.6: Testing the bottom friction coefficient of ADCIRC

To improve the parameters a fort.13 file should be created. In these simulation no fort.13 file was used due to the time restriction, therefore all parameters are constant across the domain, even though it is hetero-

geneous. It is possible that this would also improve the stability of the model. The bottom friction coefficient for example has a very big influence on the stability but also varies considerably across the domain and it is therefore highly recommended to take those variations into account. This is the case for many parameters which led to believe that having a fort.13 would solve the instabilities. However the parameters are not the only explanation for the instabilities.

5.1.2. Sources of instabilities

Other explanations for the instabilities are the boundary conditions, the steep elevations changes and the length of the mesh. The first reason was tested as follows.

The mesh was run with different boundary conditions:

- 1/100 flood with the discharge governing input;
- 1/100 flood with the storm governing input;
- No discharge and only the 1/100 year storm with discharge as governing input;
- No discharge and a tidal boundary downstream;
- Only the 1/100 year discharge with discharge as governing input and a tidal boundary downstream;
- Constant discharge of 1000 m^3/s for the Potomac river and a constant discharge of $10m^3/s$ for the Anacostia river.

With these runs mostly the default hydraulic conditions were used for the fort.15 file. Unfortunately none of the runs with the different boundaries showed stability. With the exception of the original mesh model without river discharge and only a tidal boundary, see appendix F. The same boundary, no river discharge and a tidal boundary downstream was tested with the created model without dikes but it also showed instabilities. It was therefore concluded that the large amount of water in the model had a significant influence on the stability, but that it was not the main reason of the instabilities. An improvement point would be to test these different boundaries using the same parameters for all simulations, as this was not done in this case which makes it difficult to rule out the boundaries as source of instabilities completely. The volume of water that the model was computing in such a short time (2days) was considerable and it is very likely that this was or had a significant influence on the stability of the model.

Another explanation, adding to the fact that the boundaries created a significant amount of water, is the mesh length. The existing mesh which was used to create the model was cut to be adjusted to the downstream boundary. This shortening of the mesh gave ADCIRC less space to dissipate the large amount of water imposed to the system. ADCIRC is a delicate model that has difficulty with large amount of water by shorelines and therefore needs enough distance to dissipate, especially due to the high elevation changes. Adding extensive amounts of water from the upstream and downstream boundaries which are very close to each other does not allow ADCIRC to process all the volume of water. This can then lead to the instabilities near the downstream boundary found in the simulations. A good solution for this problem would be to use the previously existing mesh and to add the dikes to that mesh. Caution is required boundary that will need a new data source for the water levels. If this extension of the mesh doesn't work, an even longer mesh that goes deeper into the Chesapeake bay should be created and tested.

A second explanation is the discharge and water levels distribution used by the boundaries. The length of the distribution was from 2.5 to 3 days. This created a considerably rapid increase in water elevation which then could have led to the instabilities. A solution for this would be to make the time of the peak discharge and water level arrive more gradually, this would give ADCIRC enough time to process the amount of water. This also leads to longer simulations that last more than 3 days and therefore more time would be needed to run the simulations.

Another explanation is the rapid changes in water level due to the tidal variation in the tidal boundary. ADCIRC has difficulties with rapidly changing water levels, therefore a constant water level by the tidal boundary at the beginning could be imposed by the downstream boundary in order to fill the system with water before adding the tidal fluctuation to the system.

The last potential cause of instabilities is the steep gradient in shallow areas. Because problems with the mass balance can occur in case of wetting and drying.

With all these explanation the influence of the parameters still plays an important role. Therefore it is important to keep in mind which parameters are used each time and make sure the same parameters are used during an experiment. An overview of the outcomes created by ADCIRC with instabilities can be found in appendix F.

5.2. Levee design

At first the bathtub style flood maps for the optimal return period will be presented. The settlement estimations will be provided for the two cases described below. Finally a stability analysis against rotational failure will be carried out.

In order to make the new levees comply with the 1/100 standard it was decided to consider that they will be rebuilt. From a stress path approach destroying a levee to rebuild it is similar to heightening it. Two cases will be compared in the settlement analysis: the heightening of a levee and the construction of an entire new one. The groundtable was assumed to be at +2m NAVD 88 (Nat) for the National Mall levee and +0m NAVD 88 for the Anacostia, for it is straight at the river bank.

5.2.1. Flood map

DC area: 1/273 year flood

The flood map of the optimal return period of 1/273 years, equivalent to a water level of 6.0 m was used to determine which locations needed a completely new levee and at which location the old one could be heightened. It is presented in Figure 5.7. A new levee west of the national mall needs to be constructed, as well as a the temporary defense at P street in the south of DC.

Since no soil data was available for the south levee it was assumed as the same lithography as the location for the National Mall, making its design identical to the junction added in the North-West.

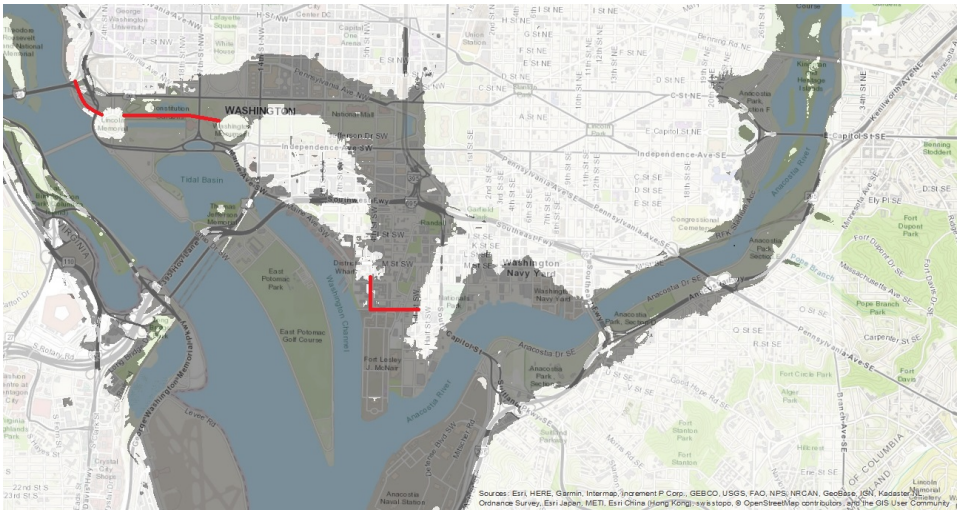

Figure 5.7: Location of required levee's in downtown DC to prevent a 1/263 year flood

Anacostia bank: 1/373 year flood

The return period for the design of the levee in the region East of downtown DC along the Anacostia bank was calculated to be 1/373 years. This is equivalent for a design water level of +6.9 m NAVD 88. The resulting flood map is presented in Figure 5.8.

The Anacostia bank levee is mostly protective of the military base in the South. It was decided to prolong it to also protect habitations in the North.

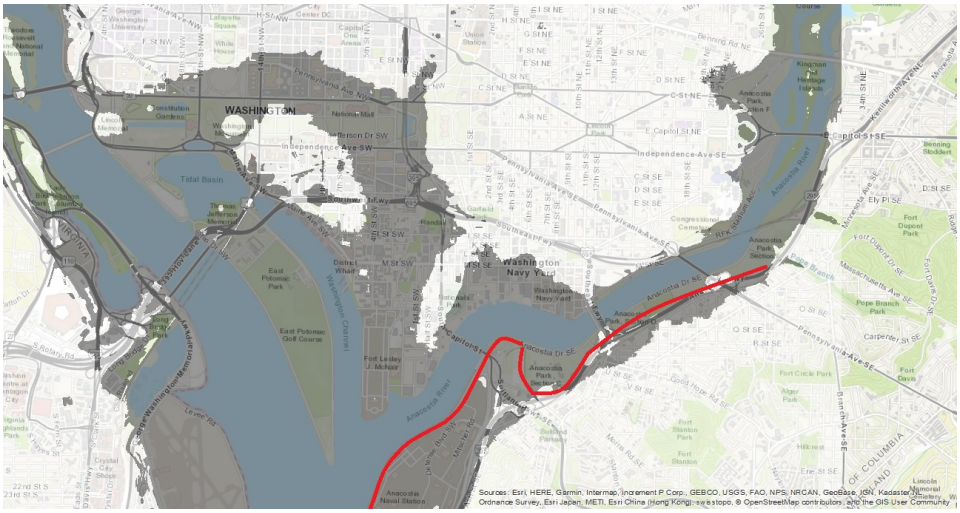

Figure 5.8: Location of required levee's at the Anacostia bank to prevent a 1/373 year flood

5.2.2. Levee design and settlement calculations

With the design water levels known, it is possible to determine the levee construction height. 2 Cases will be analyzed. First the settlement calculations for the reconstruction of a higher levee will be determined. The second case to be studied are the settlements induced by the construction of a levee at a place where no levee was present yet. A summary of the return period water height and levee design height is presented in Table 5.1.

Table 5.1: Design water level and levee height for design return periods

Return Period	Design Water level [m]	Levee Design height [m]
1/100	4.0	5.4
1/263	6.0	7.4
1/373	6.9	8.3

Rebuilding of existing levee

The levees at the National Mall and South Anacostia river bank needed to be rebuilt as discussed previously. Removing the levee will lead to unloading of the subsurface, and rebuilding it until the original height to reloading. Since this will be done in a short time period it can be assumed that the soil will undergo the same magnitude of deformation in unloading as reloading.

As was described in the undrained shear strength determination section the OCR of the different layers was assumed to be 1. This means that every loading applied by the elevation of the levee above its original height can be declared as primary compression, which is why the primary consolidation parameter Cc should be used.

The draining layers are assumed to be the sandy layers. The layers under MH3 for the National Mall and CL for the Anacostia bank are assumed to be drained. Since the hydraulic conductivity for the silty layers of the National Mall levee are in the same order of magnitude the drainage path for these layers was chosen as the shortest distance of the furthest point in the undrained layer towards the drained layer.

A summary of the settlements for the case of rebuilding existing levees for the two locations is presented in Figure 5.9.

Rebuilding of existing levees	1/100 year National Mall	1/263 year National Mall
Requiered Height [m]	5.40E+00	7.40E+00
Added height [m]	5.00E-01	2.60E+00
ΔH Total [m]	7.92E-02	1.49E-01
ΔH Primary Total [m]	2.01E-02	9.01E-02
ΔH Secondary Total [m]	5.90E-02	5.90E-02
ΔH ML1 [m]	6.38E-03	1.20E-02
ΔH MH1 [m]	9.62E-03	1.90E-02
ΔH ML2 [m]	1.56E-02	3.21E-02
ΔH MH2 [m]	2.40E-02	4.76E-02
ΔH MH3 [m]	2.36E-02	3.85E-02

Rebuilding of existing levees	1/100 year Anacostia Bank	1/373 year Anacostia Bank
Requiered Height [m]	5.40E+00	8.30E+00
Added height [m]	1.50E+00	4.50E+00
ΔH Total [m]	5.02E-02	8.88E-02
ΔH Primary Total [m]	2.03E-02	5.89E-02
ΔH Secondary Total [m]	2.99E-02	2.99E-02
ΔH ML [m]	3.61E-02	5.98E-02
ΔH CL [m]	1.41E-02	2.90E-02

Figure 5.9: Summary of the settlements for the case of rebuilding the existing levees

Construction of new levee

At the locations where no levee is present yet the load applied on the subsurface will be bigger. This will lead to more excess pore pressures being generated than in the case of rebuilding an embankment higher, therefore leading to more consolidation. This will increase the amount of settlement that can be expected.

Note can be taken that the amount of secondary settlement does not increase from the first situation. The time for the layer to consolidate is independent of the applied load, and creep settlements will only occur from the moment that a certain amount of pore pressures are dissipated (often 90 percent of consolidation is chosen).

Construction of new levees	1/100 year National Mall	1/263 year National Mall
Requiered Height [m]	5.40E+00	7.40E+00
Added height [m]	3.60E+00	5.70E+00
ΔH Total [m]	1.73E-01	2.22E-01
ΔH Primary Total [m]	1.14E-01	1.63E-01
ΔH Secondary Total [m]	5.90E-02	5.90E-02
ΔH ML1 [m]	1.39E-02	1.74E-02
ΔH MH1 [m]	2.24E-02	2.84E-02
ΔH ML2 [m]	3.78E-02	4.89E-02
ΔH MH2 [m]	5.60E-02	7.25E-02
ΔH MH3 [m]	4.34E-02	5.52E-02

Construction of new levees	1/100 year Anacostia Bank	1/373 year Anacostia Bank
Requiered Height [m]	5.40E+00	8.30E+00
Added height [m]	5.50E+00	8.50E+00
ΔH Total [m]	9.39E-02	1.28E-01
ΔH Primary Total [m]	6.40E-02	9.79E-02
ΔH Secondary Total [m]	2.99E-02	2.99E-02
ΔH ML [m]	6.64E-02	8.38E-02
ΔH CL [m]	2.74E-02	4.40E-02

Figure 5.10: Summary of the settlements for the case of building new levees

5.2.3. Stability analysis

The stability analysis for the construction of new levees was carried out with Morgenstine-Price slice method. Only rotational failure was considered. 2 situations were analyzed, one after the construction of the new levee and one for a long term high water flood. The long term high water analysis was based on the theory that steady state flow would be present from the high water towards the toe of the levee. It was deemed unnecessary to also carry out the stability analysis for the reconstruction of the embankments as it would be safer than constructing a new embankment from the start. In all the cases it was this analysis that proved to have the lowest Factor of Safety as the pore water pressures were the highest through the levee.

All the designed slopes were estimated to be safe in the tested situations with the subsurface parameters that were estimated. A summary of the results is presented in Table 5.2. The different failure envelopes are presented in Appendix G.

Table 5.2: Factor of safety against rotational sliding after construction and during long term flood for new levees

Levee designed	FOS After construction	FOS long term flood
1/100 National Mall	2.360	2.033
1/263 National Mall	1.542	1.408
1/100 Anacostia bank	2.997	2.202
1/373 Anacostia bank	2.153	1.747

5.2.4. Final levee geometry

The designed levees are predicted to be high enough to withstand the design period floods for which they were designed for 50 years based on the settlement estimations. The slope stability analysis proved that the 1:3 slopes for which they were designed should also remain safe. A summary of the final levee height design with respect to the ground table is presented below in Figures 5.11, 5.12, 5.13 and 5.14. The ground table at National Mall levee was assumed at +2m NAVD 88, and at the Anacostia bank levee at +0m NAVD 88.

A final word need to be said about underseepage. Because the top layers of the subsurface are made of material with a high hydraulic conductivity, there is a risk that seepage under the levee might occur. In order to prevent that the top layer should be extracted and replaced with the levee material with low hydraulic conductivity, or injected with a material that will reduce the hydraulic conductivity (like grout).

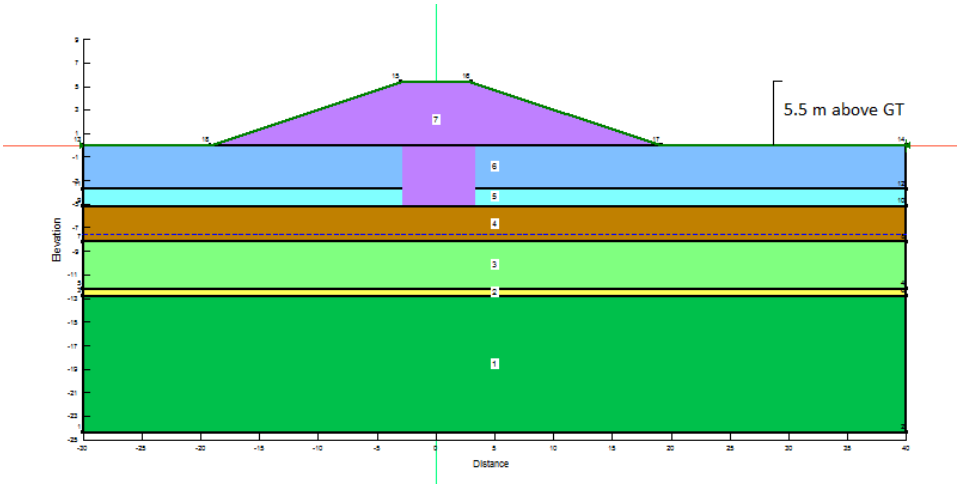

Figure 5.11: Final design height of new 100 year return period Anacostia bank levee

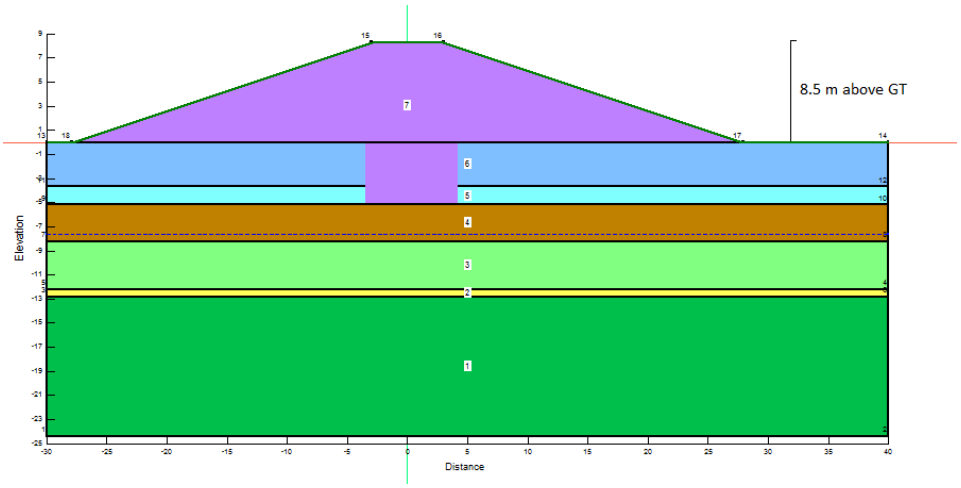

Figure 5.12: Final design height of new 373 year return period Anacostia bank levee

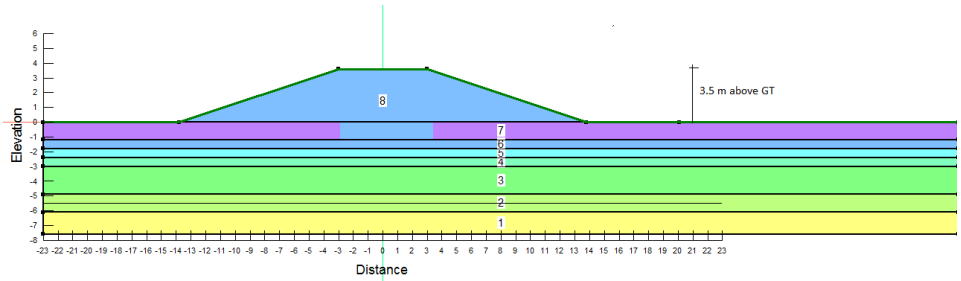

Figure 5.13: Final design height of new 100 year return period National Mall levee

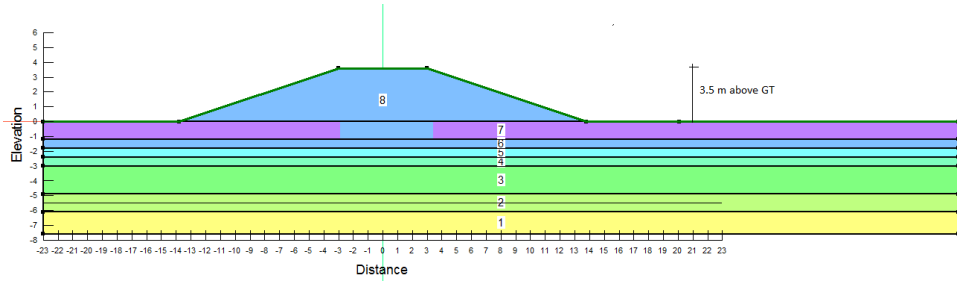

Figure 5.14: Final design height of new 263 year return period National Mall levee

6

Discussion

A general improvement to the results mentioned above would be to collect more data, especially for the soil data it is important, since correlations lack the accuracy required for the design. Furthermore the design of the levees and the determination of the optimal return period should be based upon the ADCIRC model, instead of historic water levels, near Washington DC, since these water levels do not capture the effects of flow.

Design flood

In this study, a bathtub overflow model was used to determine damage cost. The original intent of this research was however, to look at flooding scenarios modeled within ADCIRC. This method would have given dynamic flooding scenarios which more closely resembles a physical flood, in turn giving more accurate results. Yet, where the same number of estimations used for the damage curve and investment curve, this would not have reduced any errors significantly. First and foremost, more reference flood maps should be used to better fit the damage curves and investment curves. At the moment five flood maps were created for elevations of 4, 5, 6, 10 and 12 meters. Every additional flood map changed the optimal return period considerably, which is why more flood maps should be added.

Furthermore, considering the scope of this study, only levee overtopping is used to estimate damage caused by flooding. A more accurate way of damage estimation would include damage for multiple failure mechanisms. In this case, geotechnical failure models would estimate the failure probability of a levee over different water elevations. Nevertheless, given that the levee in question is in good condition, failure is unlikely to occur at low water levels. This means that for new levees, as is the case for this study, failures other than overtopping would not account for much of the damage. Near the end of the lifespan of the levee system, failure probability due to geotechnical instabilities might be higher, depending on the level of maintenance.

Additionally, in this study only investment cost and damage cost are taken into account. To make the analysis complete, it should also include maintenance cost, rescue cost and unquantifiable cost including environmental cost, cultural loss and general disruption of society.

Lastly, the time series for the boundary conditions can be made more realistic, by applying conditions from historic events. This will improve the accuracy of the simulations. In determining the boundary conditions the dependence was assumed negligible, however, to improve the accuracy of the simulations, the dependence should be taken into account. It is likely that the high water levels are associated with storm surges, in which case the downstream boundary should be a Dirichlet boundary. However due to a lack of data, this could not be incorporated in the research, in further research this should be estimated or simulated based on nearby stations.

Flood modelling

To make the model stable the boundary conditions could be adjusted in order to let the water in the model flow slower and more gradually. Due to significant elevation changes in the model the significant volume of water computed in such a short time induced many elevation errors by the downstream boundary. Therefore it is advised to let the water level by the downstream boundary be constant and increase gradually over an appropriate amount of days. This would give ADCIRC enough time to compute the water levels while having high elevation differences. Another option would be to smoothen the elevation across the model.

Another possible solution to make the model stable is to extend the model in order to have the downstream boundary by the Chesapeake bay. It is possible that because the model gets a significant amount of water by both the upstream and downstream boundaries, the volume of water coming in the model does not have enough space to dissipates and creates instabilities.

Finally creating a fort.13 for the mesh would improve the stability of the model considerable. The domain is considerably heterogeneous and therefore a too high bottom friction coefficient by a shallow water for example can cause the model to become unstable.

When the model is stable more improvements are still possible, because some forcing terms were neglected in simulations, even though they are relevant. No baroclinic effect have been taken into account because, however due to the proximity to the Atlantic Ocean, it is very likely to have a considerable influence over the flow. To include the baroclinic effects the floods should be modelled using a 3 dimensional model, which would also include dispersion. Most historic storms are related to hurricanes, to accurately model this air pressure and wind velocities should not be neglected in the modelling. Since both can cause a significant raise in the water level.

A new levees has been placed near the National Mall in Washington DC, because no elevation data for this levee is available it could not be added to the model. In further studies these should be added, to accurately describe the region.

One of the main problems in Washington DC is caused by rainfall, this however is not included in the model. The effect of flooded sewers should be analyzed as well, for a full understanding of the flood risk.

Soil Conditions

Soil is an extremely variable medium. More boreholes at the specific locations of the levees would have been required in order to get an accurate knowledge of the lithography and groundwater conditions. Spatial variability was totally unaccounted for in this analysis, making the conclusion concerning stability and settlements unreliable.

Further tests on the soil samples obtained from these boreholes would have been required in order to estimate the settlements and stability.

For the settlement parameters an Oedometer test would be vital for each compressible layers in order to estimate the magnitude of settlements. Results on the compression coefficients, as well as the initial void ratio, OCR or coefficient of consolidation were estimated here, but induced errors in the estimation of the settlements. Falling head tests would also be of importance to estimate the hydraulic conductivity, needed to have a better overview of the drainage path in multiple stacked compressible layers. The hydraulic conductivity of the levee material also needs to be determined in order to make sure that it would not behave in a drained matter.

For the stability Triaxial Compression tests or Direct Simple Shear tests would be required to obtain parameters like the friction angle or the undrained shear strength. Without accurate results for these parameters no real conclusions can be drawn concerning the stability.

A final words need to be added on the slope stability analysis. The levee material presented here is a sandy silt. A critical stability case for a levee of this could be in the case of a fast drawdown of the water level after a long flood. Due to the pore pressures that would accumulate in the levee during a drawdown the effective stress in the soil would reduce. This could lead to a critical situation. If better data concerning the actual soil parameters would be present, a fully coupled hydro-mechanical possible failure could be tested.

7

Conclusion

The current flood protection in Washington DC includes 2 levees, with one located at the National Mall and one near the Anacostia river. The heights of the levees are 5.0 and 3.9 meters respectively. Additionally there are some locations with temporary levees. These flood protection measures do not offer sufficient protection according to the local safety standards, assuming the water level to spread equally over the studied area.

However this method is less accurate than numerical modelling of the flow, because the steepness of the bathymetry is not included in this method. In the case of a flat bathymetry next to the banks of the river, the water level would increase beyond the physical limitations that are imposed by the continuity equation. Following the same principle, the design water level would be underestimated for a steep bathymetry. When the velocity of flow is taken into consideration, more accurate water levels would be obtained due to their inverse relationship which follows from energy conservation. In addition, run up originates from flow which is not considered in a stagnant bathtub model. However instabilities in the numerical model represented a drawback to this method.

The instabilities were assumed to be caused by the hydraulic conditions, such as bottom friction and lateral eddy viscosity. However, after analyzing all input parameters, no stable solution could be found. In combination with the CFL condition being met, this indicated that the previous assumption was incorrect and that there is another cause of instabilities. Possible explanations of the instabilities could be the steepness of the bathymetry in shallow areas. the length of the ramp time, the length of the time series for the boundary conditions or the location and the type of boundary condition. Because no conclusive answer was found the bathtub floods were used to design the flood protections.

Based on the historic data found near Washington DC the once in a 100 year flood has an elevation of 4.0 meters based on a bathtub model. When sea levels rise and an estimation of the wave over topping are included, the design water level amounts to 5.4 meters. Disregarding the current state of the levees, it can be concluded that these levees inherently do not comply with the safety standards set by the Army Corps of Engineers.

To ensure proper protection which would withstand a 100 year flood, the levee at the National Mall has to be increased by 0.5 meters and by 1.5 meters at the Anacostia bank. These proposed reinforcements include the predicted settlements of less than 0.1 meters during the 50 years of the design lifetime. The permeable layers directly under the levees should also be replaced with an impermeable layer or injected with grout.

A cost-benefit analysis was conducted to minimize the total flood related costs. An optimal levee height which offers protection against a once in 263 year flood near the National Mall district and against a once in 373 year flood near the Anacostia river was determined to be the most cost efficient. To comply with these flood events, the levees need to be elevated to 7.4 meters and 8.3 meters for the National Mall levee and the Anacostia levee respectively. An additional height of 2.6 and 4.5 meters respectively is required to account for settlements.

When building new levees they should be built to a height of 5.7m in the National Mall area and 8.5m at the Anacostia Bank to account for settlements.

8

Acknowledgements

First of all we would like to thank Feline Fox who contributed considerably to the project by working with us throughout the whole 2 months and finding the optimal return period for us which was essential to our project.

We would like to extend our sincere gratitude to our main supervisor Dr. ir. Jeremy Bricker for making this project and this travel to the United States of America possible, and especially for guiding us throughout the project by taking the time to meet online every other week. We would also like to extend our sincere gratitude to our local supervisor Dr. ir. Celso Ferreira for helping us with all the logistics that needed to be done including finding us a place to work, for always being available to answer our questions and for making our stay extremely pleasant.

We would also like to thank Dr. ir. Marcel Zijlema and Prof. Dr. ir. Cristina Jommi for accepting to supervise this project and giving us advise when needed.

Additionally we would like to thank Arslaan Khalid for giving us two meshes to work with and for always taking the time to help and answer our questions about ADCIRC. Another thank you to Selina Jahan Sumi for providing us with discharge data of the Anacostia river, for explaining ARCGIS to us and for answering all our questions.

Additionally we would like to thank Tyler W Miesse, Gustavo De Almeida, Ali M. Rezaie and Brayan Pozo for the warm welcome given and for always being ready to help.

Lastely we would like to thank the International Internship Grant and 'Het waterbouw fonds' for providing financial support.

Bibliography

National levee database. https://levees.sec.usace.army.mil/#/levees/system/2305300002/summary. Accessed: 2018-10-29.

Structx soil properties hydraulic conductivity. http://structx.com/Soil_Properties_007.html. Accessed: 2018-10-29.

D. Albouy and G. Ehrlich. *Metropolitan land values and housing productivity*. National Bureau of Economic Research, 2012.

association of Swiss Road and traffic Engineers. Characteristic coefficients of soils. Standard SN 670 010b.

ASTMD85492. Section iv. specific-gravity-of-solids determination, 2013.

Shahidzadeh-Bonn N. Azouni, A., A. Tournie, S. Bichon, P. Vie, S. ROodtsDTS, P. Faure, and F. Bertrand. Effect of wetting on the dynamics of drainage in porous media. 1957.

J. Bachmann, J. Ramírez-Flores, and A. Marmur. Direct determination of contact angles of model soils in comparison with wettability characterization by capillary rise. *Journal of hydrology*, 2010.

C.A. Blain, R.S. Linzell, P. Chu, and C. Massey. Validation test report for the advanced circulation model (adcirc) v45. 11. Technical report, NAVAL RESEARCH LAB STENNIS SPACE CENTER MS OCEANOGRAPHY DIV, 2010.

T Brown and H Hettiarachchi. Estimating shear strength properties of soils using spt blow counts: An energy balance approach. (No. 179, ISBN 978-0-7844-0972-5), 2008.

W. D. III Carrier. Consolidation parameters derived from index tests. *Geotechnique*, 36(0016-8505):211–213, 1985.

Cheryl Ann Blain, Robert S. Linzell, Philip Chu. Validation test report for the advanced circulation model (adcirc) v45.11. Memorandum Report OMB No. 07040188, 2010.

CIRIA. The international levee handbook, 2013. C731.

C R I Clayton. The standard penetration test (spt): methods and use. (R143), 1985.

K. Colbo. Lateral reynolds stress and eddy viscosity in a coastal strait. *Journal of Physical Oceanography*, 36, 2005.

J.C. Dietrich, R.L. Kolar, and R.A. Luettich. Assessment of adcirc's wetting and drying algorithm. *Proceedings of Computational Methods in Water Resources, CT Miller, MW Farthing, WG Gray, and GF Pinder, eds*, 2: 1767–1778, 2004.

J.C. Dietrich, R.L. Kolar, and J.J. Westerink. Refinements in continuous galerkin wetting and drying algorithms. In *Estuarine and Coastal Modeling (2005)*, pages 637–656. 2006.

ECS-Midatlantic-LTD. Kingman island improvement. Report of subsurface exploration and geotechnical engineering analysis ECS Job No. 15431, 2009.

Inc. Froehling Robertson. Report of geotechnical data nama rehabilitate potable water lines. Report of Geotechnical Data FR Project No. 72U0289, 2014.

K. Gavin. Parameter selection handout.

J.P. Giroud. Charts for foundations design, 1973.

R. Hui, E. Jachens, and J. Lund. Risk-based planning analysis for a single levee. *Water Resources Research*, 52 (4):2513–2528, 2016.

R.L. Kolar J.C. Dietrich and R.A. Luettich. Assessment of adcirc's wetting and drying algorithm. Technical report, School of Civil Engineering and Environmental Science, University of Oklahoma and Institute of Marine Sciences, University of North Carolina.

S.N. Jonkman, R.D.J.M. Steenbergen, O. Morales-Nápoles, A.C.W.M. Vrouwenvelder, and J.K. Vrijling. Probabilistic design: Risk and reliability analysis in civil engineering. Technical report, Delft University of Technology, 2011.

K Kootahi and P.W. Mayne. Index test method for estimating the effective preconsolidation stress in clay deposits. *Journal of Geotechnical and Geoenvironmental Engineering*, (04016049), 2016.

Foot R. Ladd, C.C., K. Ishihara, and H. G. Polous. Stress-deformation and strength characteristics. *9th International Conference on Soil Mechanics and Foundation Engineering*, 1977.

R. Luettich and J. Westerink. *Formulation and Numerical Implementation of the 2D/3D ADCIRC Finite Element Model Version 44.XX*. University of North Carolina at Chapel Hill, Institute of Marine Sciences and Department of Civil Engineering and Geological Sciences, University of Notre Dame.

G Mesri and P M Godlewski. Time and stress-compressibility interrelationship. *Journal of the Geotechnical Engineering Division*, 103:417—-430, 1977.

NCPC. Report on flooding and stormwater in washington dc. Technical report, National Capital Planning Commission, 2008.

J. O. Osterberg. Influence values for vertical stresses in a semi-infinite mass due to an embankment loading. *Proc fourth int conf on soil mechanics and foundation engineering*, 1:393–396, 1957.

K.J. Roberts and W.J. Pringle. Ocean2dmesh: User guide. Technical report, University of Notre Dame, United States Computational Hydraulics Lab, 2018.

K. Slager and D. Wagenaar. Standaardmethode 2017. Technical report, Deltares, 2017.

SMS. User manual (v12.2), the surface water modelling system, 2018.

National Cooperative Soil Survey. Soil survey of district of columbia. Report of soil conditions, 1976.

US.Army.Corps. Engineering and design – design and construction of levees, 2000. EM 1110-2-1913.

A

Return period

To determine the damage in the event of a certain flood height, the following flood maps were created.

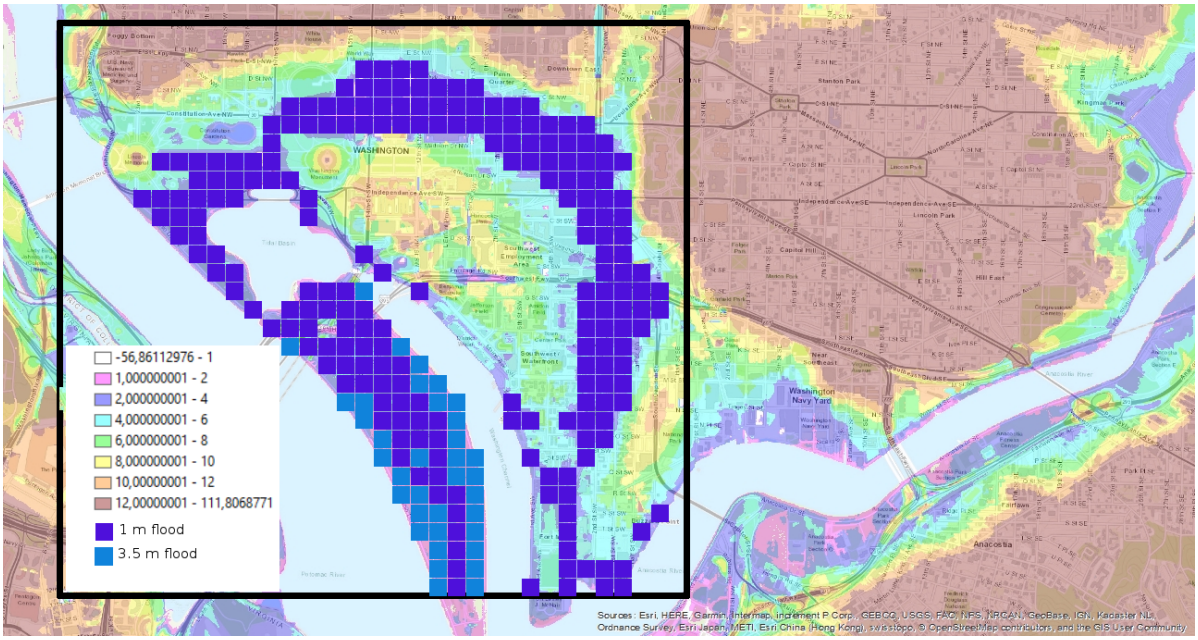

Figure A.1: Washington DC, 4 m flood

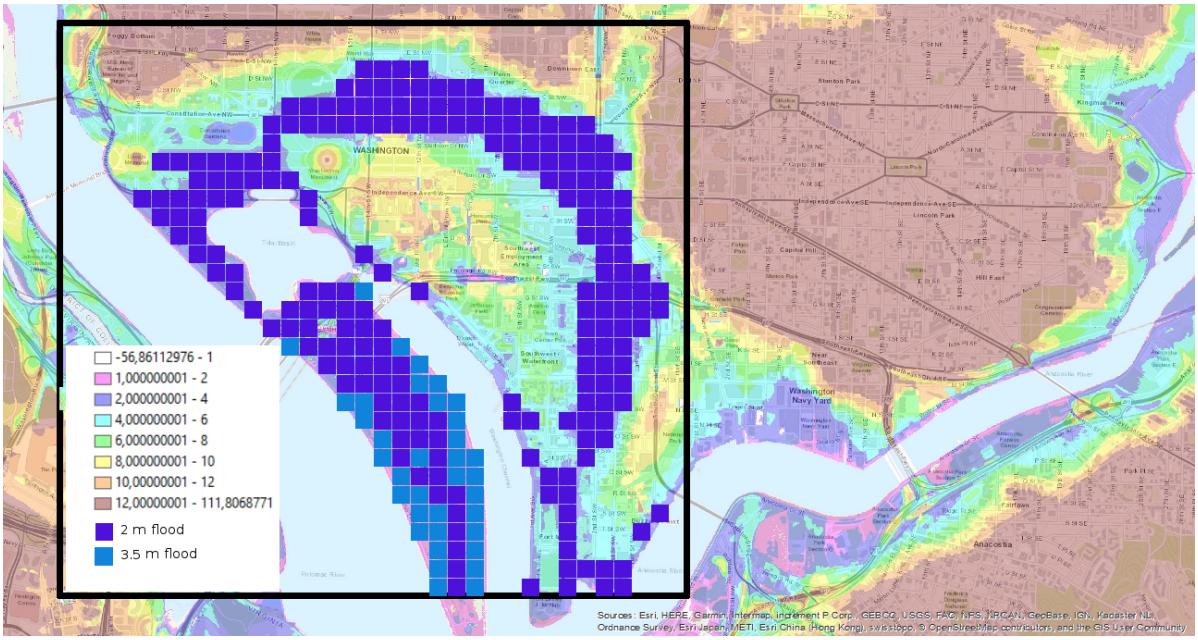

Figure A.2: Washington DC, 5 m flood

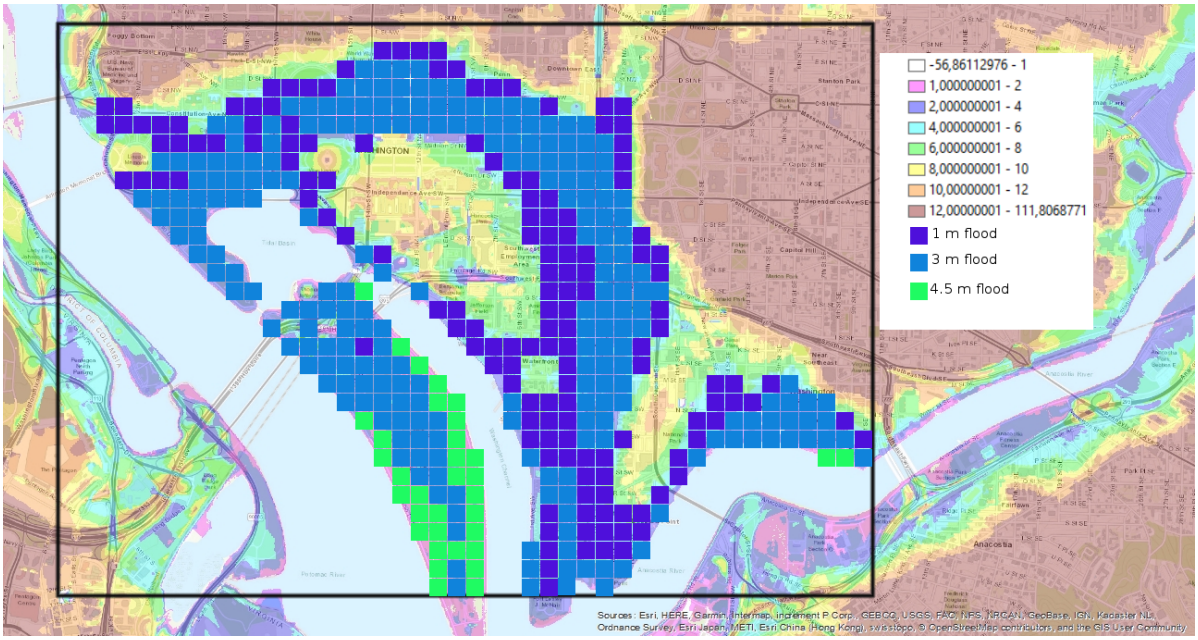

Figure A.3: Washington DC, 6 m flood

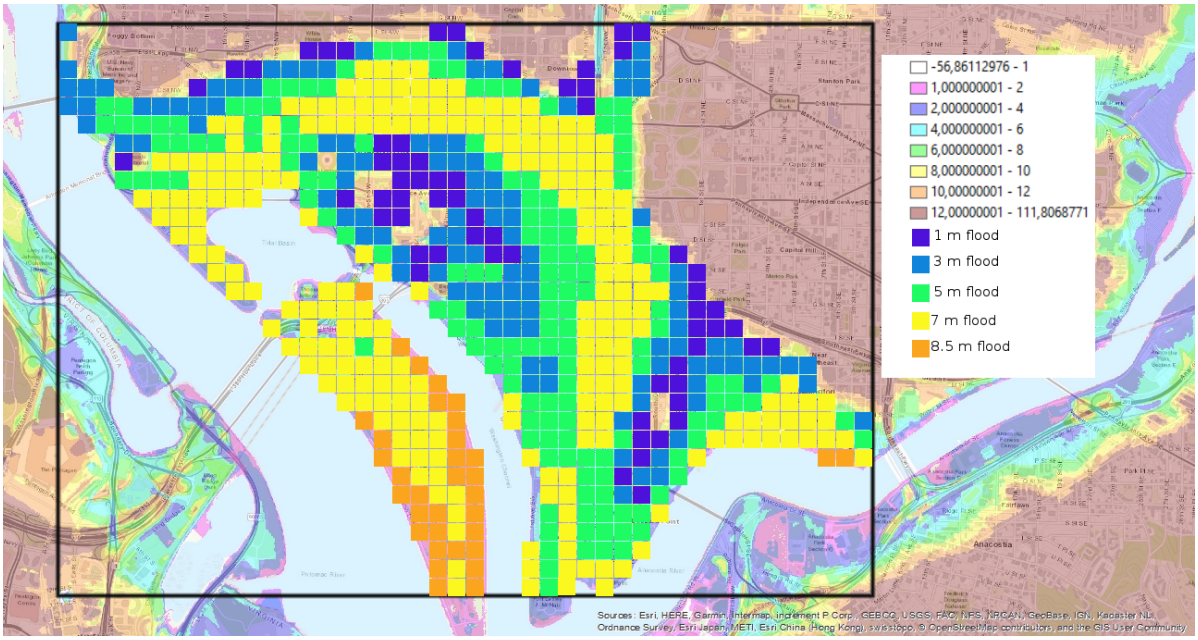

Figure A.4: Washington DC, 10 m flood

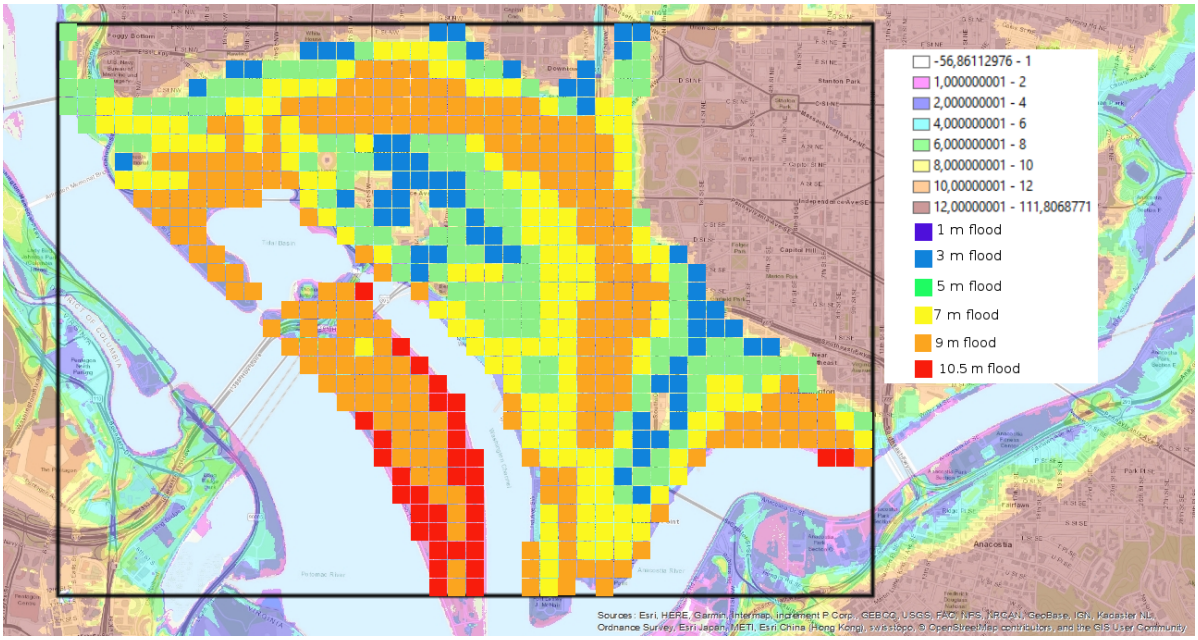

Figure A.5: Washington DC, 12 m flood

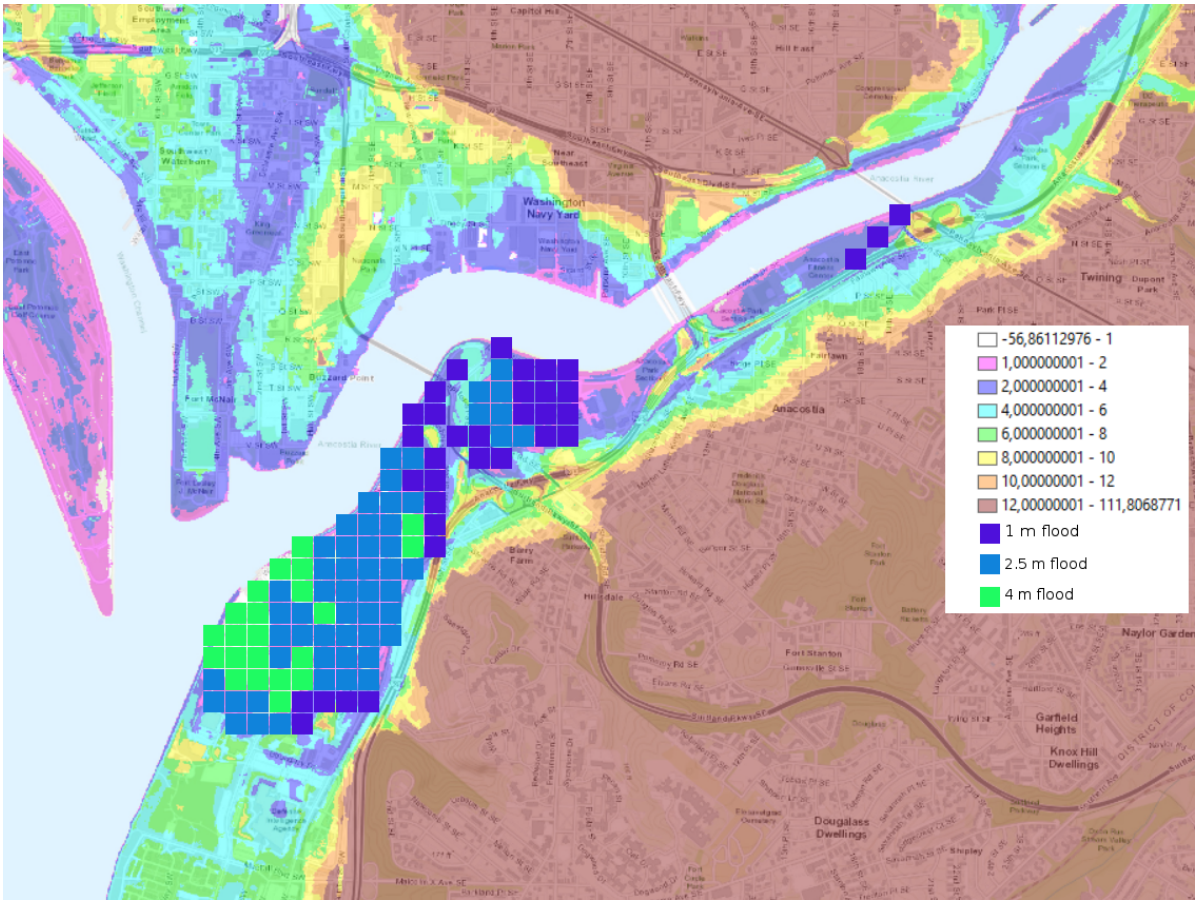

Figure A.6: Anacostia river bank, 4 m flood

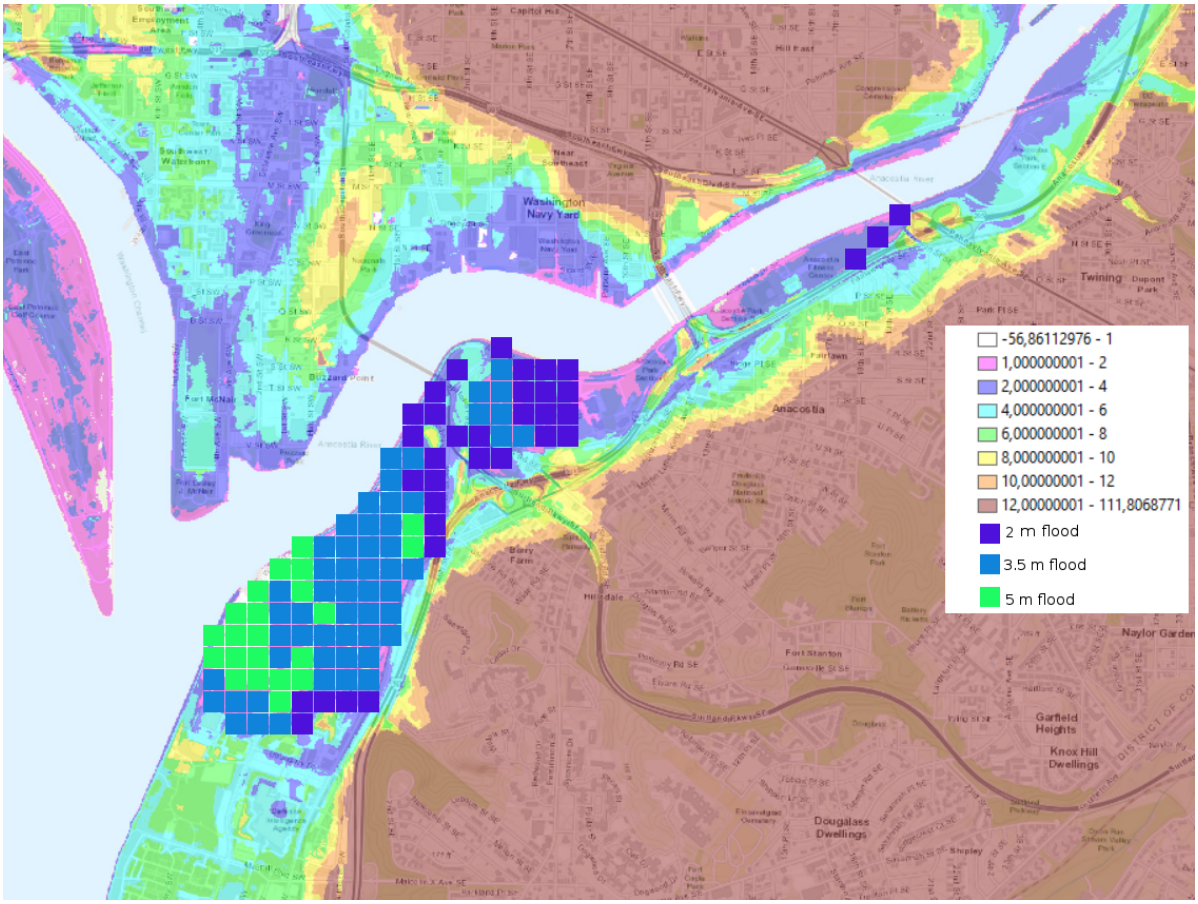

Figure A.7: Anacostia river bank, 5 m flood

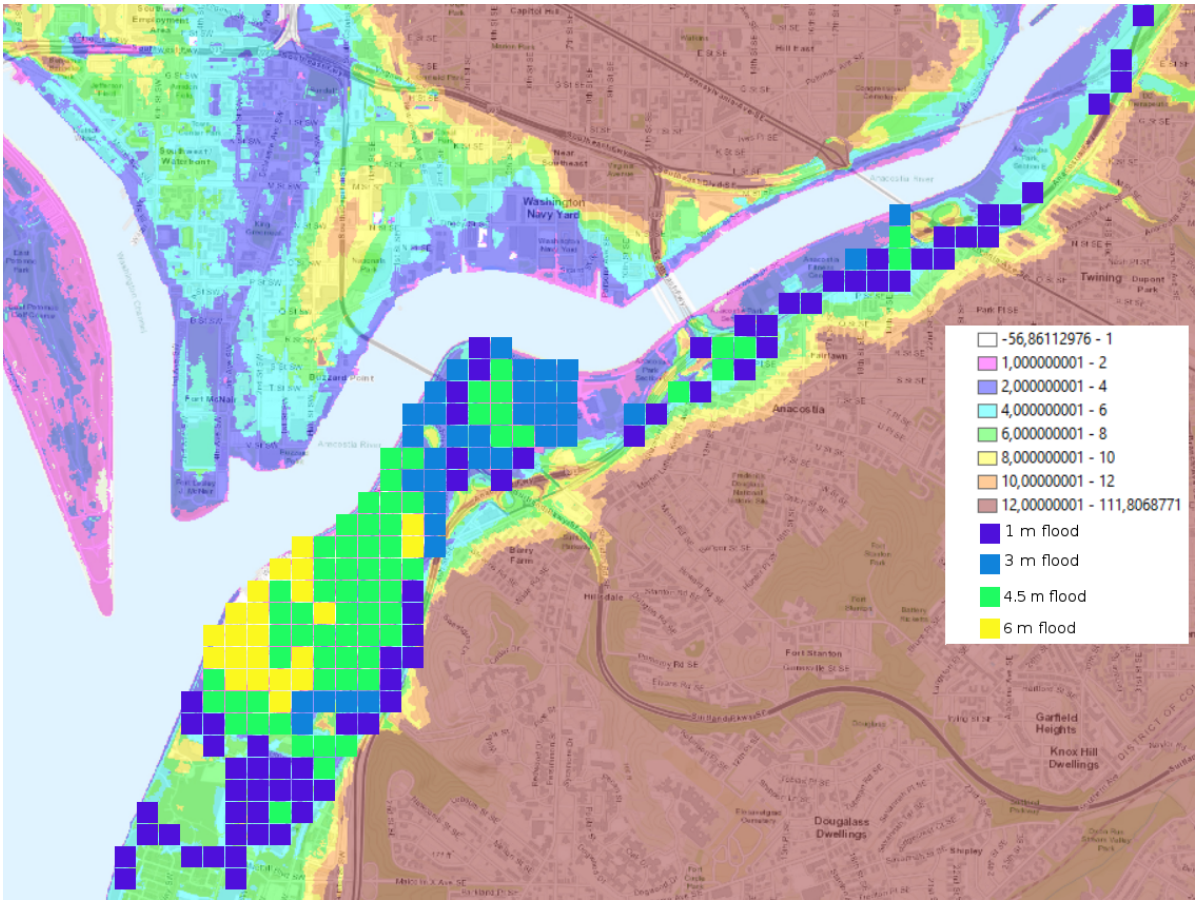

Figure A.8: Anacostia river bank, 6 m flood

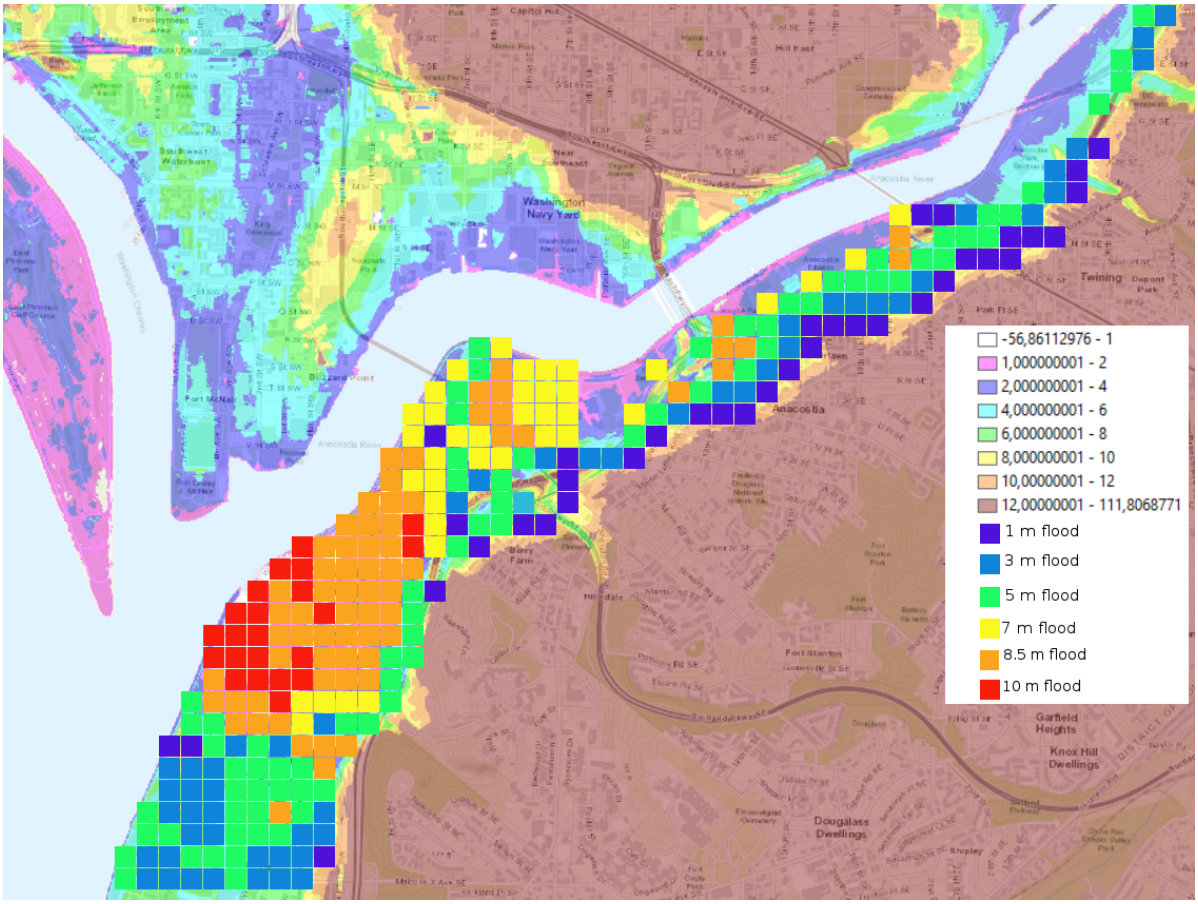

Figure A.9: Anacostia river bank, 10 m flood

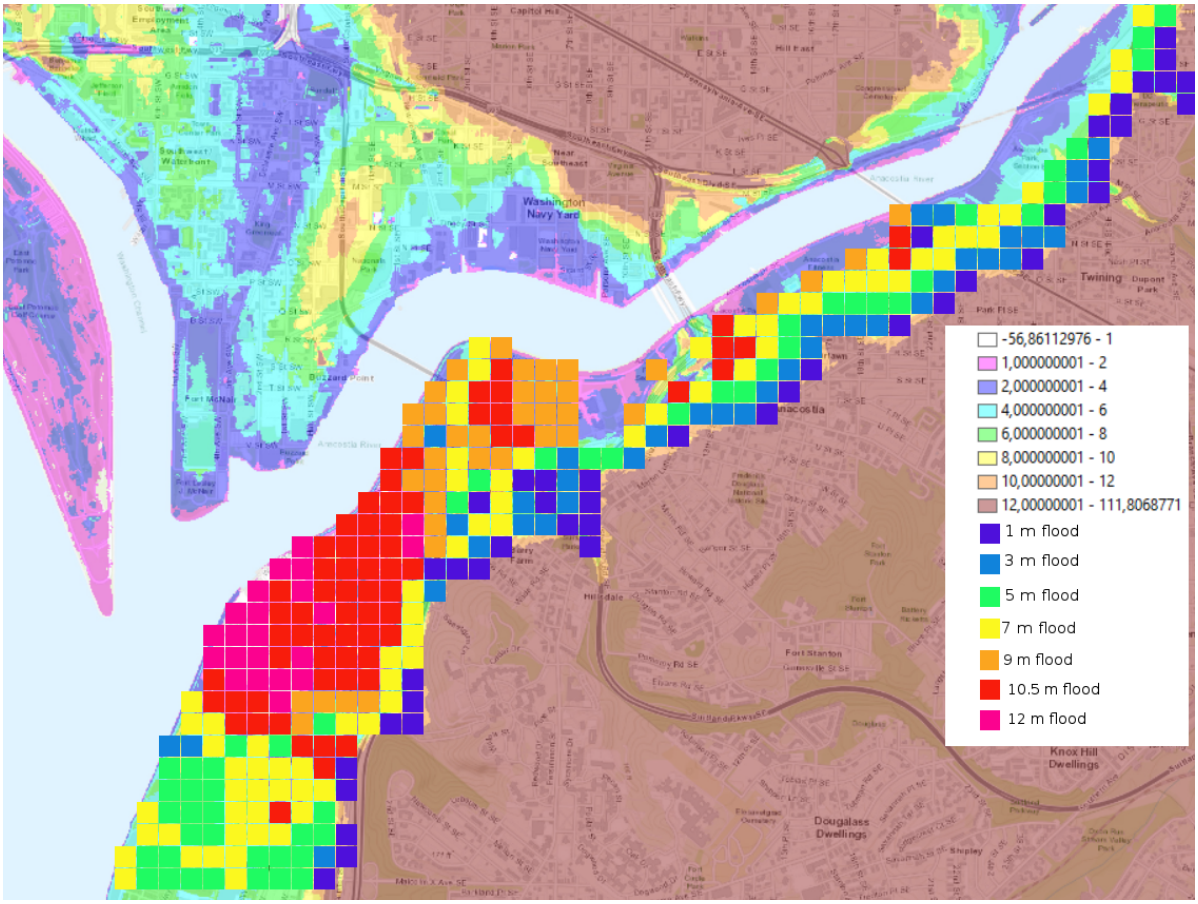

Figure A.10: Anacostia river bank, 12 m flood

Every raster point was given a damage factor and damage value based on the water depth and land usage. This can be found in the tables below.

	1 m flood				
	Damage factor	Amount	Amount per block	Price per item [10^3 $]	Total cost [10^3 $]
Housing	0,07	94	3,5	1225	28219
Household	0,48	94	3,5	70	11054
Parks	0,6	14	1	8019	67359
Monuments	0,65	1	1	206	134
Industry	0,4	24	2	10530	202174
Business shutdown	0,8	24	5000	1	96000
Roads	0,58	133	600	1,2	55541
Vehicles	1	94	3,01	8	2264
					462744

Table A.1: Downtown Washington DC, 4 m flood

	2 m flood				
	Damage factor	Amount	Amount per block	Price per item [10^3 $]	Total cost [10^3 $]

Table A.2 continued from previous page

Housing	0,1	94	3,5	1225	40313
Household	0,5	94	3,5	70	11515
Parks	0,8	14	1	8019	89811
Monuments	0,75	1	1	206	154
Industry	0,55	24	2	10530	277989
Business shutdown	0,97	24	5000	1	116400
Roads	0,8	133	600	1,2	76608
Vehicles	1	94	3,01	8	11318
					624108

Table A.2: Downtown Washington DC 5 m flood

	1 m flood		3 m flood			
	Damage factor	Amount	Damage factor	Amount	Amount per block	Price per item [10^3 $]
Housing	0,07	86	0,35	95	3,5	1225
Household	0,48	86	0,66	95	3,5	70
Parks	0,6	7	0,92	12	1	8019
Monuments	0,65	1	1	2	1	206
Industry	0,4	10	0,75	24	2	10530
Business shutdown	0,8	10	1	24	5000	1
Roads	0,58	104	0,93	133	600	1,2
Vehicles	1	86	1	95	3,01	8

Table A.3: Downtown Washington DC, 6 m flood

	1 m flood		3 m flood		5 m flood		7 m flood
	Damage factor	Amount	Damage factor	Amount	Damage factor	Amount	Damage factor
Housing	0,07	43	0,35	97	1	86	1
Household	0,48	43	0,66	97	1	86	1
Parks	0,6	1	0,92	0	1	7	1
Monuments	0,65	0	1	0	1	1	1
Industry	0,4	5	0,75	6	1	10	1
Business shutdown	0,8	5	1	6	1	10	1
Roads	0,58	49	0,93	103	1	104	1
Vehicles	1	43	1	97	1	86	1

Table A.4: Downtown Washington DC, 10 m flood

	1 m flood		3 m flood		5 m flood		7 m flood
	Damage factor	Amount	Damage factor	Amount	Damage factor	Amount	Damage factor
Housing	0,07	0	0,35	43	1	97	1
Household	0,48	0	0,66	43	1	97	1
Parks	0,6	0	0,92	1	1	0	1
Monuments	0,65	0	1	0	1	0	1
Industry	0,4	0	0,75	5	1	6	1
Business shutdown	0,8	0	1	5	1	6	1
Roads	0,58	0	0,93	49	1	103	1
Vehicles	1	0	1	43	1	97	1

Table A.5: Downtown Washington DC, 12 m flood

	1 m flood		2.5 m flood			
	Damage factor	Amount	Damage factor	Amount	Amount per block	Price per item [10^3 $]
Housing	0,07	0	0,23	0	3,5	1225
Household	0,48	0	0,59	0	3,5	70
Parks	0,6	0	0,85	0	1	8019
Monuments	0,65	1	0,91	0	1	206
Industry	0,4	50	0,63	22	2	10530
Business shutdown	0,8	50	1	22	5000	1
Roads	0,58	51	0,85	22	600	1,2
Vehicles	1	0	1	0	3,01	8

Table A.6: Anacostia riverbank, 4 m flood

	1 m flood		2.5 m flood		4 m flood		
	Damage factor	Amount	Damage factor	Amount	Damage factor	Amount	Amount per bloc
Housing	0,07	0	0,23	0	0,69	0	3,5
Household	0,48	0	0,59	0	0,82	0	3,5
Parks	0,6	0	0,85	0	0,98	0	1
Monuments	0,65	1	0,91	0	1	0	1
Industry	0,4	32	0,63	55	0,83	22	2
Business shutdown	0,8	32	1	55	1	22	5000
Roads	0,58	33	0,85	55	0,98	22	600
Vehicles	1	0	1	0	1	0	3,01

Table A.7: Anacostia riverbank, 5 m flood

	1 m flood		3 m flood		4.5 m flood		6 m flood
	Damage factor	Amount	Damage factor	Amount	Damage factor	Amount	Damage factor
Housing	0,07	23	0,35	3	0,91	6	1
Household	0,48	23	0,66	3	0,95	6	1
Parks	0,6	0	0,92	0	0,98	0	1
Monuments	0,65	0	1	1	1	0	1
Industry	0,4	46	0,75	26	1	60	1
Business shutdown	0,8	46	1	26	1	60	1
Roads	0,58	69	0,93	30	0,98	66	1
Vehicles	1	23	1	3	1	6	1

Table A.8: Anacostia riverbank, 6 m flood

	1 m flood		3 m flood		5 m flood		7 m flood
	Damage factor	Amount	Damage factor	Amount	Damage factor	Amount	Damage factor
Housing	0,07	25	0,35	21	1	27	1
Household	0,48	25	0,66	21	1	27	1
Parks	0,6	0	0,92	0	1	0	1
Monuments	0,65	0	1	0	1	0	1
Industry	0,4	12	0,75	33	1	50	1
Business shutdown	0,8	12	1	33	1	50	1
Roads	0,58	37	0,93	54	1	77	1
Vehicles	1	25	1	21	1	27	1

Table A.9: Anacostia riverbank, 10 m flood

	1 m flood		3 m flood		5 m flood		7 m flood
	Damage factor	Amount	Damage factor	Amount	Damage factor	Amount	Damage factor
Housing	0,07	19	0,35	25	1	21	1
Household	0,48	19	0,66	25	1	21	1
Parks	0,6	0	0,92	0	1	0	1
Monuments	0,65	0	1	0	1	0	1
Industry	0,4	22	0,75	12	1	33	1
Business shutdown	0,8	22	1	12	1	33	1
Roads	0,58	41	0,93	37	1	54	1
Vehicles	1	19	1	25	1	21	1

Table A.10: Anacostia riverbank, 12 m flood

To determine the cost of constructing new levees, the land value for the areas designated for the levees was computed. The landvalue Unit Cost (UC) depends on the distance of the land from downtown Washington DC. Land values depend on the distance from the city center in a quartic polynomial distribution (Albouy and Ehrlich, 2012), as seen in figure A.11.

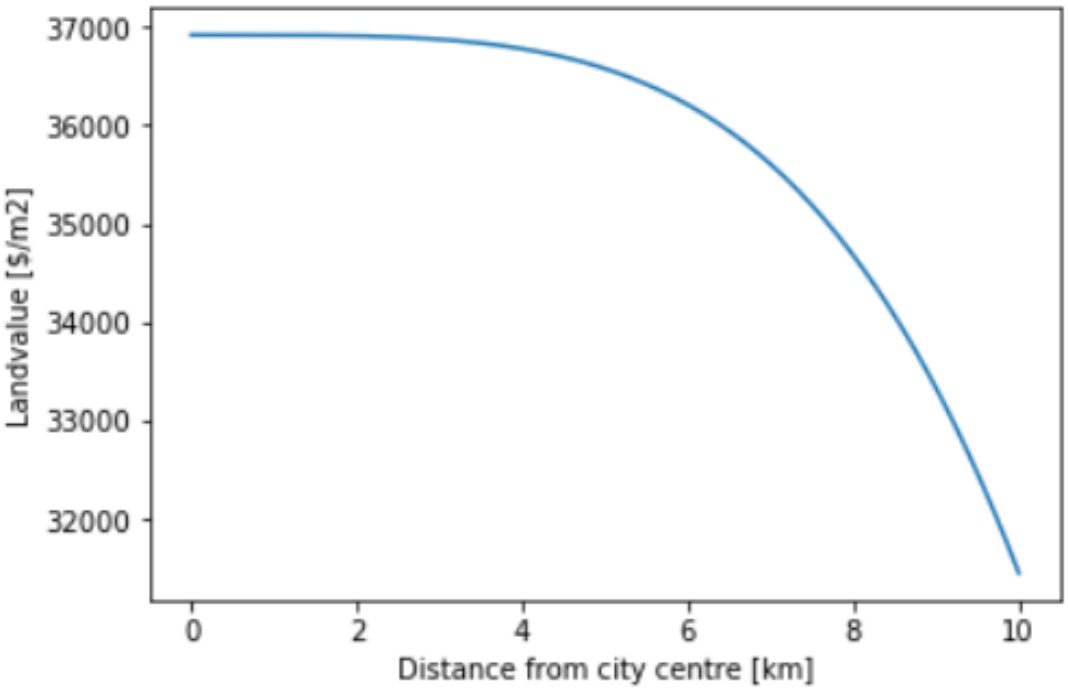

Figure A.11: Land values in Washington DC

B

ADCIRC equations

ADCIRC uses the generalized wave continuïty equation (GWCE) to compute the elevation at each node. The continuïty equation is given below.

$$\frac{\partial H}{\partial t} + \frac{\partial}{\partial y}(VH) + \frac{\partial}{\partial x}(UH) = 0 \tag{B.1}$$

Where U and V are the depth averaged velocity in x and y direction. H is the total water depth consisting of the depth and the surface elevation.

$$\frac{\partial^2 \zeta}{\partial t^2} + \frac{\partial}{\partial t \partial y}(VH) + \frac{\partial}{\partial t \partial x}(UH) + \tau_0 \frac{\partial H}{\partial t} + \tau_0 \frac{\partial}{\partial y}(VH) + \tau_0 \frac{\partial}{\partial x}(UH) = 0 \tag{B.2}$$

Using the product rule on the equation above gives the following equation

$$\frac{\partial^2 \zeta}{\partial t^2} + \frac{\partial \tilde{J}_x}{\partial x}(VH) + \frac{\partial \tilde{J}_y}{\partial y}(VH) - UH\frac{\partial \tau_0}{\partial x} - VH\frac{\partial \tau_0}{\partial y} = 0 \tag{B.3}$$

where

$$\begin{aligned} \tilde{J}_x &\equiv \frac{\partial}{\partial t}(UH) + \tau_0 UH = H\frac{\partial U}{\partial t} + U\frac{\partial \zeta}{\partial t}\tau_0 UH \\ \tilde{J}_y &\equiv \frac{\partial}{\partial t}(VH) + \tau_0 VH = H\frac{\partial V}{\partial t} + V\frac{\partial \zeta}{\partial t}\tau_0 VH \end{aligned} \tag{B.4}$$

The GWCE is multiplied with a weighing factor and integrated over the computational domain.

$$\left\langle \frac{\partial^2 \zeta}{\partial t^2}, \phi_j \right\rangle + \left\langle \frac{\partial \tilde{J}_x}{\partial x}, \phi_j \right\rangle + \left\langle \frac{\partial \tilde{J}_y}{\partial y}, \phi_j \right\rangle - \left\langle UH\frac{\partial \tau_0}{\partial x}, \phi_j \right\rangle - \left\langle VH\frac{\partial \tau_0}{\partial y}, \phi_j \right\rangle = 0 \tag{B.5}$$

$$\left\langle \frac{\partial^2 \zeta}{\partial t^2}, \phi_j \right\rangle + \left\langle \tilde{J}_x, \frac{\partial \phi_j}{\partial x} \right\rangle + \left\langle \tilde{J}_y, \frac{\partial \phi_j}{\partial y} \right\rangle - \left\langle UH\frac{\partial \tau_0}{\partial x}, \phi_j \right\rangle - \left\langle VH\frac{\partial \tau_0}{\partial y}, \phi_j \right\rangle + \int_\Gamma \left[\frac{\partial Q_x}{\partial t} + \tau_0 Q_N \right] \phi_j d\Gamma = 0 \tag{B.6}$$

$$\begin{aligned} \tilde{J}_x &= J_x - gh\frac{\partial \zeta}{\partial x} \\ \tilde{J}_y &= J_y - gh\frac{\partial \zeta}{\partial y} \end{aligned} \tag{B.7}$$

Now the momentum equation is subsituted into the equation for the $\tilde{J}$.

$$\begin{aligned} J_x &= -Q_x\frac{\partial U}{\partial x} - Q_y\frac{\partial U}{\partial y} + fQ_y - \frac{g}{2}\frac{\partial \zeta^2}{\partial x} - gH\frac{\partial [P_s/g\rho_0 - \alpha\eta]}{\partial x} + \frac{\tau_{sx}}{\rho_0} - \frac{\tau_{bx}}{\rho_0} + M_x - D_x - B_x + U\frac{\partial \zeta}{\partial t} + \tau_0 Q_x \\ J_y &= -Q_y\frac{\partial V}{\partial y} - Q_x\frac{\partial V}{\partial x} - fQ_x - \frac{g}{2}\frac{\partial \zeta^2}{\partial y} - gH\frac{\partial [P_s/g\rho_0 - \alpha\eta]}{\partial y} + \frac{\tau_{sy}}{\rho_0} - \frac{\tau_{by}}{\rho_0} + M_y - D_y - B_y + V\frac{\partial \zeta}{\partial t} + \tau_0 Q_y \end{aligned} \tag{B.8}$$

$$\left\langle \frac{\partial^2\zeta}{\partial t^2},\phi_j \right\rangle + \left\langle \tau_0\frac{\partial\zeta}{\partial t},\phi_j \right\rangle + \left\langle gh\frac{\partial\zeta}{\partial x},\frac{\partial\phi_j}{\partial x} \right\rangle + \left\langle gh\frac{\partial\zeta}{\partial y},\frac{\partial\phi_j}{\partial y} \right\rangle =$$
$$\left\langle J_x,\frac{\partial\phi_j}{\partial x} \right\rangle + \left\langle J_y,\frac{\partial\phi_j}{\partial y} \right\rangle - \left\langle UH\frac{\partial\tau_0}{\partial x},\phi_j \right\rangle - \left\langle VH\frac{\partial\tau_0}{\partial y},\phi_j \right\rangle + \int_\Gamma \left[\frac{\partial Q_x}{\partial t} + \tau_0 Q_N\right]\phi_j d\Gamma = 0 \tag{B.9}$$

$$\sum_{n=1}^{NE_j}\left\{\frac{A_n}{12}\left[\sum_{i=1}^{3}\phi_{i,j}\frac{\partial\zeta_i}{\partial t} + \overline{\tau}_{0,n}\sum_{i=1}^{3}\phi_{i,j}\frac{\partial\zeta_i}{\partial t}\right] + \frac{g\overline{h}_n}{4A_n}\left[b_j\sum_{\hat{i}=1}^{3}\zeta_i b_i + a_i\sum_{i=1}^{3}\zeta_i a_i\right]\right\}_n =$$
$$\sum_{n=1}^{NE_j}\frac{1}{2}\left\{\overline{J}_{xn}b_j + \overline{J}_{yn}a_j + \overline{Q}_{xn}\sum_{i=1}^{3}\tau_{0i}\frac{b_i}{3} + \overline{Q}_{yn}\sum_{i=1}^{3}\tau_{0i}\frac{a_i}{3}\right\}_n \tag{B.10}$$
$$-\sum_{n=1}^{2}\frac{L_n}{6}\left\{\sum_{n=1}^{2}\phi_{i,j}\left[\frac{\partial Q_{Ni}}{\partial t} + \overline{\tau}_{0n}Q_{Ni}\right]\right\}_n$$

Discretized in time using a finite difference method, gives the scheme shown below. Where $\alpha_{1,2,3}$ represent the time weighting factors, which can be used to specify a numerical scheme.

$$\sum_{n=1}^{NE_j}\left\{\frac{A_n}{12\Delta t}\left(\frac{1}{\Delta t}+\frac{\overline{\tau}_{0n}}{2}\right)\sum_{i=1}^{3}\phi_{i,j}\zeta_i^{*s+1} + \frac{g\overline{h}_n\alpha_1}{4A_n}\left[b_j\sum_{i=1}^{3}\zeta_i^{*s+1}b_i + a_j\sum_{i=1}^{3}\zeta_i^{*s+1}a_i\right]\right\} =$$
$$\sum_{n=1}^{NE_j}\left\{\frac{A_n}{12\Delta t}\left(\frac{1}{\Delta t}+\frac{\overline{\tau}_{0n}}{2}\right)\sum_{i=1}^{3}\phi_{i,j}\zeta_i^{*s} - \frac{g\overline{h}_n\alpha_1}{4A_n}\left[(\alpha_1+\alpha_2)\left(b_j\sum_{i=1}^{3}\zeta_i^s b_i + a_j\sum_{i=1}^{3}\zeta_i^s a_i\right) + \alpha_3\left(b_j\sum_{i=1}^{3}\zeta_i^{s-1}b_i + a_j\sum_{i=1}^{3}\zeta_i^{s-1}a_i\right)\right]\right.$$
$$\left. + \frac{1}{2}\left[\overline{J}_{xn}^s b_j + \overline{J}_{yn}^s a_j\right] + \frac{1}{6}\left[\overline{Q}_{x_n}^s\sum_{i=1}^{3}\tau_{0i}b_i + \overline{Q}_{y_n}^s\sum_{i=1}^{3}\tau_{0i}a_i\right]\right\}$$
$$-\sum_{n=1}^{2}\left\{\frac{L_n}{6}\sum_{i=1}^{2}\phi_{i,j}\left[\frac{Q_{Ni}^{s+1}-Q_{Ni}^{s-1}}{2\Delta t} + \overline{\tau}_{0n}Q_{Ni}^s\right]\right\} \tag{B.11}$$

$$\overline{J}_{xn}^s \equiv -\frac{\overline{Q}_{xn}^s}{2A_n}\sum_{i=1}^{3}U_i^s b_i - \frac{\overline{Q}_{yn}^s}{2A_n}\sum_{i=1}^{3}U_i^s a_i + f\overline{Q}_{yn}^s - \frac{g}{4A_n}\sum_{i=1}^{3}\zeta_i^{2^s}b_i - \frac{g\overline{H}_i^s}{2A_n}\sum_{i=1}^{3}\left[P_s/g\rho_0 - \alpha\eta\right]_i^s b_i$$
$$+\overline{\left(\frac{\tau_{sx}}{\rho_0}\right)}_n^s - \overline{\left(\frac{\tau_{bx}}{\rho_0}\right)}_n^s + \overline{M}_{xn}^s - \overline{D}_{xn}^s - \overline{B}_{xn}^s + U_n^s\frac{\zeta_n^{*s}}{\Delta t} + \overline{(\tau_0 Q_x)}_n^s \tag{B.12}$$

$$\overline{J}_{yn}^s \equiv -\frac{\overline{Q}_{xn}^s}{2A_n}\sum_{i=1}^{3}V_i^s b_i - \frac{\overline{Q}_{yn}^s}{2A_n}\sum_{i=1}^{3}V_i^s a_i - f\overline{Q}_{xn}^s - \frac{g}{4A_n}\sum_{i=1}^{3}\zeta_i^{2^s}a_i - \frac{g\overline{H}_i^s}{2A_n}\sum_{i=1}^{3}\left[P_s/g\rho_0 - \alpha\eta\right]_i^s a_i$$
$$+\overline{\left(\frac{\tau_{sy}}{\rho_0}\right)}_n^s - \overline{\left(\frac{\tau_{by}}{\rho_0}\right)}_n^s + \overline{M}_{yn}^s - \overline{D}_{yn}^s - \overline{B}_{yn}^s + V_n^s\frac{\zeta_n^{*s}}{\Delta t} + \overline{(\tau_0 Q_y)}_n^s \tag{B.13}$$

$$M_x \equiv \frac{\partial H\tau_{xx}}{\partial x} + \frac{\partial H\tau_{yx}}{\partial y}$$
$$M_y \equiv \frac{\partial H\tau_{xy}}{\partial x} + \frac{\partial H\tau_{yy}}{\partial y} \tag{B.14}$$

These equations cannot be easily solved, because of the importance of the flow fluctuations. Instead an approximation is made by means of the lateral eddy viscosity as shown below.

$$H\tau_{i,j} = E_h\left[\frac{\partial Q_j}{\partial i} + \frac{\partial Q_i}{\partial j}\right]; i = x,y; j = x,y \tag{B.15}$$

To obtain information about the velocity the momentum equations are solved in the x,y plane.

$$\begin{aligned}\frac{\partial U}{\partial t}+U\frac{\partial U}{\partial x}+V\frac{\partial U}{\partial y}-fV&=-g\frac{\partial[\zeta+P_s/g\rho_0-\alpha\eta]}{\partial x}+\frac{\tau_{sx}}{H\rho_0}-\frac{\tau_{bx}}{H\rho_0}+\frac{M_x}{H}-\frac{D_x}{H}-\frac{B_x}{H}\\ \frac{\partial V}{\partial t}+U\frac{\partial V}{\partial x}+V\frac{\partial V}{\partial y}-fU&=-g\frac{\partial[\zeta+P_s/g\rho_0-\alpha\eta]}{\partial y}+\frac{\tau_{sy}}{H\rho_0}-\frac{\tau_{by}}{H\rho_0}+\frac{M_y}{H}-\frac{D_y}{H}-\frac{B_y}{H}\end{aligned} \tag{B.16}$$

The bottom friction is estimated as follows

$$\frac{\tau_{bx}}{\rho_0}=K_{slip}U\frac{\tau_{by}}{\rho_0}=K_{slip}V \tag{B.17}$$

Where the drag coefficient K_{slip} can be a constant or approximated quadratically using the following equation.

$$K_{slip}=C_D\sqrt{U^2+V^2} \tag{B.18}$$

Similar to the GWCE this the momentum equation is multiplied with a weighing factor ϕ and integrated over the computational domain.

$$\begin{aligned}\left\langle\frac{\partial U}{\partial t},\phi_j\right\rangle+\left\langle U\frac{\partial U}{\partial x},\phi_j\right\rangle+\left\langle V\frac{\partial U}{\partial y},\phi_j\right\rangle-\left\langle fV,\phi_j\right\rangle&=-\left\langle g\frac{\partial[\zeta+P_s/g\rho_0-\alpha\eta]}{\partial x},\phi_j\right\rangle+\\ \left\langle\frac{\tau_{sx}}{H\rho_0},\phi_j\right\rangle-\left\langle\frac{\tau_{bx}}{H\rho_0},\phi_j\right\rangle+\left\langle\frac{M_x}{H},\phi_j\right\rangle-\left\langle\frac{D_x}{H},\phi_j\right\rangle-\left\langle\frac{B_x}{H},\phi_j\right\rangle&\\ \left\langle\frac{\partial V}{\partial t},\phi_j\right\rangle+\left\langle U\frac{\partial V}{\partial x},\phi_j\right\rangle+\left\langle V\frac{\partial V}{\partial y},\phi_j\right\rangle-\left\langle fU,\phi_j\right\rangle&=\left\langle-g\frac{\partial[\zeta+P_s/g\rho_0-\alpha\eta]}{\partial y},\phi_j\right\rangle+\\ \left\langle\frac{\tau_{sy}}{H\rho_0},\phi_j\right\rangle-\left\langle\frac{\tau_{by}}{H\rho_0},\phi_j\right\rangle+\left\langle\frac{M_y}{H},\phi_j\right\rangle-\left\langle\frac{D_y}{H},\phi_j\right\rangle-\left\langle\frac{B_y}{H},\phi_j\right\rangle&\end{aligned} \tag{B.19}$$

Discretizing the integral gives the following results

$$\begin{aligned}\frac{\partial U_j}{\partial t}+\frac{1}{A_{NE_j}}\sum_{n=1}^{NE_j}A_n\left[\overline{U}_n\left(\frac{\partial U}{\partial x}\right)_n+\overline{V}_n\left(\frac{\partial U}{\partial y}\right)_n\right]-fV_j&=-\frac{g}{A_{NE_j}}\sum_{n=1}^{NE_j}A_n\left(\frac{\partial[\zeta+P_s/g\rho_0-\alpha\eta]}{\partial x}\right)_n+\\ \left(\frac{\tau_{sx}}{H\rho_0}\right)_n-\left(\frac{K_{slip}U}{H\rho_0}\right)-\frac{3}{H_jA_{NE_j}}\sum_{n=1}^{NE_j}A_n\left(H\tau_{xx}\frac{\partial\phi_j}{\partial x}+H\tau_{yx}\frac{\partial\phi_j}{\partial y}\right)_n-\frac{1}{A_{NE_j}}\sum_{n=1}^{NE_j}A_n\left(\frac{B_x}{H}\right)_n&\\ \frac{\partial V_j}{\partial t}+\frac{1}{A_{NE_j}}\sum_{n=1}^{NE_j}A_n\left[\overline{U}_n\left(\frac{\partial V}{\partial x}\right)_n+\overline{V}_n\left(\frac{\partial V}{\partial y}\right)_n\right]+fU_j&=-\frac{g}{A_{NE_j}}\sum_{n=1}^{NE_j}A_n\left(\frac{\partial[\zeta+P_s/g\rho_0-\alpha\eta]}{\partial y}\right)_n+\\ \left(\frac{\tau_{sy}}{H\rho_0}\right)_n-\left(\frac{K_{slip}V}{H\rho_0}\right)-\frac{3}{H_jA_{NE_j}}\sum_{n=1}^{NE_j}A_n\left(H\tau_{xy}\frac{\partial\phi_j}{\partial x}+H\tau_{yy}\frac{\partial\phi_j}{\partial y}\right)_n-\frac{1}{A_{NE_j}}\sum_{n=1}^{NE_j}A_n\left(\frac{B_y}{H}\right)_n&\end{aligned} \tag{B.20}$$

The equation is discretized in time as follows.

$$\begin{aligned}\left[1+\frac{\Delta tK^s_{slip_j}}{2H_j^{s+1}}\right]U_j^{s+1}-\frac{f\Delta t}{2}V_j^{s+1}&=\left[1+\frac{\Delta tK^s_{slip_j}}{2H_j^{s+1}}\right]U_j^s-\frac{\Delta t}{A_{NE_j}}\sum_{n=1}^{NE_j}A_n\left[\overline{U}^s_n\left(\frac{\partial U^s}{\partial x}\right)+\overline{V}^s_n\left(\frac{\partial U^s}{\partial y}\right)\right]\\ &+\frac{\Delta tfV_j^s}{2}-\frac{g\Delta t}{A_{NE_j}}\sum_{n=1}^{NE_j}A_n\left(\frac{\partial[\zeta+P_s/g\rho_0-\alpha\eta]^s}{\partial x}+\frac{\partial[\zeta+P_s/g\rho_0-\alpha\eta]^{s+1}}{\partial x}\right)_n\\ &+\frac{\Delta t}{2}\left[\frac{\tau^{s+1}_{sx_j}}{H_j^{s+1}\rho_0}+\frac{\tau^s_{sx_j}}{H_j^s\rho_0}\right]-\frac{3\Delta t}{H_j^sA_{NE_j}}\sum_{n=1}^{NE_j}A_n\left(H\tau^s_{xx}\frac{\partial\phi_j}{\partial x}+H\tau^s_{yx}\frac{\partial\phi_j}{\partial y}\right)_n-\frac{\Delta t}{A_{NE_j}}\sum_{n=1}^{NE_j}A_n\left(\frac{B_x}{H}\right)^s_n\\ \left[1+\frac{\Delta tK^s_{slip_j}}{2H_j^{s+1}}\right]V_j^{s+1}+\frac{f\Delta t}{2}U_j^{s+1}&=\left[1+\frac{\Delta tK^s_{slip_j}}{2H_j^{s+1}}\right]V_j^s-\frac{\Delta t}{A_{NE_j}}\sum_{n=1}^{NE_j}A_n\left[\overline{U}^s_n\left(\frac{\partial V^s}{\partial x}\right)+\overline{V}^s_n\left(\frac{\partial V^s}{\partial y}\right)\right]\\ &-\frac{\Delta tfU_j^s}{2}-\frac{g\Delta t}{A_{NE_j}}\sum_{n=1}^{NE_j}A_n\left(\frac{\partial[\zeta+P_s/g\rho_0-\alpha\eta]^s}{\partial y}+\frac{\partial[\zeta+P_s/g\rho_0-\alpha\eta]^{s+1}}{\partial y}\right)_n\\ &+\frac{\Delta t}{2}\left[\frac{\tau^{s+1}_{sy_j}}{H_j^{s+1}\rho_0}+\frac{\tau^s_{sy_j}}{H_j^s\rho_0}\right]-\frac{3\Delta t}{H_j^sA_{NE_j}}\sum_{n=1}^{NE_j}A_n\left(H\tau^s_{xy}\frac{\partial\phi_j}{\partial x}+H\tau^s_{yy}\frac{\partial\phi_j}{\partial y}\right)_n-\frac{\Delta t}{A_{NE_j}}\sum_{n=1}^{NE_j}A_n\left(\frac{B_y}{H}\right)^s_n\end{aligned} \tag{B.21}$$

C

Levee elevation

The levees used in this research were:

- The Washington DC National Mall levee;
- The Washington DC temporary flood defense;
- The Anacostia levee;

All levees and temporary defenses heights were taken from the National Levee database and can be found in the figures below. The Washington DC National Mall contains in its levee a temporary defense that is in normal times not close, this can be seen with figure E.1. However this temporary defense can be closed in times of flooding and therefore a height of 5,5m was assumed due to the lack of information, this can be seen in figure C.2.

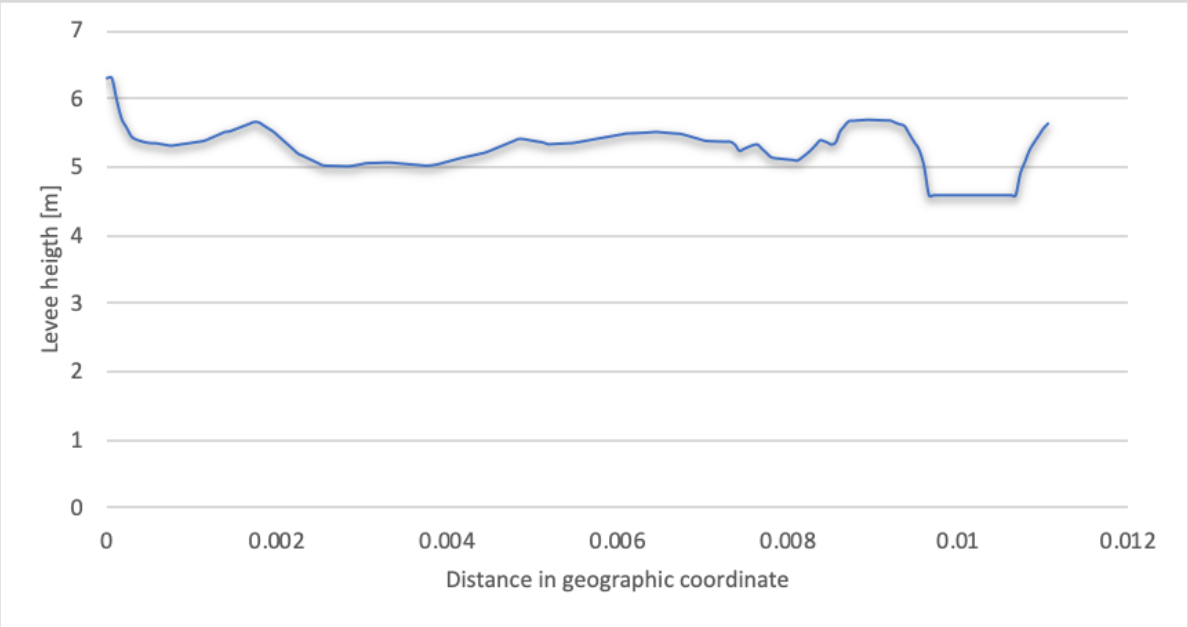

Figure C.1: Washington DC National Mall Levee without temporary flood defense

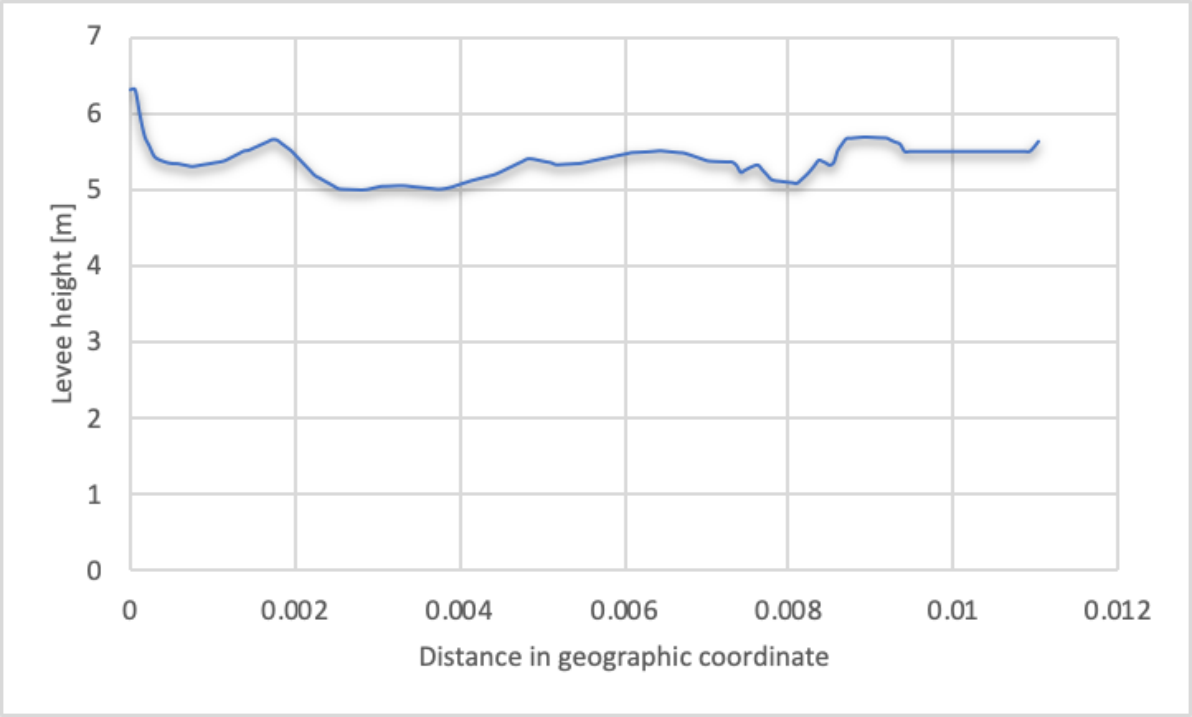

Figure C.2: Washington DC National Mall Levee with temporary flood defense

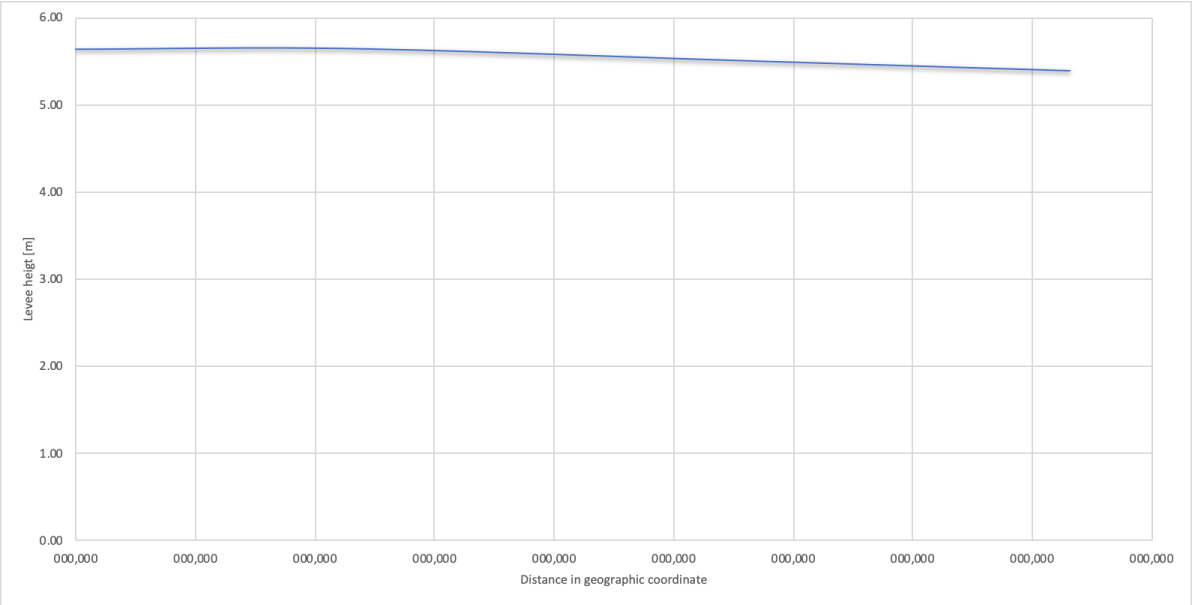

Figure C.3: Washington DC temporary flood defense

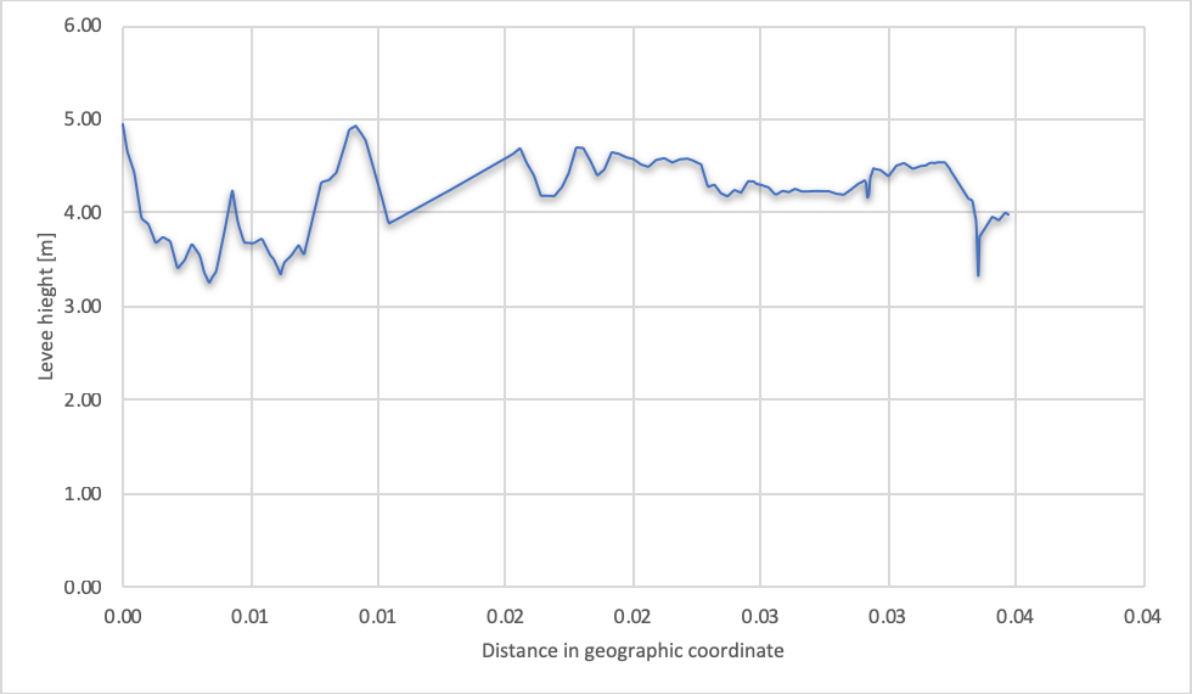

Figure C.4: Anacostia levee

D

Stampede2

Stampede2 is the platform used to access a supercomputer needed to run the model due to its high number of nodes. Stampede2 was used with 2 other tools:

- winSPC, used to prepare the files for the simulation;
- Putty, used to send the simulations to the super computer

Two queue lines could be used in stampede 2, see figure D.1. The faster queue line was the development queue which was made for new users that were still learning how to use the supercomputer. The second one was the normal queue line where longer job could be submitted and multiple job could be sent at the same time. The development queue line had a limit of 2hours to run and could run only one job at the time but was faster in the waiting line. Therefore this queue line was often used to test out the parameters. For longer runs of maximum 48hours the normal queue was used which could also compute multiple simulations at the time.

Queue Name	Node Type	Max Nodes per Job (assoc'd cores)*	Max Duration	Max Jobs in Queue*	Charge Rate (per node-hour)
development	KNL cache-quadrant	16 nodes (1,088 cores)*	2 hrs	1*	1 Service Unit (SU)
normal	KNL cache-quadrant	256 nodes (17,408 cores)*	48 hrs	50*	1 SU
large**	KNL cache-quadrant	2048 nodes (139,264 cores)*	48 hrs	5*	1 SU
long	KNL cache-quadrant	32 nodes (2,176 cores)*	120 hrs	2*	1 SU
flat-quadrant	KNL flat-quadrant	32 nodes (2,176 cores)*	48 hrs	5*	1 SU
skx-dev	SKX	4 nodes (192 cores)*	2 hrs	1*	1 SU
skx-normal	SKX	128 nodes (6,144 cores)*	48 hrs	25*	1 SU
skx-large**	SKX	868 nodes (41,664 cores)*	48 hrs	3*	1 SU

Figure D.1: Queue lines in Stampede2

Furthermore the model itself was cut in a number of elements, usually 48 or 96, in order for it to run faster. This was all done in win SPC, see figure D.2 with the job2.2 file. The simulation could be ran with the following input files: fort.14, fort.15, fort.19 and fort.20. Once these files were copied to winSPC, an ADCPREP command needed to be done to prepare the model and the job could be sent with the 'sbatch' command on putty, see figure D.3

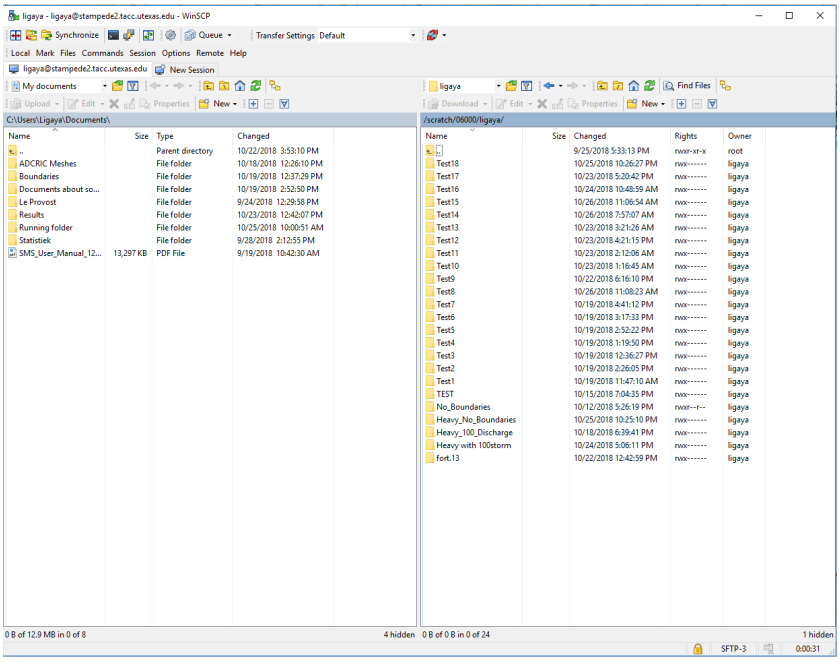

Figure D.2: winSPC window

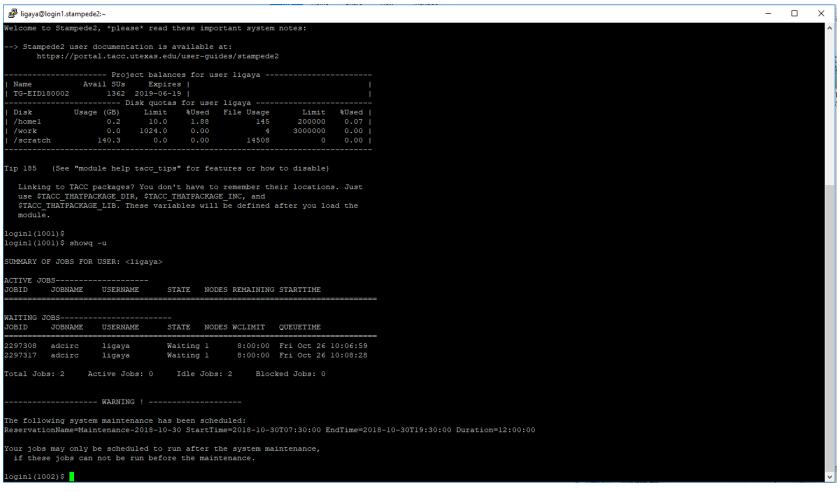

Figure D.3: Putty window

E

Simulations

For this research many simulations were made in order to find the best parameters for the simulation. Below the table with the different simulations made can be found.

The first simulation were ran without dikes, using only the cut model of the existing mesh.

Later other simulations were made using the model with dikes and with the temporary defense at the National Mall levee. The tables E.2 and E.3 contains the runs with the 1/100 year flooding dominated by the Potomac discharge and the table E.4 with the 1/100 year flooding dominated by the storm water levels.

File computer name		No_Dikes_4	No_Dikes_4	No_Dikes_4
Dikes		NO	NO	NO
File super computer		Test6	Test5	Test3
Running process		Super computer (normal)	Super computer (dev)	Super computer (dev)
Comments		Testing Tau0	More time	Testing the default parameters
Testing parameters	Bottom friction [-]	0.0025	0.0025	0.0025
	Tau0 [-]	-1	0.005	0.005
	Eddy [m2/s]	**2**	**2**	**2**
	Hmin [m]	0.01	0.01	0.05
	Umin [m/s]	0.01	0.01	0.05
Model control	Model	2DDI	2DDI	2DDI
	Ramp time [days]	2	2	2
	Time step [sec]	0.1	0.1	0.1
Running info	n	1	1	1
	N	96	96	96
	Software (dev, normal...)	normal	dev	dev
	Run model time	02:30	02:00:00	02:00
	Run ID	2268838	2269065	2268108
Results	Error	Elevation error	Elevation error	Elevation error
	Time started	13:19:25	13:52:22	11:19:31
	Time stopped	14:17:33	14:30:02	11:36:27
	Time runned	00:58:08	00:37:40	00:16:56
Time runned in Model [sec]		2.48E+04	1.69E+04	8.15E+03
Comments		Error nead the potomac river	Error nead the potomac river	Error by the Potomac River

Figure E.1: Simulations without dikes

File computer name		Me_Idiot	Me_Idiot	Me_Idiot	Me_Idiot	Me_Idiot	Me_Idiot	Me_Idiot	Me_Idiot	Me_Idiot	Me_Idiot
Dikes		YES	YES	YES	YES	YES	YES	YES	YES	YES	YES
File super computer		ME_IDIOT	Cf_DRAMP	ME_IDIOT	U0 + DRAMP	TestU0	TestU0 with 120/120	Extreme_eddy	Extreme_eddy	cf	Tau0
Running process		Super computer (dev)	Super computer (dev)	Super computer (dev)	Super computer (dev)	Super computer (dev)	Super computer (dev)	Super computer (dev)	Super computer (dev)	Super computer (dev)	Super computer (dev)
Comments		Influence of ramp time	check cf (longer)	Check the new tidal boundary with default friction	Check the new tidal boundary with default friction	Check the new tidal boundary with default friction	Check the new tidal boundary with default friction	Check the new tidal boundary with default friction	Check the new tidal boundary with default friction	cf+DRAMP+U0	cf+DRAMP+U0
Testing parameters	Bottom friction [-]	0.0025	0.025	0.0025	0.0025	0.0025	0.0025	0.0025	0.0025	0.025	0.025
	Tau0 [-]	0.01	0.05	0.01	0.01	0.01	0.01	0.05	0.01	0.05	-1
	Eddy [m2/s]	10	10	10	10	10	10	50	50	10	10
	Hmin [m]	0.01	0.01	0.01	0.01	0.01	0.01	0.01	0.01	0.01	0.01
	Umin [m/s]	0.05	0.05	0.05	0.01	0.01	0.01	0.05	0.05	0.01	0.01
Model control	Model	2DDI	2DDI	2DDI	2DDI	2DDI	2DDI	2DDI	2DDI	2DDI	2DDI
	Ramp time [days]	1	1	0.5	1	0.5	0.5	0.5	0.5	1	1
	Time step [sec]	0.1	0.1	0.1	0.1	0.1	0.1	0.1	0.1	0.1	0.05
Running info	n	1	1	1	1	1	1	1	1	1	1
	N	96	96	96	96	96	96	96	96	96	96
	Software (dev, normal...)	normal	dev	normal	normal	normal	normal	normal	normal	dev	normal
	Run model time	05:55	02:55	05:55	05:55	05:55	05:55	05:55	00:55	02:55	06:55
	Run ID	2267821	2269235	22678119	2268559	2268165	2268314	2268853	2268853	2269238	2273002
Results	Error	Elevation error	Elevation error	Elevation error	Elevation error	Elevation error	Elevation error	Elevation error	Elevation error	elevation error	Elevation error
	Time started	11:19	15:10	10:23	12:35:00	11:38	12:07	13:22	15:54	15:17	16:16
	Time stopped	11:44	18:00	10:34	12:57	11:53	12:21	13:22	15:54	17:22	21:00
	Time runned	00:25	02:50	00:11	00:22	00:15	00:14	00:00	00:00	02:05	04:44
Time runned in Model [sec]		1.15E+04	8.05E+04	4.40E+03	1.06E+04	6.87E+03	6.87E+03	4.96E+01	4.97E+01	5.92E+04	5.31E+04
Comments		downstream err			Combination not perfect	downstream err	No effect from mid params				tau -1 is not perfect

Figure E.2: Simulation with 1/100 flooding dominated by the Potomac discharge

File computer name		Tau/longrun	Tau/Heightened eddy	Dike_4	Dike_4	Dike_4	Dike_4	Dike_4	Dike_4	Dike_4	Dike_4
Dikes		YES	YES	YES	YES	YES	YES	YES	YES	YES	YES
File super computer		Tau0	Tau0	Test10	Test13	Test9	Test11	Test8	Test8	Test8	Test12
Running process		Super computer (dev)	Super computer (dev)	Super computer (normal)	Super computer (normal)	Super computer (normal)	Super computer (normal)	Super computer (normal)	Super computer (normal)	Super computer (normal)	Super computer (normal)
Comments		cf+DRAMP+U0	cf+DRAMP+U0	Testing the time step	Testing the time step	Testing the time step	Testing the time step	Testing the time step	Testing the time step	Testing the time step	Testing the time step
Testing parameters	Bottom friction [-]	0.05	0.05	0.05	0.05	0.05	0.05	0.0025	0.0025	0.025	0.05
	Tau0 [-]	0.5	0.5	-1	-1	-1	-1	-1	-1	-1	-1
	Eddy [m2/s]	10	20	10	10	2	10	2	10	10	2
	Hmin [m]	0.01	0.01	0.05	0.01	0.05	0.01	0.01	0.05	0.05	0.01
	Umin [m/s]	0.01	0.01	0.05	0.05	0.05	0.01	0.01	0.05	0.05	0.05
Model control	Model	2DDI	2DDI	2DDI	2DDI	2DDI	2DDI	2DDI	2DDI	2DDI	2DDI
	Ramp time [days]	1	1	2	2	2	1	2	2	2	1
	Time step [sec]	0.05	0.05	0.1	0.1	0.1	0.1	0.02	0.1	0.1	0.1
Running info	n	1	1	1	1	1	1	1	1	1	1
	N	96	96	96	96	96	96	96	48	48	96
	Software (dev, normal...)	normal	normal	normal	normal	normal	normal	normal	normal	normal	normal
	Run model time	14:55	06:55	04:00	04:00	02:00	04:30	04:30	04:00	04:00	03:00
	Run ID	2274202	2278990	2281569	2281577	2280450	2281588	2269742	2288307	2288740	2283953
Results	Error	Elevation error	Elevation error	Elevation error	Elevation error	Elevation error	Elevation error	Elevation error	Elevation error	Elevation error	Elevation error
	Time started	08:07	23:14	21:38:53	23:41:46	15:18:04	00:18:20	14:55:01	11:09	11:57	13:23
	Time stopped	15:11	05:52	00:16:45	02:21:26	17:16:10	01:12:06	18:59:29	11:41	14:48	15:21
	Time runned	07:04	06:38	02:37:52	02:39:40	01:58:06	00:53:46	04:04:28	00:31	02:50	01:57
Time runned in Model [sec]		9.77E+04	8.00E+04	7.36E+04	6.82E+04	5.60E+04	2.58E+04	2.48E+04	1.33E+04	7.17E+04	5.50E+04
Comments		errors downstream		Short elevation warning. Error at boundary downstream	Short elevation warning. Error at boundary downstream	Long elevation error. Error at downstream boundary	Short elevation warning. Error at boundary downstream	Error by the downstream boundary		a lot of elevation error	

Figure E.3: Simulation with 1/100 flooding dominated by the Potomac discharge

File computer name		Dike_4	Dike_4	Dike_4	Dike_4	Dike_4	Dike_4
Dikes		YES	YES	YES	YES	YES	YES
File super computer		Test15	Test15	Test15	Test15	Test15	Test15
Running process		Super computer (normal)	Super computer (normal)	Super computer (normal)	Super computer (normal)	Super computer (normal)	Super computer (normal)
Comments		100storm	100storm	100storm	100storm	100storm	100storm
Testing parameters	Bottom friction [-]	0.05	0.0025	0.05	**0.025**	0.05	0.05
	Tau0 [-]	-1	-1	-1	-1	-1	-1
	Eddy [m2/s]	10	10	10	10	10	10
	Hmin [m]	0.05	0.05	**0.01**	0.05	0.05	0.1
	Umin [m/s]	0.05	0.05	0.05	0.05	0.05	0.05
Model control	Model	2DDI	2DDI	2DDI	2DDI	2DDI	2DDI
	Ramp time [days]	1	1	1	1	**2**	**2**
	Time step [sec]	**0.1**	**0.1**	**0.1**	**0.1**	**0.1**	**0.1**
Running info	n	1	1	1	1	1	1
	N	96	96	48	48	48	48
	Software (dev, normal...)	dev	normal	normal	normal	normal	normal
	Run model time	03:00	03:00	03:00	03:00	04:00	06:00
	Run ID	2285963	2288250	2288544	2289666	2293062	2294894
Results	Error	Elevation error	Elevation error	Elevation error	Elevation error	Elevation error	Elevation error
	Time started	16:35	10:34:53	11:21:56	14:48	09:05:37	21:21:18
	Time stopped	19:28:22	10:57:08	14:03:10	17:00	12:29:42	23:17:05
	Time runned	02:53:17	00:22:15	02:41:14	02:11	03:24:05	01:55:47
Time runned in Model [sec]		8.35E+04	8.92E+03	7.17E+04	5.30E+04	9.04E+04	4.95E+04

Figure E.4: Simulation with 1/100 flooding dominated by the storm water levels

F

Results of ADCIRC model

The created model was tested with many different parameters and boundary conditions. However, none of those simulations were stable and therefore most of the results were disregarded. A few water elevation files (fort.63) were kept and the results can be seen below.

The existing mesh was ran in ADCIRC using no upstream river boundaries and a tidal boundary at the downstream end, this was done to test if the existing model worked. The model ran for 1day 23hours but was then unfortunately stopped due to the lack of time given to run. The water elevation of the simulation can be found below. This simulation was done using only the standard parameters of ADCIRC.

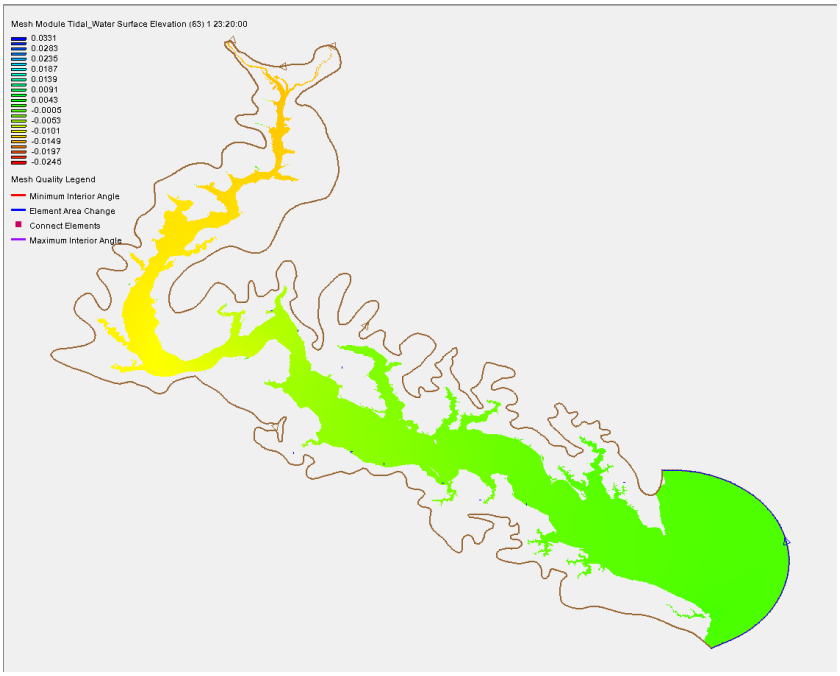

Figure F.1: Result of the simulation of the existing mesh

Later the model was tested with as boundary conditions the 1/100 year flood with maximum discharge. This model ran for almost one day and the results can be found with figure F.2. The same model was ran for the 1/100 year flood with maximum storm and computed water elevation for almost a day, the results are found with figure F.3.

The parameters used for both simulations can be found in Appendix E.

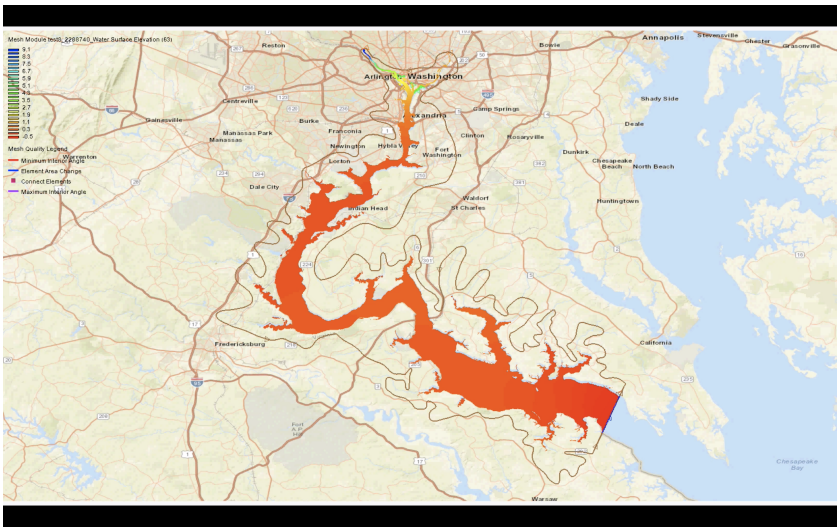

Figure F.2: Result of the simulation with run ID 2288740

Figure F.3: Result of the simulation with run ID 2293062

G

Stability Analysis

The results of the failure envelopes of the stability analysis carried out in W-Slope are presented below.

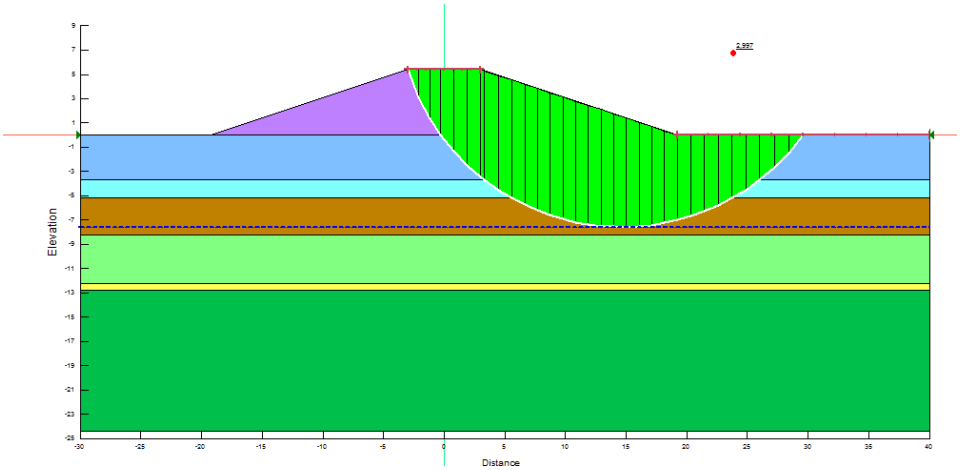

Figure G.1: Factor of Safety against rotation and failure envelope of the 1/100 year levee at the Anacostia bank just after construction

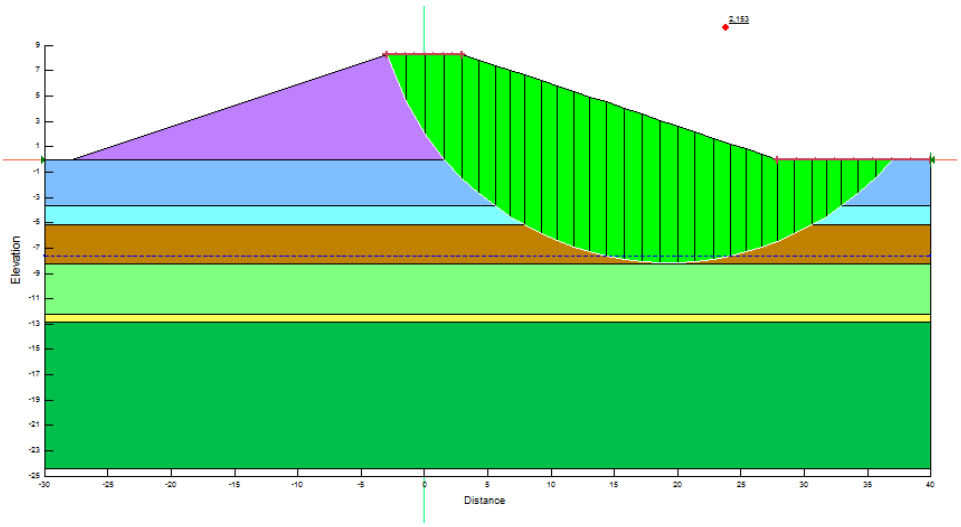

Figure G.2: Factor of Safety against rotation and failure envelope of the 1/373 year levee at the Anacostia bank just after construction

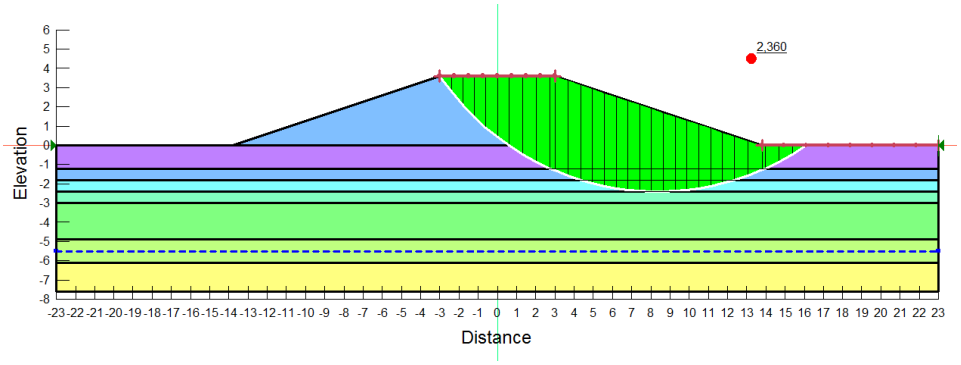

Figure G.3: Factor of Safety against rotation and failure envelope of the 1/100 year levee at the National Mall just after construction

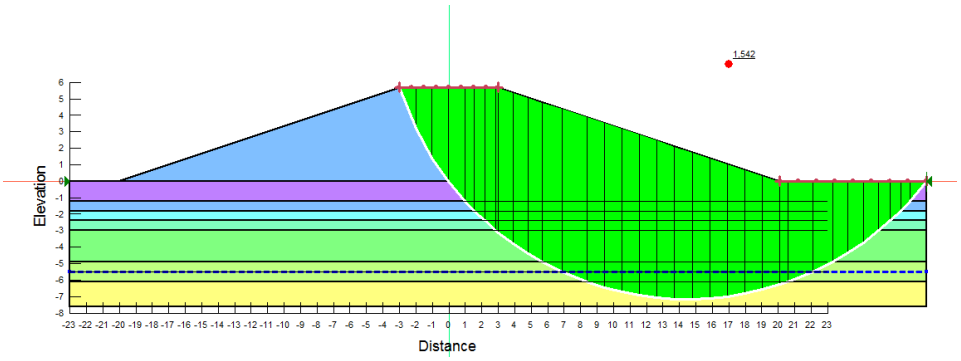

Figure G.4: Factor of Safety against rotation and failure envelope of the 1/263 year levee at the National Mall just after construction

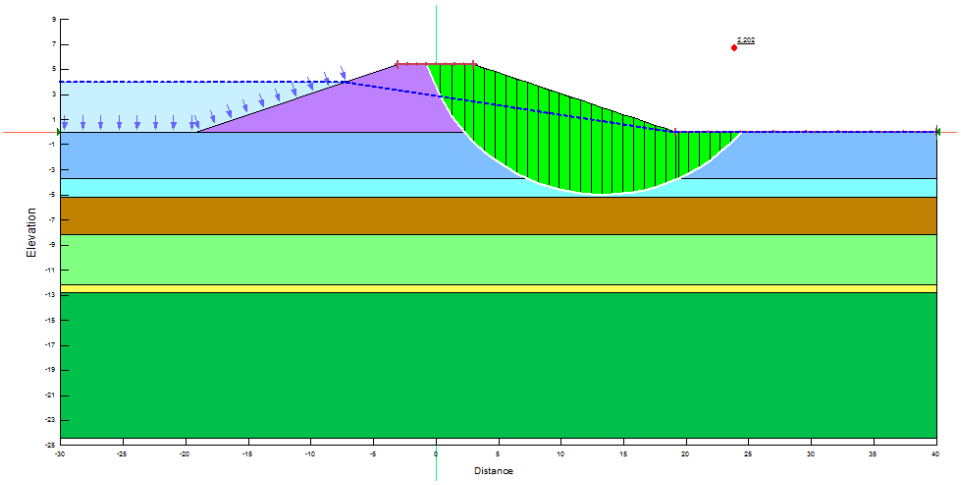

Figure G.5: Factor of Safety against rotation and failure envelope of the 1/100 year levee at the Anacostia bank during a long term flood event

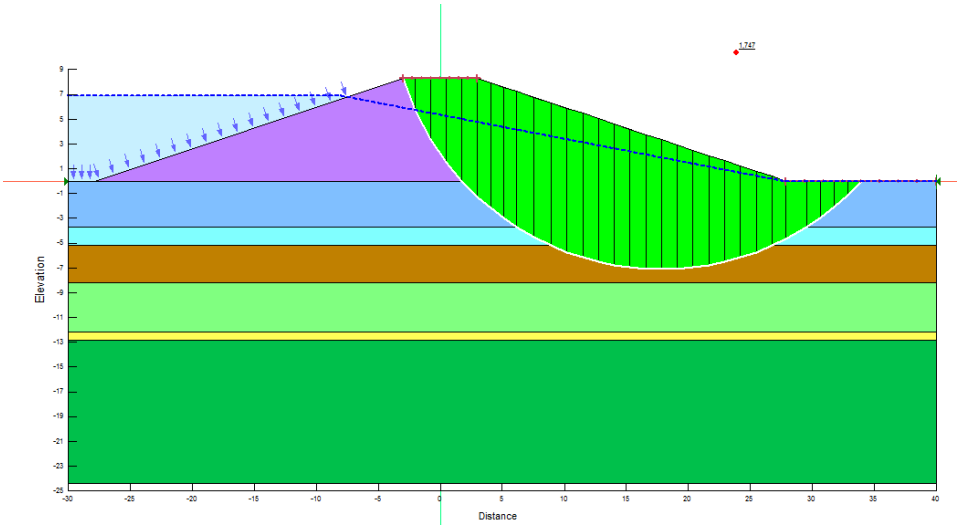

Figure G.6: Factor of Safety against rotation and failure envelope of the 1/373 year levee at the Anacostia bank during a long term flood event

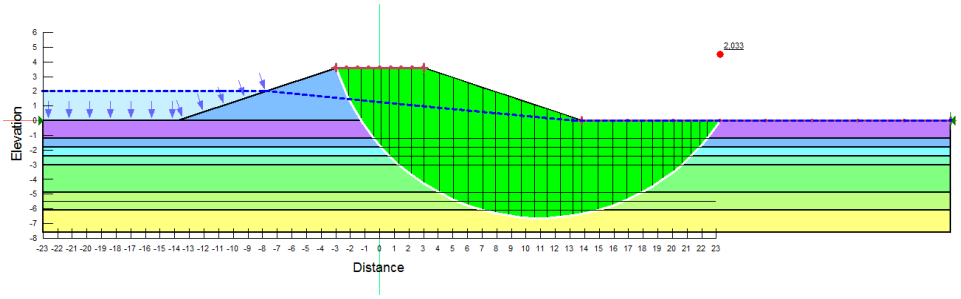

Figure G.7: Factor of Safety against rotation and failure envelope of the 1/100 year levee at the National Mall during a long term flood event

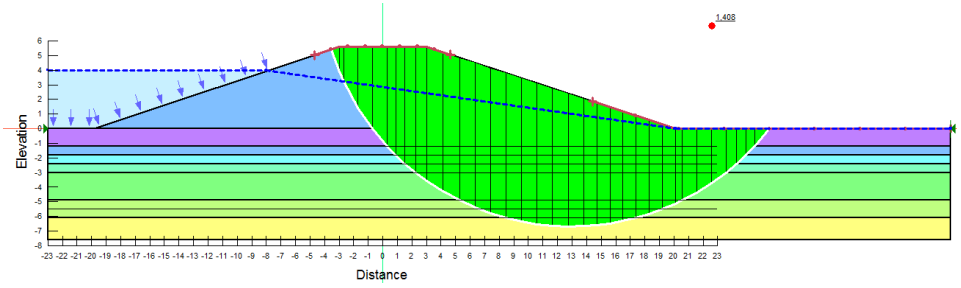

Figure G.8: Factor of Safety against rotation and failure envelope of the 1/263 year levee at the National Mall during a long term flood event

Boundary time series

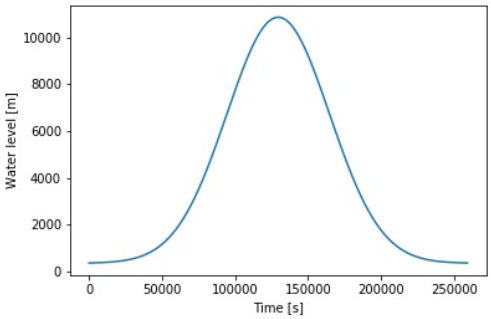

Figure H.1: Upstream boundary, 100 year, river dominance

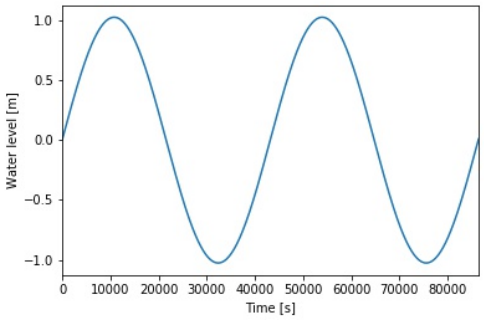

Figure H.2: Downstream boundary, 100 year, river dominance

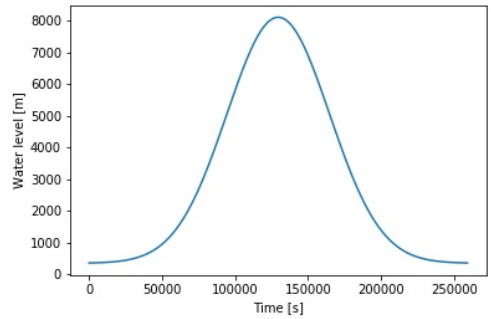

Figure H.3: Upstream boundary, 100 year, river dominance

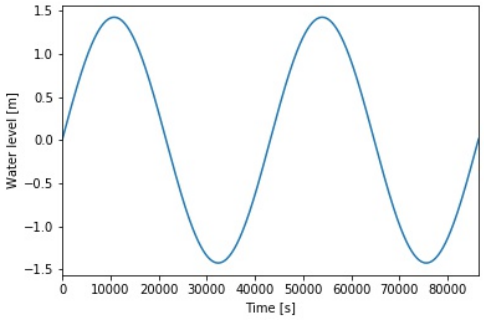

Figure H.4: Downstream boundary, 100 year, river dominance

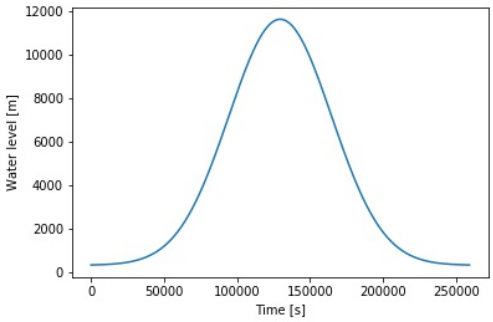

Figure H.5: Upstream boundary 263 year, river dominance

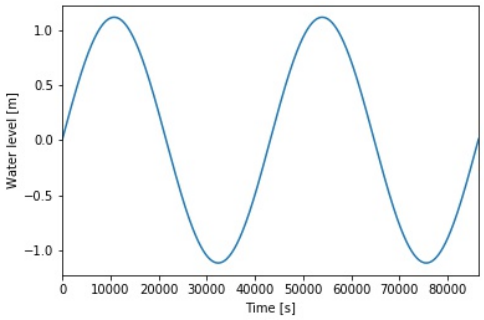

Figure H.6: Downstream boundary 263 year, river dominance

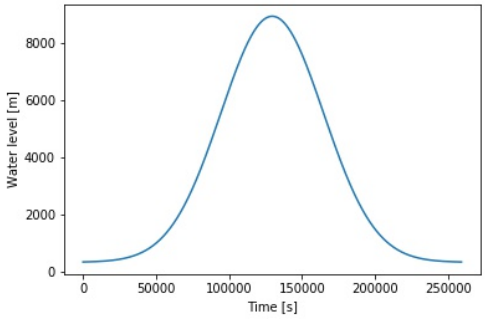

Figure H.7: Upstream boundary 263 year, river dominance

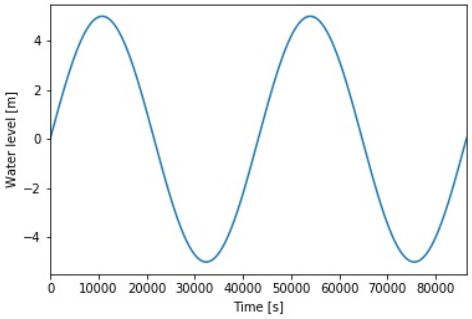

Figure H.8: Downstream boundary 263 year, river dominance

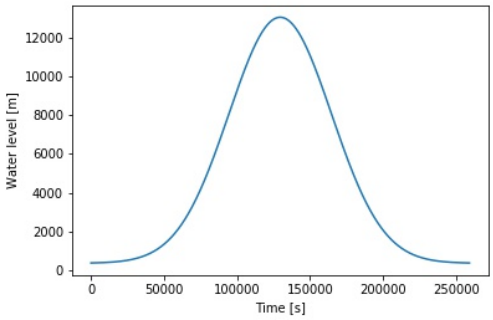

Figure H.9: Upnstream boundary, 373 year. tidal dominance

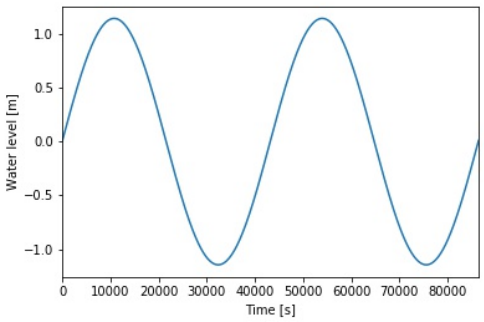

Figure H.10: Downstream boundary, 373 year, tidal dominance

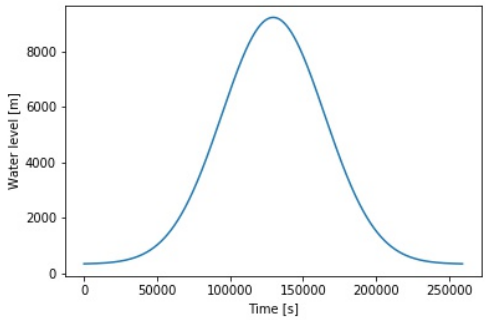

Figure H.11: Upnstream boundary, 373 year, tidal dominance

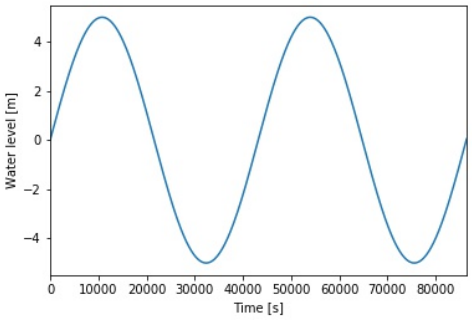

Figure H.12: Downstream boundary, 373 year, tidal dominance

Geological map DC

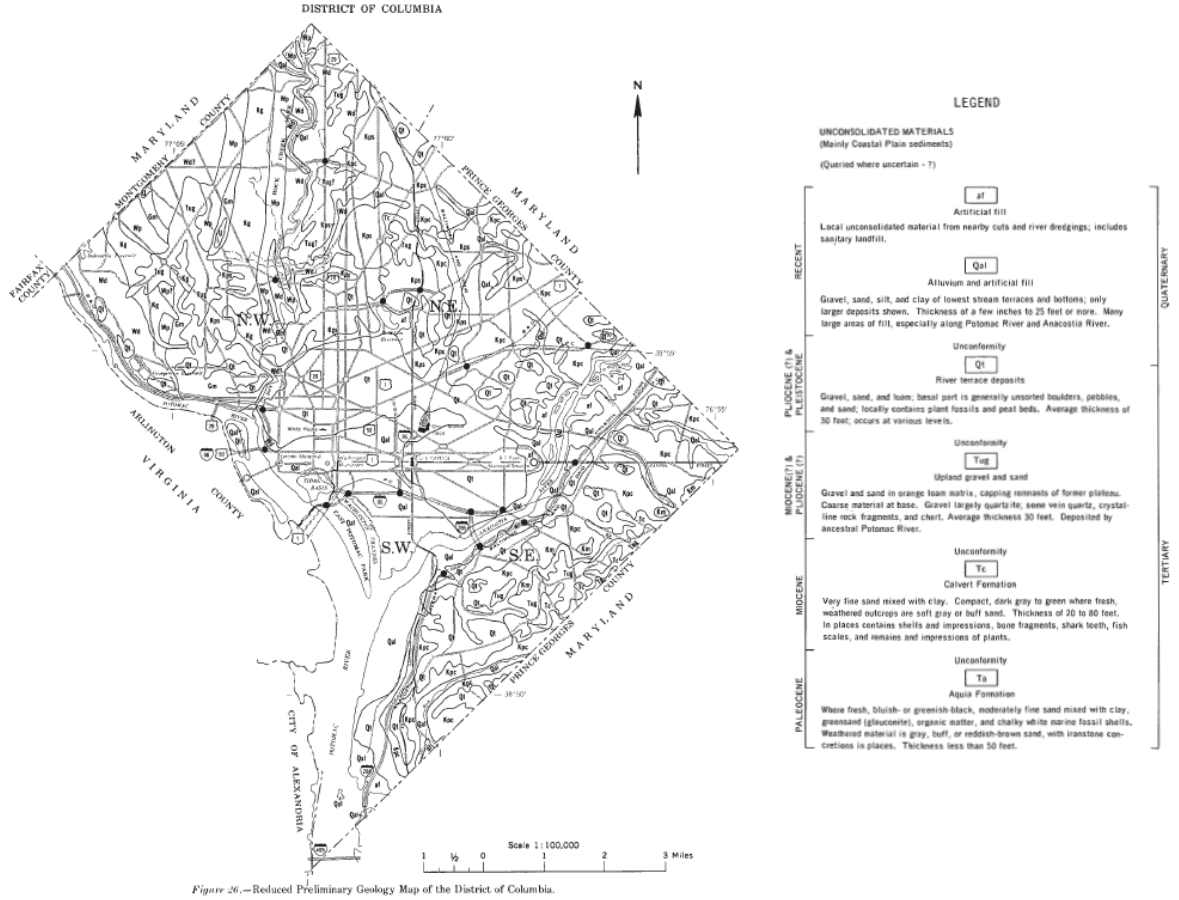

Figure 26.—Reduced Preliminary Geology Map of the District of Columbia.

Figure I.1: Geological map of the soil surface of DC (Survey, 1976)

Figure 27.—Map showing thickness of overburden in the District of Columbia.

Figure I.2: Geological map of the soil overburden of DC (Survey, 1976)

J

Sight investigation

Figure J.1: Sight investigation National Mall (Nat)

Figure J.2: Sight investigation Anacostia (Nat)

K

Boreholes

K.1. Borehole ECS LLC Kings Island improvement

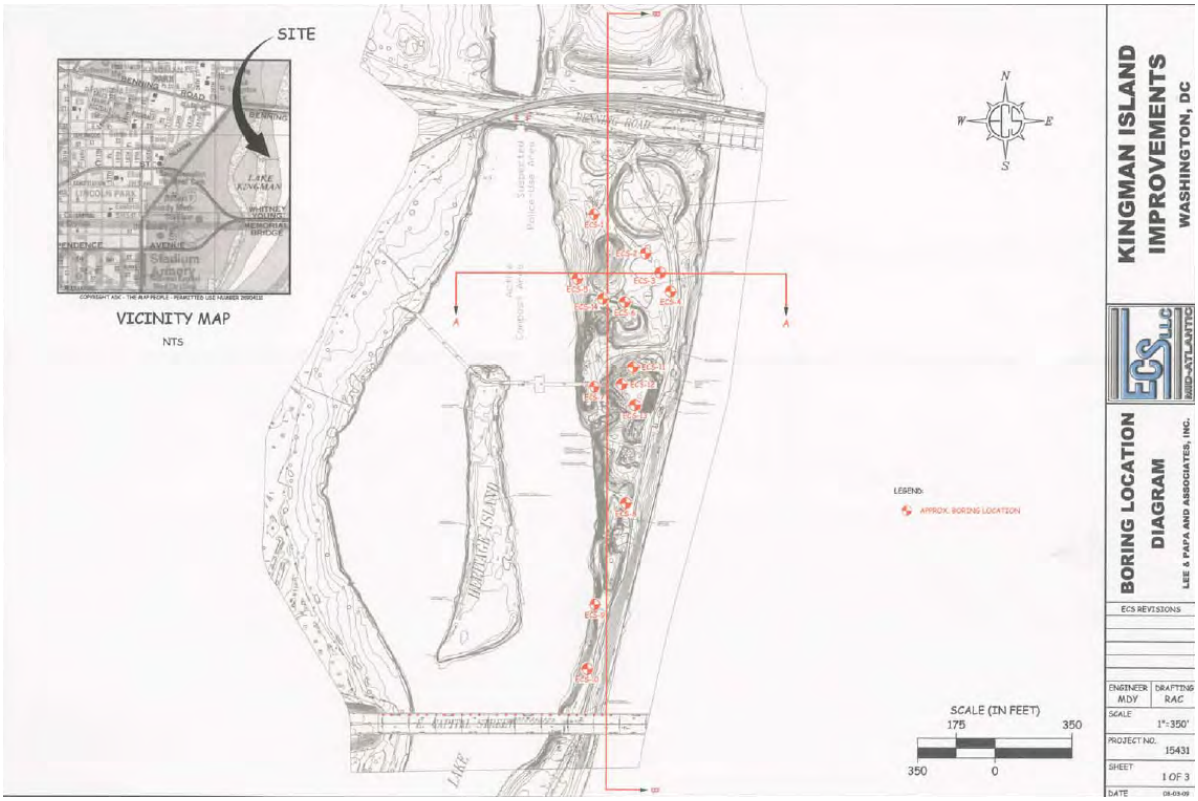

Figure K.1: Location of the different boreholes at Kingman Island (ECS-Midatlantic-LTD, 2009)

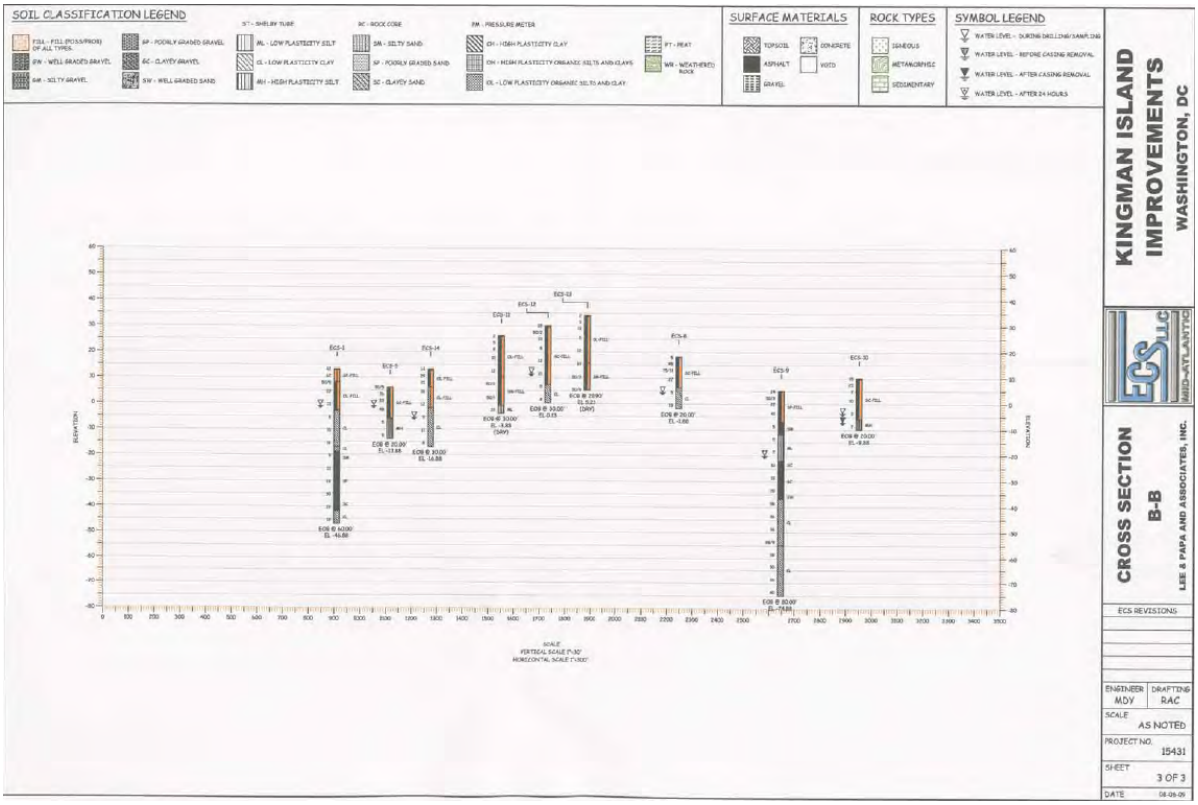

Figure K.2: Summary of the lithography of boreholes at Kingman Island crossection B-B (ECS-Midatlantic-LTD, 2009)

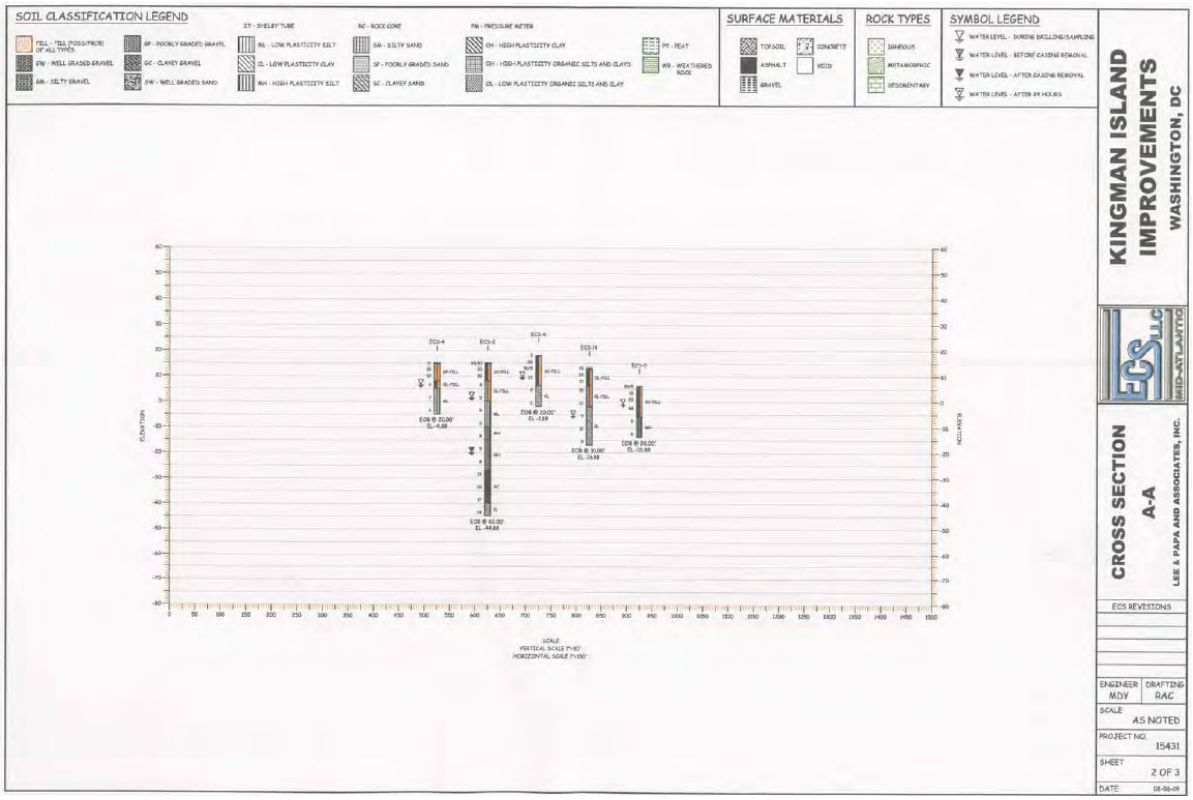

Figure K.3: Summary of the lithography of boreholes at Kingman Island crossection A-A (ECS-Midatlantic-LTD, 2009)

K.2. Borehole NAMA Rehabilitate Potable Water Lines

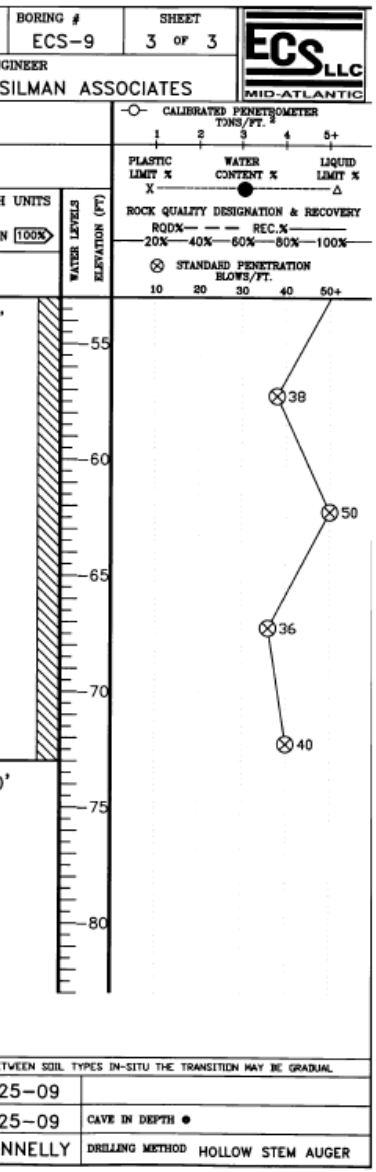
BORING # ECS-9
SHEET 3 OF 3
SILMAN ASSOCIATES
CALIBRATED PENETROMETER TONS/FT.²
PLASTIC LIMIT %
WATER CONTENT %
LIQUID LIMIT %
ROCK QUALITY DESIGNATION & RECOVERY
RQD% REC.%
STANDARD PENETRATION BLOWS/FT.
WATER LEVELS
ELEVATION (FT)
38
50
36
40
TWEEN SOIL TYPES IN-SITU THE TRANSITION MAY BE GRADUAL
25-09
25-09
NNELLY
CAVE IN DEPTH ●
DRILLING METHOD HOLLOW STEM AUGER

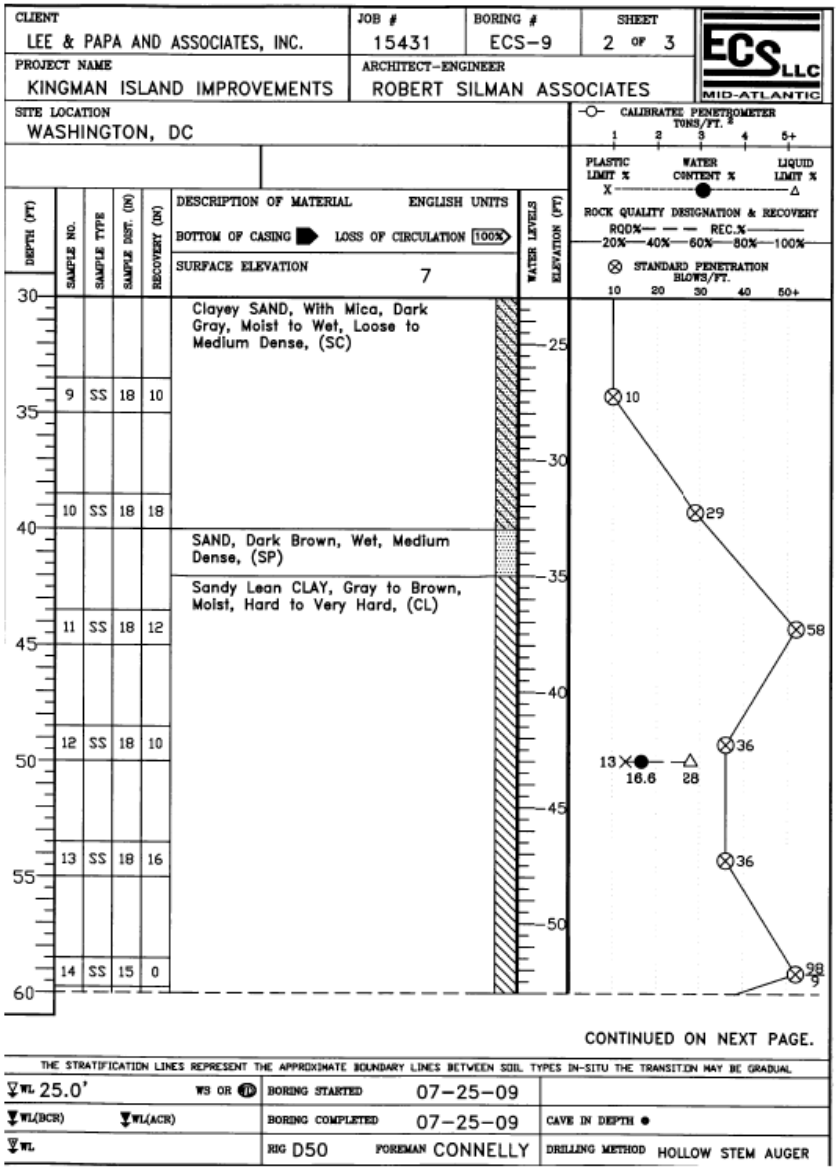
CLIENT
LEE & PAPA AND ASSOCIATES, INC.
JOB # 15431
BORING # ECS-9
SHEET 2 OF 3
PROJECT NAME
KINGMAN ISLAND IMPROVEMENTS
ARCHITECT-ENGINEER
ROBERT SILMAN ASSOCIATES
SITE LOCATION
WASHINGTON, DC
DEPTH (FT)
SAMPLE NO.
SAMPLE TYPE
SAMPLE DIST. (IN)
RECOVERY (IN)
DESCRIPTION OF MATERIAL ENGLISH UNITS
BOTTOM OF CASING LOSS OF CIRCULATION 100%
SURFACE ELEVATION 7
Clayey SAND, With Mica, Dark Gray, Moist to Wet, Loose to Medium Dense, (SC)
SAND, Dark Brown, Wet, Medium Dense, (SP)
Sandy Lean CLAY, Gray to Brown, Moist, Hard to Very Hard, (CL)
9 SS 18 10
10 SS 18 18
11 SS 18 12
12 SS 18 10
13 SS 18 16
14 SS 15 0
10
29
58
36
36
13
16.6
28
CONTINUED ON NEXT PAGE.
THE STRATIFICATION LINES REPRESENT THE APPROXIMATE BOUNDARY LINES BETWEEN SOIL TYPES IN-SITU THE TRANSITION MAY BE GRADUAL
WL 25.0'
WS OR ▽D
BORING STARTED 07-25-09
WL(BCR)
WL(ACR)
BORING COMPLETED 07-25-09
CAVE IN DEPTH ●
WL
RIG D50
FOREMAN CONNELLY
DRILLING METHOD HOLLOW STEM AUGER

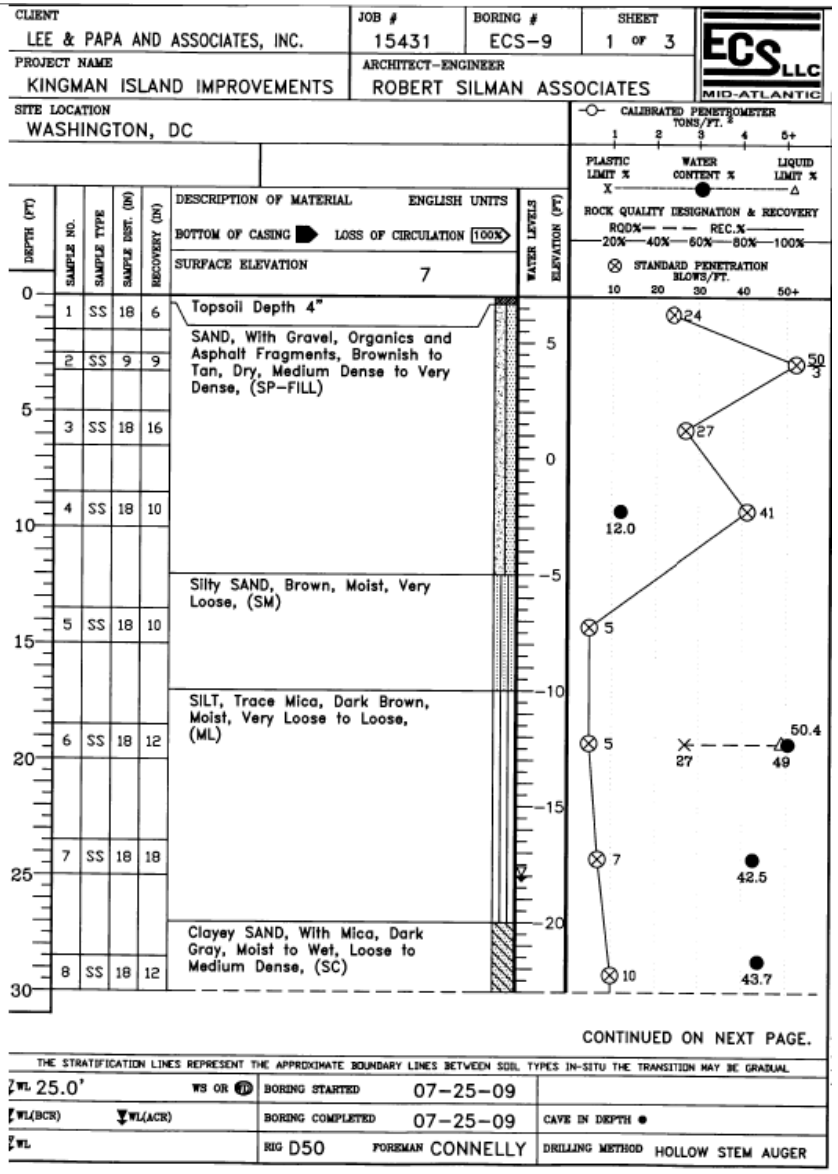
CLIENT
LEE & PAPA AND ASSOCIATES, INC.
JOB # 15431
BORING # ECS-9
SHEET 1 OF 3
PROJECT NAME
KINGMAN ISLAND IMPROVEMENTS
ARCHITECT-ENGINEER
ROBERT SILMAN ASSOCIATES
SITE LOCATION
WASHINGTON, DC
DESCRIPTION OF MATERIAL ENGLISH UNITS
BOTTOM OF CASING LOSS OF CIRCULATION 100%
SURFACE ELEVATION 7
1 SS 18 6
2 SS 9 9
3 SS 18 16
4 SS 18 10
5 SS 18 10
6 SS 18 12
7 SS 18 18
8 SS 18 12
Topsoil Depth 4"
SAND, With Gravel, Organics and Asphalt Fragments, Brownish to Tan, Dry, Medium Dense to Very Dense, (SP-FILL)
Silty SAND, Brown, Moist, Very Loose, (SM)
SILT, Trace Mica, Dark Brown, Moist, Very Loose to Loose, (ML)
Clayey SAND, With Mica, Dark Gray, Moist to Wet, Loose to Medium Dense, (SC)
24
50/3
27
41
12.0
5
5
27
49
50.4
7
42.5
10
43.7
CONTINUED ON NEXT PAGE.
THE STRATIFICATION LINES REPRESENT THE APPROXIMATE BOUNDARY LINES BETWEEN SOIL TYPES IN-SITU THE TRANSITION MAY BE GRADUAL
WL 25.0'
WS OR ▽D
BORING STARTED 07-25-09
WL(BCR)
WL(ACR)
BORING COMPLETED 07-25-09
CAVE IN DEPTH ●
WL
RIG D50
FOREMAN CONNELLY
DRILLING METHOD HOLLOW STEM AUGER

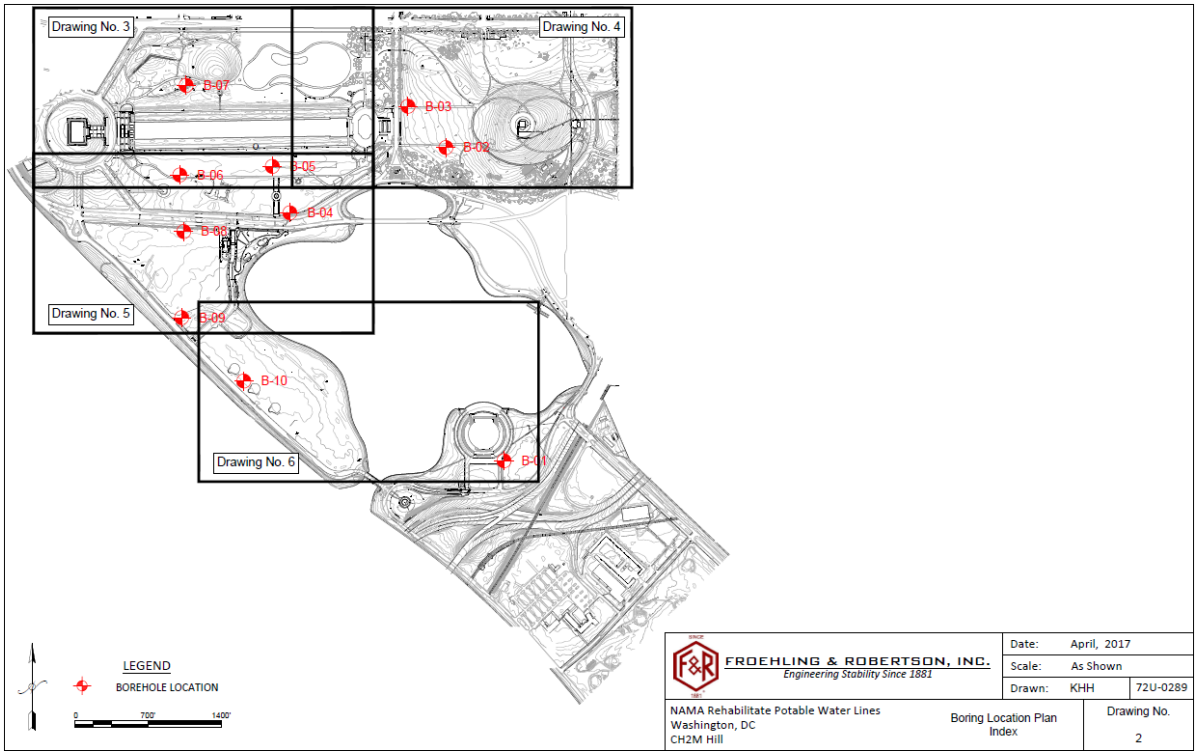

Figure K.5: Location of the different boreholes for the Potable Water project (Froehling Robertson, 2014)

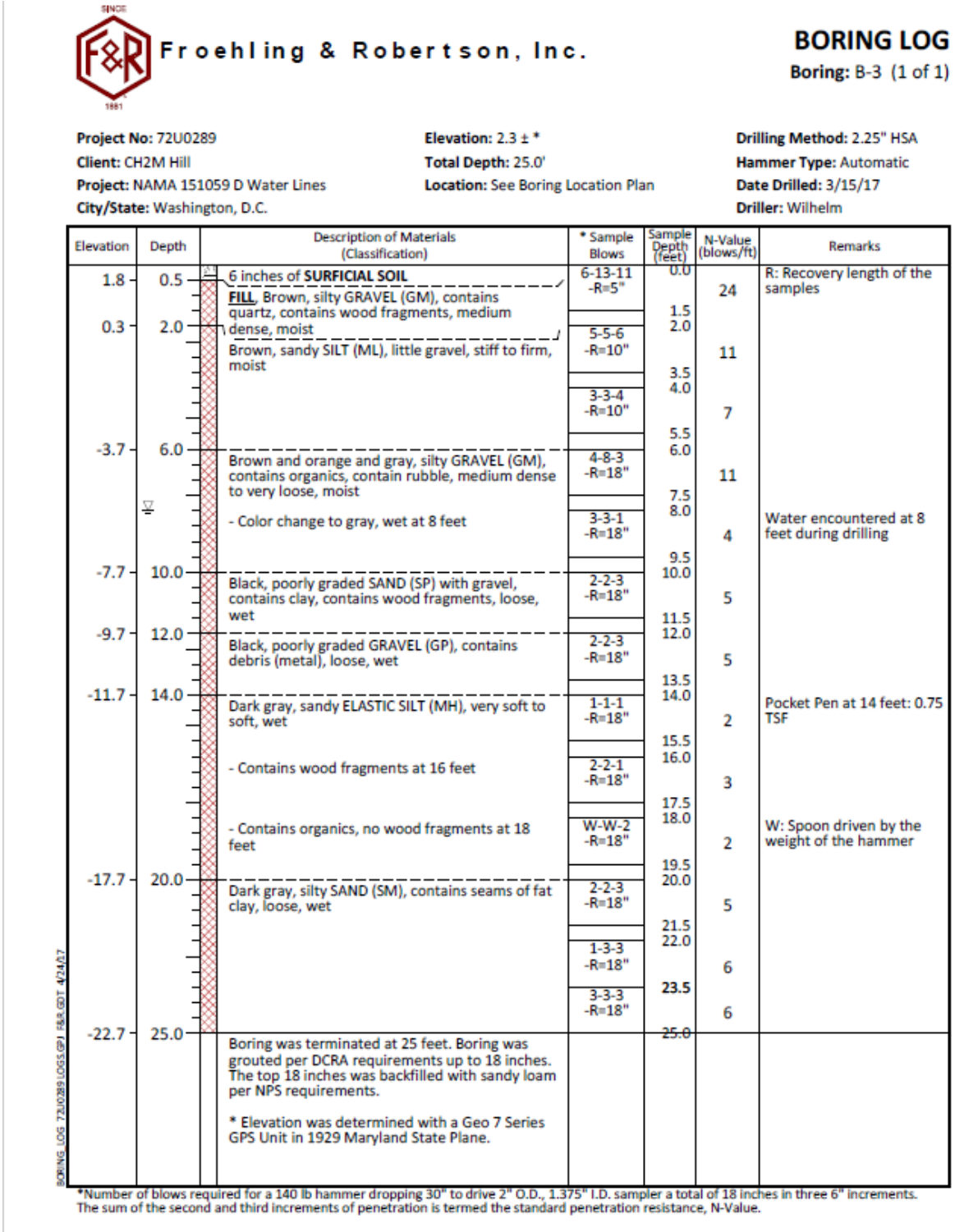

Froehling & Robertson, Inc.

BORING LOG

Boring: B-3 (1 of 1)

Project No: 72U0289
Client: CH2M Hill
Project: NAMA 151059 D Water Lines
City/State: Washington, D.C.

Elevation: 2.3 ± *
Total Depth: 25.0'
Location: See Boring Location Plan

Drilling Method: 2.25" HSA
Hammer Type: Automatic
Date Drilled: 3/15/17
Driller: Wilhelm

Elevation	Depth	Description of Materials (Classification)	* Sample Blows	Sample Depth (feet)	N-Value (blows/ft)	Remarks
1.8	0.5	6 inches of **SURFICIAL SOIL**	6-13-11 -R=5"	0.0	24	R: Recovery length of the samples
		FILL, Brown, silty GRAVEL (GM), contains quartz, contains wood fragments, medium dense, moist		1.5		
0.3	2.0	Brown, sandy SILT (ML), little gravel, stiff to firm, moist	5-5-6 -R=10"	2.0	11	
				3.5		
			3-3-4 -R=10"	4.0	7	
				5.5		
-3.7	6.0	Brown and orange and gray, silty GRAVEL (GM), contains organics, contain rubble, medium dense to very loose, moist	4-8-3 -R=18"	6.0	11	
				7.5		
		- Color change to gray, wet at 8 feet	3-3-1 -R=18"	8.0	4	Water encountered at 8 feet during drilling
				9.5		
-7.7	10.0	Black, poorly graded SAND (SP) with gravel, contains clay, contains wood fragments, loose, wet	2-2-3 -R=18"	10.0	5	
				11.5		
-9.7	12.0	Black, poorly graded GRAVEL (GP), contains debris (metal), loose, wet	2-2-3 -R=18"	12.0	5	
				13.5		
-11.7	14.0	Dark gray, sandy ELASTIC SILT (MH), very soft to soft, wet	1-1-1 -R=18"	14.0	2	Pocket Pen at 14 feet: 0.75 TSF
				15.5		
		- Contains wood fragments at 16 feet	2-2-1 -R=18"	16.0	3	
				17.5		
		- Contains organics, no wood fragments at 18 feet	W-W-2 -R=18"	18.0	2	W: Spoon driven by the weight of the hammer
				19.5		
-17.7	20.0	Dark gray, silty SAND (SM), contains seams of fat clay, loose, wet	2-2-3 -R=18"	20.0	5	
				21.5		
			1-3-3 -R=18"	22.0	6	
				23.5		
			3-3-3 -R=18"		6	
-22.7	25.0	Boring was terminated at 25 feet. Boring was grouted per DCRA requirements up to 18 inches. The top 18 inches was backfilled with sandy loam per NPS requirements.		25.0		
		* Elevation was determined with a Geo 7 Series GPS Unit in 1929 Maryland State Plane.				

*Number of blows required for a 140 lb hammer dropping 30" to drive 2" O.D., 1.375" I.D. sampler a total of 18 inches in three 6" increments. The sum of the second and third increments of penetration is termed the standard penetration resistance, N-Value.

BORING LOG 72U0289 LOGS.GPJ F&R.GDT 4/24/17

Figure K.6: Borehole 3 of the Rehabilitate Potable Water Lines project (Froehling Robertson, 2014)

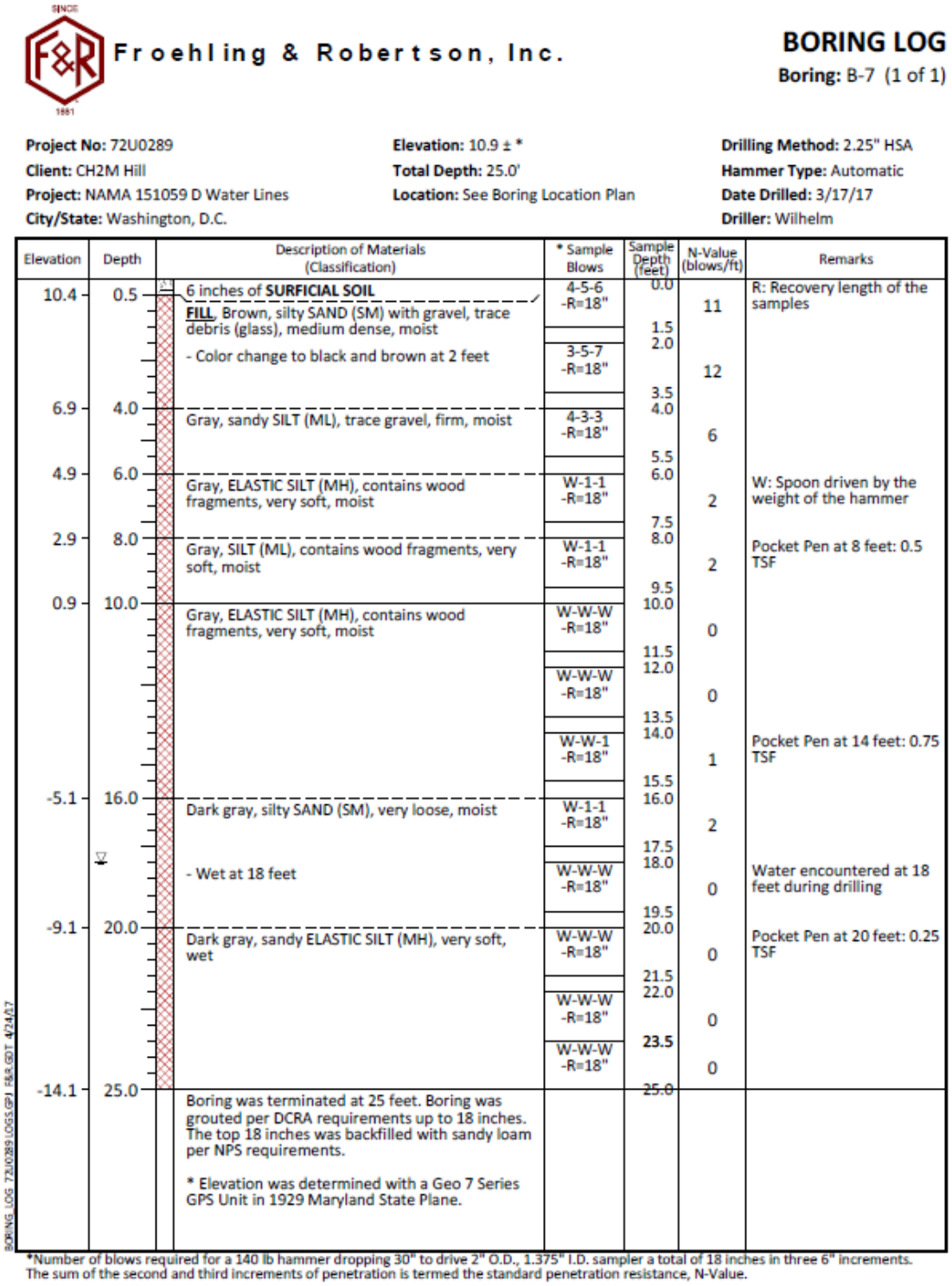

Froehling & Robertson, Inc.

BORING LOG
Boring: B-7 (1 of 1)

Project No: 72U0289
Client: CH2M Hill
Project: NAMA 151059 D Water Lines
City/State: Washington, D.C.

Elevation: 10.9 ± *
Total Depth: 25.0'
Location: See Boring Location Plan

Drilling Method: 2.25" HSA
Hammer Type: Automatic
Date Drilled: 3/17/17
Driller: Wilhelm

Elevation	Depth	Description of Materials (Classification)	* Sample Blows	Sample Depth (feet)	N-Value (blows/ft)	Remarks
10.4	0.5	6 inches of **SURFICIAL SOIL**	4-5-6 -R=18"	0.0	11	R: Recovery length of the samples
		FILL, Brown, silty SAND (SM) with gravel, trace debris (glass), medium dense, moist		1.5		
		- Color change to black and brown at 2 feet	3-5-7 -R=18"	2.0	12	
6.9	4.0	Gray, sandy SILT (ML), trace gravel, firm, moist	4-3-3 -R=18"	3.5 4.0	6	
4.9	6.0	Gray, ELASTIC SILT (MH), contains wood fragments, very soft, moist	W-1-1 -R=18"	5.5 6.0	2	W: Spoon driven by the weight of the hammer
2.9	8.0	Gray, SILT (ML), contains wood fragments, very soft, moist	W-1-1 -R=18"	7.5 8.0	2	Pocket Pen at 8 feet: 0.5 TSF
0.9	10.0	Gray, ELASTIC SILT (MH), contains wood fragments, very soft, moist	W-W-W -R=18"	9.5 10.0	0	
			W-W-W -R=18"	11.5 12.0	0	
			W-W-1 -R=18"	13.5 14.0	1	Pocket Pen at 14 feet: 0.75 TSF
-5.1	16.0	Dark gray, silty SAND (SM), very loose, moist	W-1-1 -R=18"	15.5 16.0	2	
		- Wet at 18 feet	W-W-W -R=18"	17.5 18.0	0	Water encountered at 18 feet during drilling
-9.1	20.0	Dark gray, sandy ELASTIC SILT (MH), very soft, wet	W-W-W -R=18"	19.5 20.0	0	Pocket Pen at 20 feet: 0.25 TSF
			W-W-W -R=18"	21.5 22.0	0	
			W-W-W -R=18"	23.5	0	
-14.1	25.0	Boring was terminated at 25 feet. Boring was grouted per DCRA requirements up to 18 inches. The top 18 inches was backfilled with sandy loam per NPS requirements.		25.0		
		* Elevation was determined with a Geo 7 Series GPS Unit in 1929 Maryland State Plane.				

*Number of blows required for a 140 lb hammer dropping 30" to drive 2" O.D., 1.375" I.D. sampler a total of 18 inches in three 6" increments. The sum of the second and third increments of penetration is termed the standard penetration resistance, N-Value.

BORING LOG 72U0289 LOGS.GPJ F&R.GDT 4/24/17

Figure K.7: Borehole 7 of the Rehabilitate Potable Water Lines project (Froehling Robertson, 2014)

L

Eurocode 7

Hoofd-naam	Bijmengsel	Consis-tentie [b]	γ [a] kN/m³		γ_{sat} kN/m³		q_c [a] [g] MPa			C'_p		C'_s		$C_c/(1+e_0)$ [-]		C_α [f] [-]		$C_{sw}/(1+e_0)$ [e] [-]		E_{100} [f] MPa		ϕ' [f] Graden		c' kPa		c_u kPa
grind	zwak siltig	los	17		19		15			500		∞		0,0046		0		0,0015		45		32,5		0		
		matig	18		20		25			1000		∞		0,0023		0		0,0008		75		35,0		0		n.v.t.
		vast	19	20	21	22	30			1200	1400	∞		0,0019	0,0016	0		0,0006	0,0005	90	105	37,5	40,0	0		
	sterk siltig	los	18		20		10			400		∞		0,0058		0		0,0019		30		30,0		0		
		matig	19		21		15			600		∞		0,0038		0		0,0013		45		32,5		0		n.v.t.
		vast	20	21	22	22,5	25			1000	1500	∞		0,0023	0,0015	0		0,0008	0,0005	75	110	35,0	40,0	0		
zand	schoon	los	17		19		5			200		∞		0,0115		0		0,0038		15		30,0		0		
		matig	18		20		15			600		∞		0,0038		0		0,0013		45		32,5		0		n.v.t.
		vast	19	20	21	22	25			1000	1500	∞		0,0023	0,0015	0		0,0008	0,0005	75	110	35,0	40,0	0		
	zwak siltig, kleiig		18	19	20	21	12			450	650	∞		0,0051	0,0035	0		0,0017	0,0012	35	50	27,0	32,5	0		n.v.t.
	sterk siltig, kleiig		18	19	20	21	8			200	400	∞		0,0115	0,0058	0		0,0038	0,0019	15	30	25,0	30,0	0		n.v.t.
leem [c]	zwak zandig	slap	19		19		1			25		650		0,0920		0,0037		0,0307		2		27,5	30,0	0		50	
		matig	20		20		2			45		1300		0,0511		0,0020		0,0170		3		27,5	32,5	1		100	
		vast	21	22	21	22	3			70	100	1900	2500	0,0329	0,0230	0,0013	0,0009	0,0110	0,0077	5	7	27,5	35,0	2,5	3,8	200	300
	sterk zandig		19	20	19	20	2			45	70	1300	2000	0,0511	0,0329	0,0020	0,0013	0,0170	0,0110	3	5	27,5	35,0	0	1	50	100
klei	schoon	slap	14		14		0,5			7		80		0,3286		0,0131		0,1095		1		17,5		0		25	
		matig	17		17		1,0			15		160		0,1533		0,0061		0,0511		2		17,5		5		50	
		vast	19	20	19	20	2,0			25	30	320	500	0,0920	0,0767	0,0037	0,0031	0,0307	0,0256	4	10	17,5	25,0	13	15	100	200
	zwak zandig	slap	15		15		0,7			10		110		0,2300		0,0092		0,0767		1,5		22,5		0		40	
		matig	18		18		1,5			20		240		0,1150		0,0046		0,0383		3		22,5		5		80	
		vast	20	21	20	21	2,5			30	50	400	600	0,0767	0,0460	0,0031	0,0018	0,0256	0,0153	5	10	22,5	27,5	13	15	120	170
	sterk zandig	-	18	20	18	20	1,0			25	140	320	1680	0,0920	0,0164	0,0037	0,0007	0,0307	0,0055	2	5	27,5	32,5	0	1	0	10
	organisch	slap	13		13		0,2			7,5		30		0,3067		0,0153		0,1022		0,5		15,0		0	1	10	
		matig	15	16	15	16	0,5			10	15	40	60	0,2300	0,1533	0,0115	0,0077	0,0767	0,0511	1,0	2,0	15,0		0	1	25	30
veen	niet voorbelast	slap	10	12	10	12	0,1			5	7,5	20	30	0,4600	0,3067	0,0230	0,0153	0,1533	0,1022	0,2	0,5	15,0		1	2,5	10	20
	matig voorbelast	matig	12	13	12	13	0,2			7,5	10	30	40	0,3067	0,2300	0,0153	0,0115	0,1022	0,0767	0,5	1,0	15,0		2,5	5	20	30
variatiecoëfficiënt			0,05				–			0,25										0,10				0,20			

Figure L.1: Table 2b of Eurocode 7